Addis Ababa University College of Technology and Built Environment

School of Mechanical and Industrial Engineering

EXPERIMENTAL INVESTIGATION OF MECHANICAL PROPERTY IN FRICTION STIR WELDING ON (CU2-2.041 AND SS-304L) DISSIMILAR METAL USING TAGUCHI BASED GRA

A Master Thesis Submitted to the Graduate School of Addis Ababa University in Partial Fulfillment of the Requirement for the Award Degree of Masters of Science (M.SC) In Mechanical Engineering (Manufacturing Engineering)

By: **HAILEYESUS TEGEN**

Advisor: **Dr. MESFIN GIZAW**

Addis Ababa, Ethiopia

MARCH 2025

Addis Ababa University College of Technology and Built Environment

School of Mechanical and Industrial Engineering

EXPERIMENTAL INVESTIGATION OF MECHANICAL PROPERTY IN FRICTION STIR WELDING ON (CU2-2.041 AND SS-304L) DISSIMILAR METAL USING TAGUCHI BASED GRA

By: Haileyesus Tegene

Submitted in accordance with the requirements for the degree

MASTER OF SCIENCE (M.Sc.)

Approved by Board of Directors:

Advisor	Signature	Date
Internal Examiner	Signature	Date
Internal Examiner	Signature	Date
School Head	Signature	Date

DECLARATION

I hereby declare that this Master Thesis entitled entitled: **"Experimental investigation of mechanical property in friction stir welding on (cu2-2.041 and ss-304l) dissimilar metal using Taguchi based GRA "** In partial fulfillment of the requirement for the award of the Degree of Masters of Science in Manufacturing Engineering is my Original work carried out February 2023 to March 2025 under the supervision **Dr. MESFIN GIZAW,** That is, it has not been submitted for award of any academic degree, diploma or certificate in any other university. All sources of Materials that are used for this thesis has been duly acknowledged through citation.

_____	_____	_____
Name of the student	Signature	Date

This is to certify that the above declaration made by the candidate is correct to the best of our knowledge and belief. It has been submitted for examination with our approval.

Advisor: _____ Signature: _____ Date: _____

Head of School: _____ Signature: _____ Date: _____

ACKNOWLEDGEMENT

First and foremost, I want to express my gratitude to The Almighty GOD for allowing me to begin and complete my thesis work to overcome different challenge and problems.

I am grateful to my thesis advisor, Dr. Mesfin Gizaw, Assistant Professor, School of Mechanical and Industrial Engineering, for his genuine guidance and check-ups in the thesis writing process. by seating a good example of researcher and solution maker to any problem by technical way. Those countless brainstorm enlightens me to think critically and deeply, today and tomorrow. Your methodology and advises are still guiding me find the right path. I thank you very much that you gave me perfect advices whenever I faced serious problems, you made me feel hopeful to finish this thesis. Also,

I'm also thankful to Dr. Desalng wegeso and Dr. Getasew taddese , for their assistance and cooperation During thesis progress submission as well as material selection to have a better result . I appreciate the support of Addis Ababa University's School of Mechanical and Industrial Engineering members.

I would like to thank you to Dr. Areaya for writing support letters for both Ethiopia's customs and revenue authorities and Ethio-china vocational institute to get tungsten carbide FSW tool road which imported from USA. I would like to express my sincere thanks to my friend who work in Ethio-china vocational training centre Mr. GEZHNG for facilitating the experimental workplace and machines and giving important feedback on my work and other one Mr. SAMUEL who works at Ethiopian Manufacturing Enterprise METEC for their help during the experimental work and heat treatment, respectively, on my research studies.

And also I’m thankful to Addis Ababa Science and Technology University’s work Shop Technician Mr. ISRAEL who helped me in the FSW tool preparation from tungsten carbide with energy and for preparation of copper and stillness stile plate for FSW purpose.

In addition to that I would like to give a great credential for those who do similar research titles and helps me in different circumstance during the experimental work like Mr. Wondu Tesfaye previous Msc. Student of AAIT and Mr. Eyob previous Bahirdar university student.

Finally, I'd like to express my gratitude to all of the people who assisted me in my research work like my family, friends, and classmates, for various support from the beginning to end.

ABSTRACT

FSW (Friction Stir Welding) is a solid-state welding method mostly used to join Dissimilar metals, This joining technique is energy efficient, environment friendly, and versatile. In particular, it can be used to join high-strength aerospace different metal and other metallic alloys that are hard to weld by conventional fusion welding.

During this paper experiment on a Utilizing procedure parameters of tool rotating speed (120,1400,1600), transverse speed (45,55,65) mm/min, dwell time of (4,8,12) seconds as well as pin profiles (cylindrical, conical, and square), materials of (SS-304L alloy with CU- 2.041 pure) with a thickness of 5mm Butt joint configuration was conducted by friction stir welding. The plates are successfully welded, and the welded plates are tested at room temperature to examine their tensile strength and hardness.

Assess the performance and features of the welded joints by optimizing the mechanical and metallurgical properties of the aforementioned dissimilar combination with L9 orthogonal array and the Grey relation analysis approach were used to optimize the process parameters, and the results showed larger is better quality characteristics.

During the experimental run Tungsten carbide cobalt (WC-CO) which is very strong material that can withstand sudden heat change and excessive friction was Selected as a welding tool

To look at the significant process parameters, an ANOVA was performed. This study shows that, with a joint efficiency of roughly 74.63%, tool shape,rotational speed,dwell duration,and traverse speed become relevant respectively. The experiment is deemed credible since the average values of the gray relational grade fell within the 95% confidence interval, according to the findings of three confirmatory tests.

In addition to that, this work also addresses the effects of pre welding heat treatment conditions annealing on the resulting weld joint for both copper and stainless steel with 800 and 1000 °C for half an hour

A finite element model (FEM) is developed in this work to examine the effects of dwell time and rotational speed on the micro structure, tensile strength, and hardness of the weld zone. There was ultimately a good agreement between the results of the experiments Temperature and the Transient Thermal Simulation Temperature difference on the Ansys software with regard to welding time, tool profile, and Rpm parametric relation.

After the plates are successfully welded, their hardness and tensile strength are assessed at room temperature. The results show that the ideal parameters for joining these different joints are the square pin profile, 1600 rpm rotational speed, 45 mm/min transverse speed, and 8 seconds of dwell time. In the stir zone, strengthening precipitates were distributed evenly.

Key words; - *FSW, Orthogonal array, SS -Cu, tool material, mechanical property, butt joint,*

TABLE OF CONTENTS

LIST OF FIGURES

LIST OF TABLES

LIST OF ACRONYMS AND ABBREVIATIONS

Adj SS	Adjusted sum of squares
ANOVA	Analysis of variance
ASTM	American society of testing material
HSCFRPC	Hybrid sisal-cotton fiber reinforced polyester composite
CNC	Computer numerical control
NFRP	Natural fiber reinforced polymer
FRP	Fiber-reinforced polymer
UTM	Universal testing machine
HSS	High-speed steel
RBFN	Radial basis function network
OA	Orthogonal array
MPa	Mega pascal
Ne	Number English
ml	Milliliter
Sec	Second
GPP	General Purpose polyester
KJ/m	Kilo joule per meter
Rpm	Revolution per minute
DOE	Design of experiment

DF	Degree of freedom
SS	Sum of squares
Seq SS	Sequential sum of squares
S/N	Signal to noise ratio
SN	Signal to noise
F-value	Variance
P-value	Calculated probability
μm	Micrometer
min	Minute
METEC	Metals and Engineering Corporation
10x	ten times
3D	Three Dimensional
Eq.	Equation
Fig.	Figure
SD	Standard Deviation
S/N_L	Lower the better signal to noise ratio
PLC	Diamond-like carbon
PCD	Polycrystalline diamond
PCBN	Poly Crystalline Cubic Boron Nitride
PMHSS	Powder Metallurgical High-Speed Steel

CHAPTER ONE

1.1 Introduction

Many iron objects that were riveted by hammering were created during the Middle Ages. India's Delhi Iron Pillar, which was built around 1700 years ago, is among the biggest examples of this era's welding. Professional welding as we know it today did not exist until the 19th century **[1].** Three thousand years ago, individuals in the Eastern Mediterranean region, particularly the Egyptians, learns how to fuse iron pieces together.

Following thousands of years of historical integration, the introduction of of Friction Stir Welding (FSW) which is a solid-state welding method mostly used to join Dissimilar metals was initially established 1991 at the Welding Institute in Cambridge, UK, by Thomas and Nicholas **[2].** A non-consumable spinning tool with a pin and shoulder for heat generation is used in the solid-state joining process to soften the base materials. The tool is tougher than the material being welded. There are two welded sides to the procedure. The weld axis and the progressed side are located in the same direction as the tool. The weld axis is pointing in the opposite direction from the tool's retreating side **[3].**

Due to the vast disparities in mechanical and metallurgical properties, joining different materials using any welding procedure is always challenging **[4].** The linear thermal expansion coefficient, thermal conductivity, and melting temperatures are important considerations for materials like copper and stainless steel combined. Economic benefits and a variety of mechanical parts for the international thermonuclear experimental reactor, line structure, and heat ex-changer make the joint qualities of copper to stainless steel welds highly desirable. An iron alloy with a high resistance to corrosion and rust is stainless steel. Chromium makes up at least 11% of it, and other non-metals like carbon may be added to get other desirable qualities. Because chromium produces a passive coating that can shield the material and self-heal when exposed to oxygen, stainless steel is resistant to corrosion **[5].**

Additionally, copper (Cu) has strong thermal and electrical conductivity, making it a good choice for thermal and electrical applications. connectors for electricity, bus bars, transformer foil conductors, capacitors, and tubes for refrigeration, heat exchangers, condenser foil windings, tube sheets, etc. Some typical uses for SS-CU joints are as follows. **[6].**

One of the most methods for connecting stainless steel these days is FSW. The iron alloy known as stainless steel is impervious to corrosion and rust. At least 11% of it is chromium, and additional non-metals like carbon may be added to get other desired the sector. Despite being a hard metal, FSW is still not as feasible in other alloys **[7].** When steel was first welded using FSW, tungsten and molybdenum tools were used. These FSW tools' primary drawback is that they break and distort when inserted into steel **[8].**

The advantages of having distinct thermal characteristics at both ends, cost savings and improved mechanical and thermal efficiency of heat ex-changers, as well as several intriguing engineering applications, make welding Cu-SS a significant field of attention. Given the significant challenges in welding this dissimilar combination Cu-SS connection, traditional fusion welding procedures are not appropriate to provide sound results, even with intriguing technical solutions and later implementations. and free joints without flaws **[9].**

The best welding tools for CU-SS FSW can be made of materials like commercial pure tungsten (CpW) or poly-crystalline cubic boron nitrite (PCBN). Cu and SS should not be joined by fusion welding due to the formation of massive inter metallic complexes (IMCs). Many flaws are caused by the extreme hardness and brittleness of these IMCs. Among the frequent issues with fusion welding are solidification and liquefaction cracks **[10].**

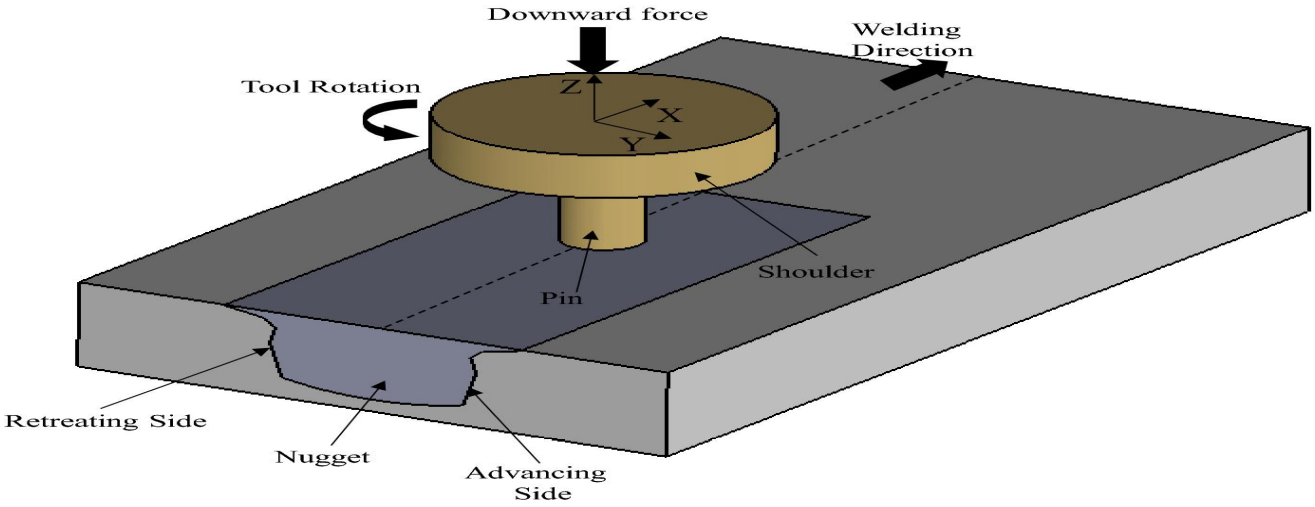

Figure 1.1 Friction stir welding set-up **[7]**

In TWI, numerous attempts have been made to assess the effectiveness of friction stir welding (FSW) in combining dissimilar and similar materials. Most of these efforts are focused on combining comparable materials, particularly alloys of stainless steel. Nandan and colleagues conducted one of the most thorough evaluations of FSW **[11].**

In this work, the basics of FSW, such as heat generation, materials flow, welding flaws, and residual stresses, were examined. Additionally, some friction stir welding defects might be described as tunneling defects, void defects, or fragment defects due to the connecting of different metals like copper, titanium, and steel alloys with FSW **[12].**

The defect that arises from low rotation speed is the emergence of joint cross section with a spongy substance. Reduced heat generation during welding will result in less flexible material flow **[13].**
In order to achieve efficient material flow, FSW tools are made to produce enough heat through friction between the base metal and the tool as well as plastic deformation of the base metal. Tool shoulder and tool pin are the two primary parts of the tool **[14].**
Hot work and cold work tooling applications frequently use HSS Tool Steel, a versatile chromium-molybdenum hot work steel. Premature heat checking is avoided, and it can tolerate fast cooling. HSS is ductile, weldable, and has good match inability. It can also be produced using standard techniques **[15].**

Two crucial elements of the design of a friction stir welding instrument are:- tool geometry and material. High temperature material application, tool material selection, tool material development, tool design, complex geometries, and dissimilar materials are the main obstacles to friction stir welding **[16].**

Three distinct tool pin geometries square, tapered conical, and cylindrical will be used in this experimental investigation in order to maximize the welding joint's outcome depending on the process variables. Utilizing the Taguchi orthogonal array design method, the effects of tool design, rotation speed, and travel speed on mechanical properties will be examined.

Friction stir welding is joining Process with a limited heat-affected zone and gives homogeneous mixture in the micro-structure level, which also improve corrosion resistance. by utilizing various optimization process parameters and proper selection of tool geometries. On this study, the key contribution of FSW welding is the addition of values in materials hardness, tensile strength and micro structural observation of thermal and electrical components for a new welding maintenance mechanism.

1.2 Problem statement

Stainless steel and copper Alloys are difficult to weld with conventional welding processes due to their disparate characteristics, which is challenging **[4].** such as Arc welding, MIG welding and TIG welding. Weld cracks are unacceptable defects that can compromise the integrity of welded structures. Most cracks are the result of solidification, cooling and stresses that develop due to weld shrinkage. Weld cracking can lead to structural failures. In the recent studies showed that fusion welding has emissions and smokes, this can cause environment to pollute and warm **[17].**

Figure 1.2 fusion and other welding for CU - SS connection

The accumulation and aggregation of undesirable materials that are deposited onto processing equipment surfaces is commonly referred to as fouling. Different types of fouling, including crystallization fouling, particle fouling, corrosion fouling, chemical reaction fouling, and solidification fouling on materials created, may significantly affect the surface's ability to perform the necessary mechanical properties of copper and stainless steel for what it was intended **[18].** because of that the welding joint area of SS - CU will come up with corrosion. Earlier than expected Corrosion causes equipment to fail in most engineering operations and commercial processes, which causes unforeseen issues. High maintenance costs, unscheduled shutdowns, and costly faults are some part of it **[19].**

For this reason, friction stir welding is one of the best materials joining mechanism for Aerospace, vehicle, manufacturing, electron-mechanical and shipping industries which gives less weight and corrosion resistance materials, so they are preferable welding methods for combination of dissimilar metals (SS - CU)

Tensile strength and hardness are crucial mechanical properties for welding joint mostly for dissimilar metals which is directly influence their corrosion resistance as well as materials strength, by optimizing the welding process parameters these properties will have better result than previous, then the overall corrosion performance of the welded component can be improved so do for materials strength too, as a stronger and harder weld zone typically exhibits better resistance to corrosive environments and recommended strength.

1.3 Objective of the study

1.3.1 General objective

General objective of this research is ''Experimental investigation of mechanical property in friction stir welding on (cu2-2.041 and ss-304l) dissimilar metal using Taguchi based (Gray relational analysis) GRA''

1.3.2 Specific objective

Specific objective, to come up objectives were identified.

- ✓ Prepare FSW tool (cylindrical ,Conical and square) shape from Tungsten carbide cobalt (WC-Co) for friction Stir welding process.
- ✓ Conduct FSW experiments with different process parameters, rotational speed, welding speed, dwell time and tool profile.
- ✓ Investigate mechanical properties of welded joints using destructive and non-destructive testing for hardness, tensile and micro-structural test.
- ✓ Evaluate the effects of pre welding heat treatment (annealing) on the resulting weld joint for both copper and stainless steel with 800 and 1000 °C for half an hour slow cooling.
- ✓ Determine the optimum parameter for FSW of dissimilar SS-304L & CU-2.04 Using the combined Taguchi and Grey relation analysis method L9 orthogonal, which has 3 levels and 4 Factors. e
- ✓ Validate the results by conducting confirmation test experiments from optimized final result.
- ✓ Confirmation test results by conducting Ansys software to examine the effects of dwell time and rotational speed between experiments Temperature and Transient Thermal Simulation Temperature difference and strain distribution on welding joint with Ansys and Abacus simulation.

1.4 Scope of the study

The study was limited to optimizing the FSW process parameters on (SS-304L alloy with CU-2.041 pure) different materials and only included the previously stated goals. The dimensions of the welding material is 110 x 50 x 5 mm with 5 mm thick. The butt joint configuration is the only joint configuration used in this thesis, and only experimental research into the joint's mechanical characteristics is included.

In addition the study using CNC milling machine while welding with a non-consumable tungsten carbide tool. Therefore, the goal of this research work was to have a successfully joint those material's using optimization tools and techniques to improve the weld material's hardness and tensile strength in order to overcome material failures including fouling, corrosion, and cracking.

The other task for this thesis is that before starting the FSW experimental method, the metals need only go through an annealing pre heat treatment procedure. Later, this research was limited to welding tools with pin profiles that were conical, square, and cylindrical. Ansys simulation is only being used to investigate the temperature differential between the experimental and simulation results.
Further mechanical characteristics of additional SS-CU alloys and composites, such as wear, toughness, brittleness, fatigue, corrosion resistance, impact strength, and other will not be covered in this study.

1.5 Significance of the study

The study's importance can be summed up by saying that it will provide a welding process adaption for long-term maintenance procedures for electrical and thermal products during their regular failures due to fouling, corrosion, and cracking. It facilitates the easy development of FSW setup on the CNC machine and provides a means of holding the work piece for local FSW practice. Adopt this method based on its advantages for welding different metals and the results of the trial.

The study is multifaceted in another sense. It will go over on future research activities about the FSW of various similar and dissimilar materials in an academic setting. It will provide scholars and industry sectors with some important information. Both the theoretical and practical parts of the subject are pertinent. Determine any gaps in the literature regarding FSW process parameter optimization is also another benefit of it.

When compared to FSW, it also offers a number of advantages over traditional welding. In the electrical and thermal manufacturing sectors, FSW is used to combine materials that are similar and dissimilar. Ethiopian industries do not have access to FSW machines, which are costly. It is not advantageous for small businesses, university labs, or anybody else to spend this much money on pricey FSW equipment. Therefore, by setting up CNC milling machines for small businesses, colleges, labs, and other establishments, the study contributes to the introduction of the possibility of the FSW process readily combining nonferrous material.

1.6 Research question

The study was to answer the following research questions:

- How can Preparing FSW tool pin profile (cylindrical ,Conical and square) shape from Tungsten carbide cobalt (WC-Co) for friction Stir welding process?
- Which type of process parameters can be used during conducted the FSW experiment to investigate the welding joint mechanical property?
- What is the most tool pin profile that affects the mechanical properties and micro-structure of welded joint?
- How does the addition of Heat treatment alters mechanical properties of the response during optimization processes ?
- Which optimization techniques are suitable for a multi-response study?
- How could be the result of mechanical properties and micro-structural observation of the welded joints validated?
- What kind of software simulation show the confirmation of experiments Temperature and Transient Thermal Simulation Temperature difference and strain distribution on welding joint overseen and validation?

1.7 Limitation and challenges of the study

Based on the existing demand in the thermal and electrical manufacturing sectors, the study only focused on dissimilar materials (SS-304L alloy with CU-2.041 pure). Another drawback of the study is that it failed to investigate the micro structure of the weld joint because the SEM machine was not operational when I intended to work.

1.8 Organization of the study

This study presents how (304L) stainless steel and (99% pure) copper materials can be welded to develop FSW adaptation in Ethiopian welding industry. The manuscript is organized into five chapters:

Chapter 1: It is an introductory part, which contains an introduction for the main part of the study, statement of the problem, the objective of the study, scope and limitations and significance of the study, methodology.

Chapter 2: Reviewed all research related to this research such as definitions of dissimilar metal welding using FSW, its Process parameters, non-consumable welding tool as well as tool geometry and tool pin profile reviews, previous researches correlated to Ss-Cu FSW results and others.

Chapter 3: Focused on the detailed explanation of materials used in the study and the methodology followed during the research work be used, dimension, design of experiment, mechanical testing, metallurgical analysis, and method of analysis.

Chapter 4: Delivers the outcomes of experimental studies. Meanwhile, it also gives a detailed discussion of the results and compares the experimental results in chapter 3

Chapter 5: Comprises conclusions of the study, recommendation, as well as directions of future works.

CHAPTER TWO
LITERATURE REVIEW

Introduction

This chapter presents a summary of the findings. of earlier studies and pertinent literature pertaining to the The friction stir welding process's parameters and related subjects involving dissimilar materials.

2.1 Overview of friction stir welding

In the solid-state welding method known as Friction Stir Welding (FSW), the name "stir" denotes the movement of the material in the form of plastic deformation, while "friction" refers to the application of frictional heat necessary for softening "BM." In general, FSW is a welding technique that makes use of heat generated by the tool-BM friction as well as the plastic deformation of BM brought on by the tool's stirring **[28].**

Innovative solid-state welding is FSW technology was was created by the Welding Institute (TWI) and patented in 1991 located in London, UK **[29].** It has a lot of potential for combining materials with radically different mechanical, chemical, and physical properties, such Cu and stainless steel, and high chemical affinity. According to numerous reports, unlike fusion welding, the mechanical characteristics and micro-structure of dissimilar materials generated with FSW are strikingly similar to those of the base materials **[30].**

It essentially consists of a rotating, non-consumable tool with a specially designed tool shoulder and pin profile, and materials stronger than the task The most important property is that it can fuse two different pieces together without melting.

The FSW technique can produce temperatures as high as 70 to 90% of the melting point of the material work piece **[31].** Just 5% of the heat produced by the friction flows into the tool; the bulk, or roughly 95%, is transported into the work-piece. Since FSW can connect any comparable or dissimilar metal, including copper and stainless steel alloys, with work-piece thicknesses ranging from 1-mm thin sheets to as thick as 75-mm thick blocks, it has been most successful in the soft metals sectors. More recently, FSW or its derivative methods have also been applied to additional alloy elements, including those based on magnesium, steel, ferrous, titanium, copper, and nickel **[32].**

High electrical and thermal conductivity materials, like copper (Cu) and staleness steel (SS), corrosion resistance, which makes it a popular choice for thermal and electrical applications. Different mechanical and metallurgical characteristics, such as melting temperatures, the linear thermal expansion coefficient, and thermal conductivity, make copper and stainless steel together a serious concern. Cu-SS dissimilar materials should be joined more easily since fusion type welding is not advised for those thermal and electrical conductors **[33].**

Materials, particularly staleness steel and copper alloys, permanently join for a distinct method. One of the more intriguing welding technologies is FSW.

2.2 Comparison between conventional welding and FSW

FSW is highly acceptably than other welding type such like MIG, TIG and FUSION literature survey indicated clearly that fusion welding has drawbacks of High heat sensitivity leading to distortion and warping, potential for poor weld quality due to different thermal conductivity, and the need for specialized filler materials and precise welding technique to achieve a strong, reliable joint **[27].** MIG often presenting less control and higher spatter compared to FSW and it less ideal for intricate welds on these materials.

Specific amount of time is needed in order for the temperature to rise to a suitable level. After that, the tool mixes the material by moving along the joint line. The quality of the weld is greatly influenced by process variables such axial force, welding speed, rotating speed, and tool dwell time **[34].**

The FSW method is widely used in many different industries, such as those that deal with copper, steel, aluminium alloys, and other non-ferrous metals, because of its bonding capacity **.**

By mixing materials with varying melting points, the FSW creates hybrid material constructions. It offers design versatility by combining materials with radically different thermal characteristics, such as steel and copper and also contributing to the development of different material functioning **[35].**

If soft material is positioned in the direction of tool rotation, better weld quality can be obtained **[36].** The FSW produces a weld that is more durable than traditional welding techniques because it operates at lower temperatures as compared to conventional welding, reducing the heat-affected zone **[37].**

2.2.1 Significance of FSW process

FSW has several advantages for the energy developing industry. Firstly, it produces high-quality welds without porosity, solidification defects, or cracking, and then FSW produces outstanding mechanical qualities, including high strength and fatigue resistance, in the welds.

This makes it ideal for different industry, which requires high-quality and high-volume production for many applications This process of joining materials is beneficial for humans, needs no consumables like (filler material, or fluxes) doesn't generate any harmful gases and its Metallurgical, environmentally and energy-efficient beneficial **[38],** as summarized in Table

Table 2.1: Metallurgical, environmental and Energy benefits of FSW **[39]**

Metallurgical benefits	Environmental benefits	Energy benefit
✓ Solid phase process ✓ Low distortion ✓ Good dimensional stability and repeatability ✓ No loss of alloying elements ✓ Excellent mechanical properties in joint area ✓ Fine recrystallized micro-structure ✓ Absence of solidification cracking ✓ Post FSW form ability	✓ Eliminate grinder request ✓ Minimal surface cleaning ✓ ✓ No harmful emission ✓ No shielding gas required ✓ Eliminate the solvent requirement ✓ Consumable material saving such as rugs, wire, or any other gases	✓ welded joints can withstand high temperatures ✓ Decreased fuel consumption in light weight automotive, aircraft, ship and others ✓ Improved material use joining different thickens allows ✓ shows a narrower HAZ ✓ reduces maintenance cost

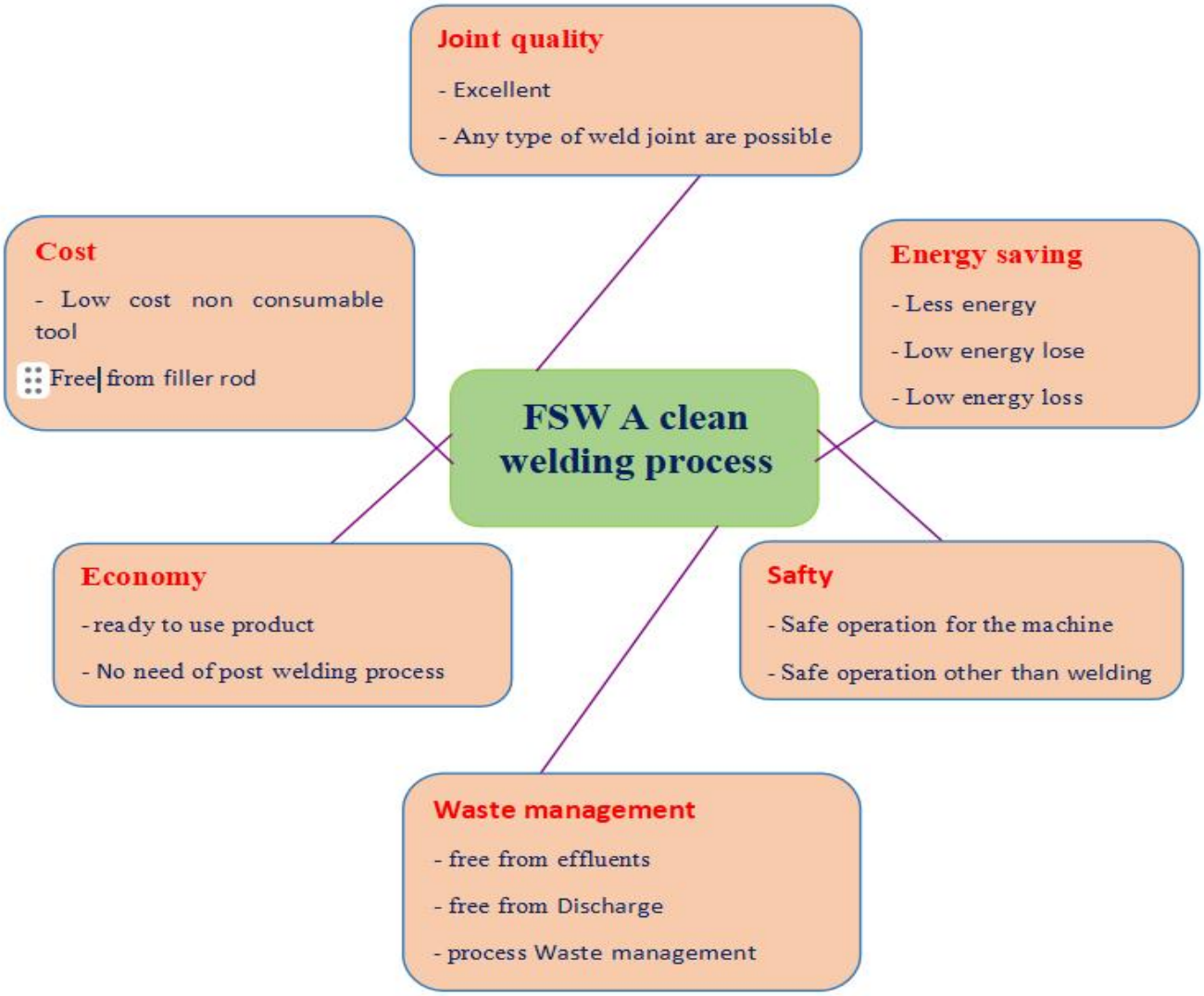

Figure 2.1 : Significance of FSW **[40]**

2.3 Dissimilar materials joining through FSW process

It was challenging to create a comprehensive system of governing equations for theoretically analyzing the behaviour of the friction stir welded joints because of the intricate geometry of some types of joints and their three-dimensional nature. Friction stir welding was a very complex process that involved multiple highly coupled physical phenomena. **[41],** examined friction stir welding, a relatively new solid state joining method that was extensively used to combine various metallic alloys in many industry domains. that are challenging for traditional fusion welding to weld.

The most recent advancements in numerical analysis, micro-structures welded joints, and friction stir welded structure attributes were examined in the article.

Additionally, numerical problems like failure criteria, meshing process, and materials flow modelling were covered. The application of FSW to the joining of dissimilar Cu alloy and stainless steel was demonstrated by their observations of seven distinct zones of the micro-structure in the welding: parent stainless steel, HAZ and TMAZ on the stainless steel on the advancing side of the weld, parent stainless steel, weld nugget, TMAZ and HAZ on the Cu alloy at retreating side of the weld, and parent Cu alloy studied on **[42].** The micro-structure revealed that the hardness of the weld nugget displayed variable values because of the presence of fine or coarsely distributed stainless steel particles on the weld nugget.

[43], examined how Al-Li alloys were most competitive or better than a composite-based design in an aircraft or space launcher, and how their remarkable strength and stiffness-to-density ratios contributed significantly to aeronautical components. Additionally, useful information regarding the processing window that leads to a successful friction welded joining of such alloys is suggested. In order to understand the effects of process parameters like temperature of the heater, rotational and traversal speeds, and the mechanical characteristics and the mechanical properties and the macro-structure of the joints.

According to the test's final results, the micro-hardness was high (112 VH0.098 and 16 VH0.024) close to the weld and reduced towards the parent material for both PMMA and AA 6061. Within the study review by varying the tool rotation speed from 500 to 1000 rpm and the traverse feed from 31.5 to 50 mm min–1, the mechanical properties of the dissimilar joint of Al Alloy (AA-6061) to PMMA (Acrylic) were investigated in **[44].**

2.4 Literature on adaptation of FSW process on milling machine

The modified milling machine successfully fully welds aluminium alloy AA 6082-T6 by FSW. **[45]** outlined a low-cost technique for converting a traditional milling machine into a basic FSW workstation. discussed procedure, which included installing equipment for measuring temperature and tracking downward and horizontal stresses, as well as designing tool fixing system.

An explanation of the process, a comparison to arc welding techniques, a discussion of welding tool design and materials, the impact of process parameters, work-piece materials, and joint geometries are some of the fundamental ideas pertinent to the usage and research of friction stir welding (FSW). **[46],** examined a few methods for adjusting vertical milling machines to accomplish FSW, a unique welding technology. Outlined the main uses of FSW in the shipbuilding, automobile, and aerospace industries and talked about their benefits. This parameter affects the configurations of the lap and butt joints.

2.4.1 Joint configuration of Fsw

The base material's position is a significant influencing factor for the dissimilar Cu-SS FSW system but does not matter in the comparable material FSW system. The quality of the welded joint during FSW is significantly influenced by the joint arrangement. Different joint configurations are affected differently by welding settings. Butt and lap joints are the most often used and appropriate joints on FSW. Corner joints, fillet joints, T-joints, pipe welds, and multiple lap joints are additional common joints **[47].** Advancement and retreating sides have a significant impact on material flow in the joint area **[48].**

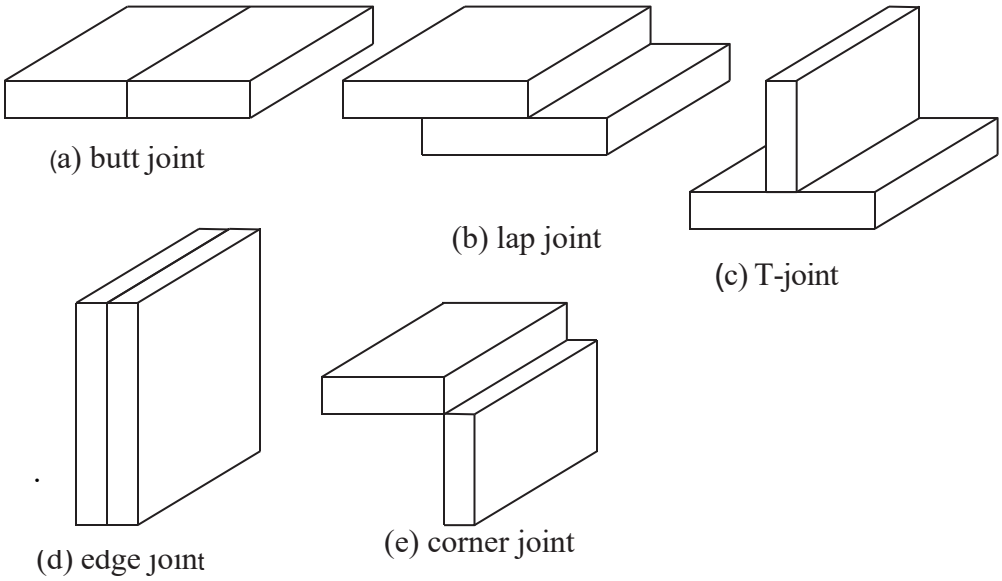

Figure 2.2 Five basic types of weld joint designs **[49]**

[50], discussed the latest advancements in FSW lap and butt welding, specifically the use of a Flared A-Skew TM probe and Trifle TM probe. Butt welds with MX-Triflute TM and Whorl TM frustum-shaped probes yielded satisfactory weld quality. Butt and lap joints are the two fundamental weld joint configurations used in FSW welding.

2.5 Welding defect of friction stir welding

Table 2.2 Welding defect on friction stir welding

No	Weld Parameters Defect Types	Rotational Speed	Travel Speed	Tilt Angle	Offset Location toward soft material	Fixing Soft Base Metal on (AS)	Main Cause
1	Micro Cracks	L	H	L	L	H	Insufficient heat & formation of IMC's **[51]**
2	Pores	H	H	L	L	H	Insufficient heat **[52]**
3	Voids & Tunnel	L	H	L	L	H	Improper mixing & pressure **[53]**
4	Fragment	L	H	L	L	H	Uneven materials flow **[54]**
5	Lack of Penetration	L	H	L	H	H	Short pin length **[55]**
6	Kissing bond	L	H	L	L	H	Insufficient material flow & oxide layer **[56]**
7	Hooking	H	L	L	L	L	Insufficient set-up Lap joint **[57]**
8	Surface Defects	H	H	L	L	H	Low heat & improper pressure **[58]**
9	Flash	H	L	H	L	H	Excess heat & improper pressure **[59]**

(H) High or increasing (L) Low or reducing

One of the main reasons why defects arise in FSW is low heat generation. By adjusting the process parameters and using the right tool geometry, the flaws can be fixed. Wormholes, kissing bonds, root sticking, incomplete fusion laps, and flash generation are examples of defects **[60].**

2.6 FSW Tool

The two components of the FSW tool are the probe and the tool body. The core of the friction stir welding method is tool technology. Weld size, welding speed, and tool strength are all determined by the geometry of the tool. Which materials can be friction stir welded is ultimately determined by the operating temperature, tool strength, and friction heating rate, all of which are influenced by the tool material **[61].**

The ideal tool shoulder diameter, which was calculated from this principle using a numerical heat transfer and material flow model, produced peak temperatures that are well within the typical range and the best weld metal strength in independent tests. Independent testing have shown that the ideal shoulder diameter of 18 mm at 1200 rpm produces exceptional tensile characteristics. **[62],** have also noted that, at a rotating speed of 1200 rpm, the tool with an 18 mm shoulder diameter produced the best weld joint strength, as seen in Table

Table 2.3 Mechanical properties of welds made using a cylindrical pin profile **[63]**

Diameter (mm)	Yield Strength (MPa)	Ultimate Tensile Strength (MPa)
15	110.5	131.7
18	130.3	161.7
21	94.0	120.0

Table 2.4 welding temperature range of various alloys **[64]**

Alloy Group	Temperature Range, ^{0}C
Aluminium alloys	440 to 550
Magnesium alloys	250 to 350
Copper alloys	600 to 900
Carbon and Low alloy steels	650 to 800
Titanium alloys	700 to 950
Stainless steel	600 to 875

Table 2.5 Tool materials used in FSW for soft alloys **[64]**

Tool Material	Work Piece Material
Mild Steel	Magnesium alloys
High Carbon Steel	Magnesium alloys
Stainless Steel	Magnesium alloys
Armour Steel	Magnesium alloys
AISI Oil hardened Tool Steel	Aluminium matrix composite materials
AISI 4140	Dissimilar Materials
Tool Steel	Aluminium alloys, Dissimilar Materials
High Speed Steel	Magnesium alloys
SKD 61 Tool Steel	Dissimilar Materials
H13 Steel	Magnesium alloys
High Carbon High Chromium Steel	Magnesium alloys, Aluminium matrix composite materials, Dissimilar Materials

The experimental investigation of the three pin geometries (threaded cylindrical, threaded conical, and pyramidal) demonstrates how tool geometry affects material flow and mechanical properties of Al-Cu bimetallic sheets that were friction stir welded using three distinct pin profile types **[65].**

The threaded conical tool yielded the highest weld strength and the fewest flaws because it offered the best compromise between the various material flow zones. Because of the micro-void on the retreating side, the joint efficiency of welding on Al-Cu bi-metals can never be 100%. In terms of weld strength and soundness, the conical threaded pin produces the best results.

[66], the impact of tool shape and weld arrangement on the mechanical characteristics and micro-structures of Al 6082 alloy FSW joints was examined. In the studies, three distinct kinds of tools with various shoulder surfaces and probe shapes were employed, along with two different weld configurations (one-sided and two-sided). Show how the form of the tool used in the FSW process affects the mechanical properties of the joints, and how the two-sided welds had poorer mechanical qualities because of increased heat transmission into the material during the second pass.

For the same number of FSW plunges and passes, the coated tool pin shrank significantly less in size than the uncoated tool pin. When the AlCrN coated FSW tool was being characterized and assessed, this study was examined by **[67].**

Using the cathode arc PVD coating process for welding structural materials, test several metallurgical hard coatings for FSW tools. The weight loss of the AlCrN-coated sample was approximately 87% lower than that of the untreated sample, demonstrating better wear resistance.

[68], introduced a technology called Tool Assisted Friction Welding (TAFW), which is related to friction stir welding (FSW). Mechanical testing made it possible to evaluate the plastic qualities and weld strength by acquiring strain data using Digital Image Correlation (DIC). Demonstrate that the TAFW process allows for extremely fast welding speeds, minimal tool wear and damage, and very good quality welds whether or not galvanized coating base materials are present. Unlike FSW, welding does not include the intermixing of basic materials.

[69], created the new dual-rotation bobbin tool friction stir welding (DBT-FSW), in which the rotational rates of the upper shoulder (US) and lower shoulder (LS) varied. Determine that the DBT-FSW can create defect-free joints across a greater range of welding conditions and has outstanding process stability.

[70], examined how the tool's rotational speed affected the friction stir-welded Al-B4C MMCs' mechanical and micro-structural characteristics. The results of an investigation by [84] demonstrate how the tool's spinning speed affects the weld joints' mechanical and metallurgical characteristics. Better mechanical qualities were noted in the joint that was welded with a tool rotation speed of 1000 rpm. suggests using a moderate tool speed (RPM) to achieve one pass welds free of defects. The micro-structure analysis showed that the weld nugget had fine re-crystallized equated grains as a result of significant plastic deformation and frictional heating.

An further study that is displayed in **[71],** examined the impact of welding parameters and tool pin profiles. To determine the optimal parameter among the ones chosen, test the tensile strength. When employing specific welding settings, the threaded straight cylindrical pin profile is appropriate for good welding.

[72], examined the shoulder in conjunction with different polygonal pin profiles for friction stir welding (FSW) 6082 aluminium alloy. Lastly, radiography and sectioned macro and microscopic observation were performed on welding joints in order to comprehend the intricate marking material flow. During the diving phase, the polygonal pins lessen the initial force needed.

The full mixing of the material on both AS and RS was responsible for the superior mechanical qualities of the welds produced with the (TR) S tool, which had a UTS of 199 MPa and a hardness of the stir zone of about 78.4 HV. Due to the fact that diffusion by the former austenite grain boundaries is significantly faster than diffusion by volume, an inter-metallic compound is formed inside the tool's metal during FSW of AMg5M aluminium alloy. The latter covers the tool's working surface, and iron/aluminum reaction diffusion is then initiated under high mechanical stress and temperature conditions. Diffusion-controlled wear mechanism of alloy steel friction stir welding (FSW) tools on aluminium alloy was presented in **[73].**

The development of a stationary FSW tool for welding thin plates of different polymers was explained in **[74].** developed FSW instruments with the goal of friction stir welding incompatible polymeric materials in a lap joint arrangement in a sound and durable manner.

In a separate paper, the joints of various tool pin profiles—such as straight cylindrical, taper cylindrical, triangular, square, trapezoidal, and hexagonal tools—with varying axial forces, welding speeds, and rotating speeds were examined. Tool shoulder-to-pin diameter ratios are crucial for the formation of stir zones, according to the literature review. The length of the pin is marginally less than the thickness of the part, and its diameter is the same as the thickness of the sections that need to be welded. Weld quality, tool wear, and performance are impacted by the qualities of the tool material, including strength, fracture toughness, hardness, thermal conductivity, and thermal expansion coefficient.

The (I) pin and (II) shoulder are the two fundamental components of the FSW tool. Shoulder diameter, shoulder surface angle, pin geometry (including size and shape), and tool surface characteristics are important components of these parts **[75].** HSS tool steel, a versatile chromium-molybdenum hot work steel that is frequently used in hot work and cold work tooling applications, is the most advised tool material for the FSW process. For FSW of different SS−Cu, the tool material and its properties are crucial **[76],** Throughout the FSW process, tool geometry and characteristics shouldn't change.

Strength at atmospheric and elevated temperatures, stability at elevated temperatures, micro-structural homogeneity, wear resistance, fracture toughness, machine-ability, tool reactivity, and sufficient density are all critical properties needed for tool material in order to perform successful welds. Aside from the user's personal preferences and experiences, two crucial factors in choosing the tool material are the work-piece material and the intended tool life **[77].**

2.6.1 Tool design

The flow of plasticized material and localized heating in the stirring zone (SZ), which have a major impact on defect development and post-weld mechanical properties, are both greatly influenced by tool design, which is a crucial component of FSW. The following are the two key features of FSW tool geometry:

To save money and time, its shape should be as straightforward as possible.

- It should be able to produce an adequate stirring effect to produce sufficient material

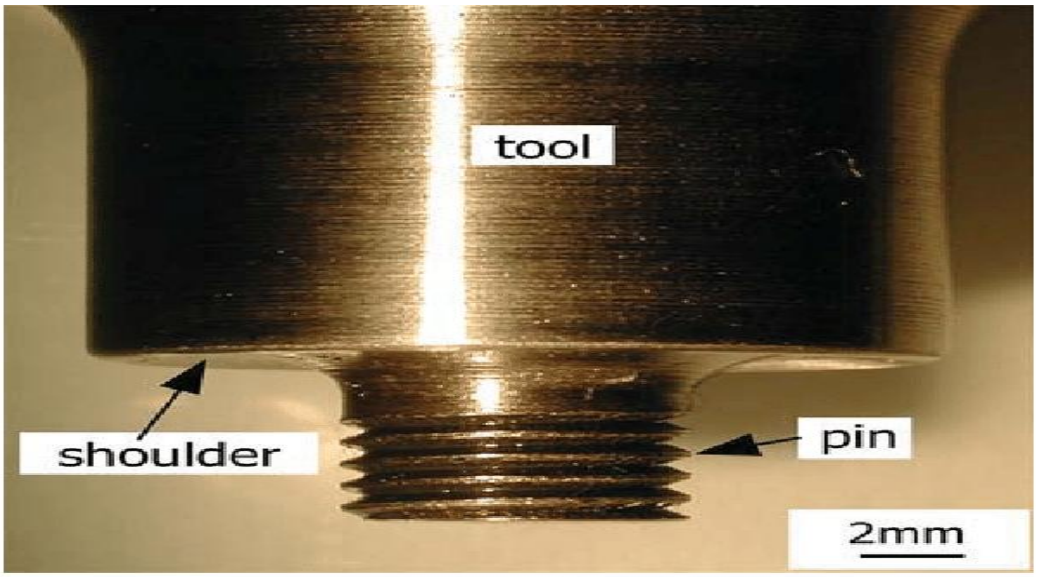

Figure 2.3 Parts of friction stir welding tool **[78].**

2.6.1.1 Tool shoulder

The welding quality is influenced by the shape of the shoulder outer surface because the shoulder plunge depth is small, which is (1-5%) of the work-piece thickness. Generally Tool shoulders are employed to provide the downward forging action required for welding consolidation and to prevent the hot metal behind the bottom shoulder surface. In the FSW process, The tool goes forward, pushing additional material into the hollow under the shoulder. FSW tools are made to produce enough heat through tool-BM friction and BM plastic deformation, as well as to achieve efficient material flow. The tool's shoulder and pin are its two primary components.

For this shoulder to function properly, the tool must be tilted 1 to 30 degrees from the work piece's regular direction of travel. In addition to a constant of 7.3 mm, the shoulder diameter is 2.2 times the thickness of the work piece. Since a greater shoulder diameter is needed to generate the heat, a greater energy input is required as thickness increases, making this relationship logical. Likewise, the probe width is equal to 0.8 times the sample thickness plus an additional 2.2 mm constant. But three is the most commonly employed shoulder-to-probe diameter ratio. Tool plunging involves feeding the material into the tool shoulder cavity from the concave shoulder at a slight angle (6-100) to the flat shoulder end surface.

Therefore, the concave surface profile of the tool shoulder acts as the escape volume or reservoir for the material that has been displaced by the probe. As downward pressure is applied to the tool, the material behind it undergoes a forging action due to the displaced material held in the concave shoulder profile.

2.6.1.2 Tool shoulder diameter, D (mm)

Due to the huge contact area, the tool shoulder diameter has a direct proportionality to the heat generated by friction, which is considerable **[78].** The shoulder generates heat through frictional sticking and sliding of the material beneath it, while friction and plastic deformation of the material generate heat in FSW.

The broader contact area, wider TMAZ and HAZ regions, and higher axial pressure required by the larger tool shoulder diameter of 21 mm result in a decline in the joints' strength characteristics. Because of the narrower contact area and less frictional heat generation caused by the smaller tool shoulder diameter of 9 mm, the weld metal consolidation is poor in the FSP region, which ultimately leads to the lowest strength attributes. The impact of the FSW process and tool parameters on the tensile strength characteristics of 7075 AA-T6 materials with butt joint configurations is demonstrated in accordance with **[79].**
Five distinct tool shoulder diameters—9, 12, 15, 18, and 21 mm were employed, According to the Article Review, the joint made utilizing a tool with a 15 mm shoulder diameter demonstrated a tensile strength of 373 MPa and a hardness of 203 HV. were an effort to comprehend how tool shoulder diameter and tool pin profile affected the creation of friction stir process zones on (300*150*6 mm, L*W*T) of 6061 AA materials with butt joint configurations **[80].**

They employed set and regulated parameters. Axial force of 7 KN, traverse speed of 75 mm/min, and tool rotational speed of 1200 rpm are among the adjustable parameters.The joints have been fabricated using fixed parameters like the tool's D/d ratios of 2.5, 3.0, and 3.5, a pin length of 5.5 mm, tool shoulder diameters of 15, 18, and 21 mm, pin diameters of 6 mm, and five distinct tool pin profiles: straight cylindrical, tapered cylindrical, cylindrical threaded, triangular, and square. According to the paper's findings, employing a square pin shaped tool with an 18 mm shoulder diameter produces welds with the highest tensile strength and no defects.

Table 2.6 Summary of tool pin profiles for different FSW/FSP systems

Pro	System and work piece material	Pin design/ profiles	Remarks/ Recommended pin design	Ref.
FSW	AA5083	Square and cylindrical	Square profile produces finer grain structure and higher tensile strength due to eccentricity, larger stir zone and higher temperature	**[81]**
FSW	Pure copper	Triangular, square, pentagonal and hexagonal	Square pin profile gives better mechanical properties due to more pulsating effect with 1.56 dynamic to static ratio	**[82]**
FSW	Al−10%TiB_2 metal matrix composite	Square, hexagonal, octagonal, tapered square and tapered octagonal	Straight square pin profile provides better mechanical properties	**[83]**
FSW	Dissimilar AA5083-H111 and AA6351-T6	Square, hexagonal and octagonal	Square pin gives highest tensile strength	**[84]**
FSW	Dissimilar AA5052-H32 and HSLA steel	Conical and cylindrical	Lesser taper angle 10° produces maximum tensile strength	**[85]**
FSW	AZ31B Mg	Cylindrical, taper, threaded cylindrical, square, triangular	Threaded cylindrical pin provides highest tensile strength	**[86]**
FSW	Dissimilar AZ31Mg and steel	Pin length variations	Shorter pin length gives better tensile properties	**[87]**
FSW	AZ31B-H24 Mg	Cylindrical pin (left hand thread and right hand thread orientation)	Left hand thread orientation produces superior properties	**[88]**

2.6.1.3 Tool pin

In the FSW process, friction stirring pins are important for material flow. The purpose of the pines is to break up the work-piece's fraying surface. Heat-treated tungsten carbide tool steel with pin profiles such a threaded pin, square, cylindrical, and cylindrical grooved with a concave shoulder was utilized to make the tool **[89].**

Concave shoulder profiles were suggested for the dissimilar Cu-Ss FSW system. For different Cu-Ss FSW systems, a cylindrical tool pin profile is advised rather than a tapered one. Additionally, they noted that a larger shoulder diameter results in a higher plunge load with adequate heat, which aids in the removal of internal joint problems. Additionally, the characteristics of various friction stir welding and processing (FSW/P) regions are greatly influenced by the tool pin design.

Additionally, the polygonal pin profiles play a significant part in altering the FSW/P region's characteristics. Because of its pulsing impact, the square tool pin profile yields higher attributes for comparable FSW systems. To the best of the author's knowledge, there haven't been many studies done on tool pin design for different Cu-Ss systems. Studying how pin designs affect the characteristics of the different Cu-Ss FSW system is therefore worthwhile. It was clarified how various pin profiles—such as square, hexagonal, cylindrical, and triangular—as well as pin diameters affected the characteristics of dissimilar FSW.

2.6.1.4 Pin length (mm)

The study states that the pin length needs to be less than 0.3 mm in comparison to the thickness of the base metal. At this length, the root was good and the shoulder reached the surface **[90].**

The pin length selection is one of the most important aspects of the FSW tool design. If the pin length is the same as base metal's thickness and the welding will not work. In order to prevent the shoulder from touching the surface and producing heat, the pin may come into contact with the support plate or it may produce material congestion.

2.6.1.5 Pin diameter, d (mm)

studied the design and characteristics of FSW tools and found that, for sheet thicknesses ranging from 1 to 8.3 mm, the pin diameter is closest to or equal to the work-piece thickness. Furthermore, unless the stirring process involves thick plate welding, the minimum pin diameter is around 3 mm.

A weld free of defects is achieved when the pin diameter is between 8 and 13 mm. The impact of the FSW tool design on the mechanical properties of as-welded AA2198 (T3)-AA2024-(T3) joints was discussed in **[91].** Therefore, one of the most important variables influencing the joint metal's tensile strength and the weld cross-sectional area was the pin diameter. This is because the pin action is mostly responsible for the stirring in the weld. **[92],** they claimed that 0.8 * plate thickness (mm) +2.2 yields the maximum outer pin diameter, whereas 0.5 * plate thickness yields the minimum pin diameter.

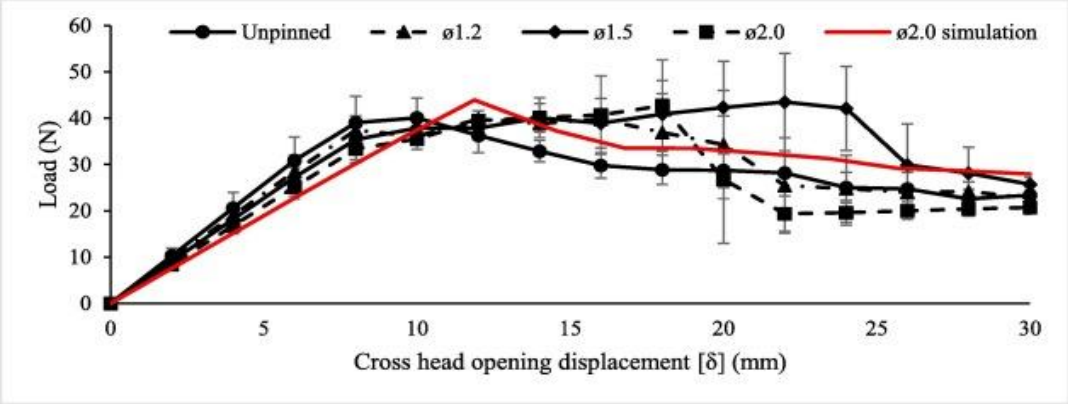

Figure 2.4 : Used pin diameter versus sample thickness **[92].**

2.6.1.6 Tilt angle

It is the angle formed by the normal line to the work-piece surface and the tool axis. The rate of heat generation, material movement, and consolidation of the flowing material behind the tool pin are all greatly impacted. As the tool tilt angle increases, so does the tool's axial force and peak temperature. Figure illustrates the tool's rotational axis's angle or inclination with relation to the work-piece surface.

Tilt angle has an impact on material flow, frictional heat generation, and the consolidation of flowing material around the tool in the FSW process. The peak temperature rises with the tool tilt angle when the tool applies vertical force.

This tilt angle of the tool helps keep the flowing material from leaking out during the FSW. To attain sufficient downward power, angle the tool slightly and adjust the plunge depth such that the tool completely penetrates the weld **[93].** The welds are free of defects due to the high tool tilt angle of about 3o. As the temperature rises and more material is plasticized as a result of the high tool tilt angle, the tool must carry more material.

The tensile strength of the welded specimen also grows as the tool-tilted angle does. Tensile strength of welded joints using 3o-tilted tools is more than that of 1.5o-tilted tools, and 0o-tilted tools is greater than 1.5o-tilted tools

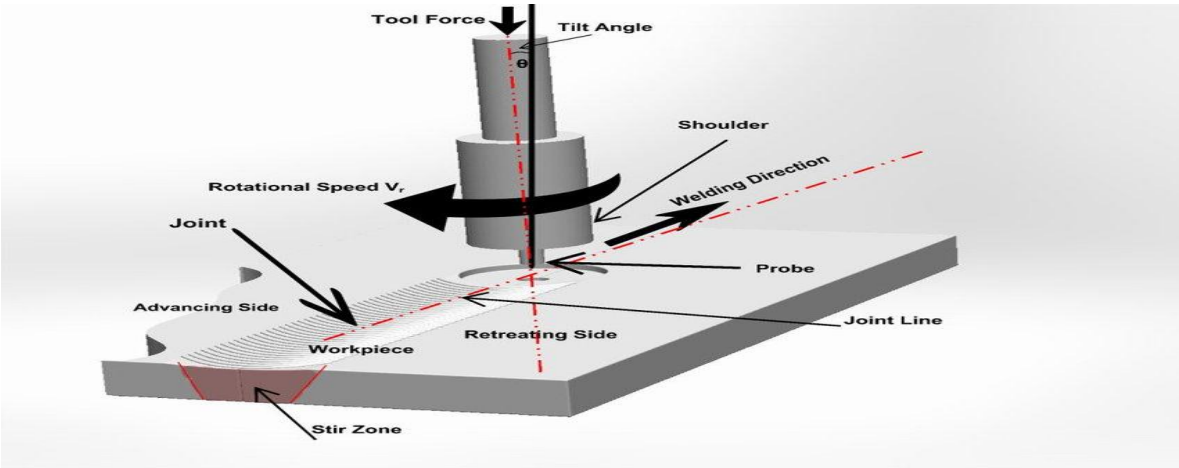

Figure 2.5 : Tool tilt angle of FSW **[94].**

The high tool tilt angle of around 3° offer defect-free welds. Due to the high tool tilt angle rise temperature and more material is plasticized, so the tool has to carry more material along with it. In addition, the tool-tilted angle increases the tensile strength of the welded specimen increases. The tensile strength of welded joints with 3°-tilted tools is more than 1.5° tilted tool and tensile strength of welded joints with 1.5° tilted tool is more than 0°.

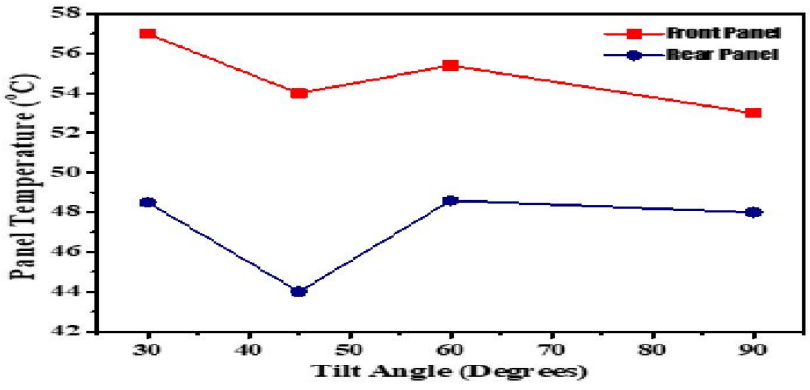

Figure 2.6 : Temperature on advancing and retreating side at a different tool tilt angle **[95].**

2.6.1.7 Tool material

Tool material is crucial in establishing the suitability of a tool for welding a particular material. A good tool material must have the following characteristics:

- Good strength and wear resistance at an elevated temperature for bearing high plunging forces,
- Good dimensional stability for repeated use,
- Good coefficient of friction with the work-piece for the adequate generation of frictional heat,
- Non-reactive with oxygen and work-piece material,
- Good machine ability for making complex geometry,
- Hot hardness should be high enough to complete long weld and
- Cost-effectiveness and others **[96].**

There are many materials are available for different materials and applications. Those are mentioned in the below table: et al.).

Table 2.7 Types of FSW tools and materials joined **[96].**

№	Tool materials	Materials welded	Characteristics
1	HC HCr	AA5083-H111 Al alloy and Magnesium alloy	High wear resistance.
2	SS310	Commercial grade Al-alloy 6 mm thick and Magnesium alloy	Very high corrosion resistance.
3	H13	AA5754 and C11000 copper 3.175 mm thick	-
4	HSS	AA2011, AA6063 alloys10 mm thick and Magnesium alloy	High wear-resistant.
5	C40	AA6082 and AA2024 4 mm thick	-
6	H13	6061-T6 Al and AISI 1018 mild steel 6 mm thickness and Magnesium alloy	Shock and abrasion resistance combined with red hardness.
7	SKD61 tool steel	For dissimilar materials	Good thermal fatigue resistance
8	Armour steel	For Magnesium alloy	-
9	Mild Steel	For Magnesium alloy	-
10	AISI oil hardened tool steel	For aluminium matrix composite materials	-
11	AISI 4341	Widely used for Al, Mg, Cu, Al-/Mg- MMC	Good elevated temperature strength.
12	PCBN	Cu, Ti, Ni alloys, steel, and Al-MMC	Chemical stability, excellent wear resistance at elevated temperature.

2.7 Process parameter for friction stir welding

2.7.1 Travel speed

Both the micro-structure and junction quality are significantly impacted by welding speed. The choice of welding speed for FSW of dissimilar metal (SS-Cu) is a challenging problem **[97].** During FSW at varying speeds, uncertain effects on welding qualities are seen **[98].** A number of factors, including work-piece material, rotational speed, joint type, and penetration depth, must be taken into account because welding speed is crucial **[99].**

The impact of FSW travel speed process parameters on various materials with a butt joint configuration is examined by **[100].** They employed three levels of three parameters: axial force of 2, 3, and 4 KN, traverse speed of 22, 40, and 75 mm/min, and rotating speed of 1000, 1200, and 1400 rpm. As a result, the maximum tensile strength of 151 MPa at a traverse speed of 40 mm/min with a rotational speed of 1200 rpm and a lower tensile strength of 110 MPa at a traverse speed of 22 mm/minutes while rotating at 1000 rpm.

[101], as per the revised article the Optimization of FSW process parameters on a 6 mm 6061 aluminium alloy using butt joint configurations in an attempt to increase the joint strength. With traverse rates of 30, 35, and 40 mm/min and tool tilt angles of 0, 1, and 2 degrees, they have taken three distinct rotating speeds: 1000, 1500, and 2000 rpm. At 30 mm/min, the traversal speed and a rotation speed of 2000 rpm, they achieved the maximum tensile strength of 132 N/mm2.

Weld flaws are brought on by the formation of different flow stresses during the FSW of SS-Cu. Therefore, determining the ideal welding speed level is essential for managing the flow stress differential. The relationship between welding speed and rotational speed determines how much heat is needed in FSW of SS-Cu to avoid the development of IMCs and other mechanical features.

Numerous flaws created during the welding process have an impact on the mechanical, micro-structural, and weld quality of friction stir welding. One of the main reasons why defects arise in FSW is low heat generation. By adjusting the process parameters and using the right tool geometry, the flaws can be fixed. Tunnel, flash, kissing bond, void/wormhole, cavity/groove, and crack faults are examples of friction stir welding flaws **[102].**

2.7.2 Tool rotational speed

One of the crucial factors that must be carefully chosen to achieve a weld free of defects is the tool's rotational speed. It involves mixing or stirring the materials around the spinning tool pin. The welding process is finished when the tool traverses the pin, moving the softened material from the front to the back. The impact of welding speed, rotational speed, and Friction Stir tool form was investigated **[103].** Butt joint designs are used in the welding of Cu and AA 6061 materials.

A vertical milling machine serving as an FSW machine was used for the experiment. Using traverse rates of 10, 15, and 20 mm/min and tool rotational speeds of 2250, 2500, and 2750 rpm, various samples were produced. The maximum tensile strength of 127.7 MPa was thus determined using a tapered pin tool geometry, a rotating speed of 2750 rpm, and a traverse speed of 15 mm/min. Likewise, a square tool pin shape, a traverse speed of 20 mm/min, and a rotation speed of 2500 rpm were found to yield the lowest tensile strength of 34.6 MPa.

The purpose of the shoulder is to keep plasticized material from escaping the weld and to provide the work-piece with extra frictional heat. The metal's strength at the point where the rotating tool and work-piece contact diminishes below rises with temperature.

Plasticized material is created to be extruded from the tool's advancing side to its retreating side when the metal's strength diminishes below the applied shear stress at the point where the rotating tool and work-piece contact reduces.

[104], examined the optimization of FSW process parameters on aluminium alloy 6061-T6 material with a butt joint configuration. Tool tilt angles of 0, 1, and 2 degrees were measured, along with traverse speeds of 20, 40, and 63 mm/min and rotational speeds of 450, 560, and 710 rpm. They discovered that at 560 and 710 rpm, with values of 230 MPa and 55.33 HV, respectively, the highest tensile and hardness strength with a defect-free union was achieved.

2.7.3 Tool Pin Profile

The tool pin profile's main job is to control the movement of the material. The flow of plasticized material is strongly influenced by the type of tool pin profile **[105].** to build the joints, they employed five distinct tool pin profiles, including square, triangular, tapered, cylindrical, and straight pins with shoulder sizes of 15, 18, and 21 mm.

The axial force, traverse speed, and tool rotating speed are 7 KN, 75 mm/min, and 1200 rpm, respectively. The study's findings shown that, in comparison to other tool pin profiles, square pin profiled tools with an 18 mm shoulder diameter provide a maximum tensile strength of about 190 MPa and a defect-free union. **[106],** examined the impact of mechanical characteristics and tool pin profile on a 6 mm plate made of different materials with butt joint configurations.

2.7.4 Dwell time

The amount of time that passes after the tool is inserted and before the welding process starts for the temperature of the tool and work-piece to stabilize, or the amount of time that the tool plunges into the weld material at the appropriate depth and rotating speed without translation motion **[107].**

Dissimilar friction stir spot wedding's mechanical characteristics and evolution across dwell times of 4, 8, and 12 seconds. After studying the impact of dwell time on micro-structure, they came to the conclusion that a longer dwell time can result in a greater peak temperature and vice versa **[108].** impacts of process variables on friction stir spot welding of aluminium alloy materials at 5, 10, and 15 mm/min with dwell times of 1, 5, and 10 seconds. The study was carried out using the sited article because they came to the conclusion that dwell time had a greater impact on joint strength than dive speed **[109].**

2.7.5 Tool geometry effects on FSW joints

Work-piece sizes, tool design and material, and standard process parameters were all included. The study of **[110],** on its review also provided a brief description of the numerical analysis of the FSW process and tool geometry influence. Four distinct pin profiles—threaded cylindrical, squared, triangular, and straight cylindrical—were used to demonstrate the impact of tool geometry on polyethylene-polypropylene dissimilar friction stir welding. The results showed that the tool with the threaded cylindrical pin had better mechanical properties for the welded joints than the tools with the squared, triangle, and straight cylindrical pin shapes, respectively. The results showed that at a low traverse speed of 8 mm/min, the stir zone's fluidity increased, leading to the formation of a non-uniform layered micro-structure. **[111],** is the other significant study.

Table 2.8 Tool design and material effects of tool geometry on FSW **[110]**

Material	Advantages	Disadvantages	Applicable Temperature Range	Applicable Welding Materials
Tool steel	Good machinable; cheap; high strength	Easy to tear	<500 ˚C	Aluminium alloy; magnesium alloy
High-temperature alloys	High strength; high toughness; high temperature resistance	Expensive	<900 ˚C	Copper alloy; titanium alloy; steel
Tungsten alloy	High strength; high temperature resistance	Difficult to process	600–800 ˚C	Aluminium alloy; magnesium alloy; titanium alloy; steel
PCBN	Good high temperature stability; high hardness	Expensive; Difficult to process	800–1000 ˚C	Wear-resistant material

2.7.6 Taguchi method

The selection of control parameters is the most crucial step in experiment design. **[112].** In order to create high-quality goods with minimal development and manufacturing parameter design, robust design is an engineering methodology that aims to establish product and process conditions that are least susceptible to the many causes of variation. It provides a straightforward and methodical way to optimize design for cost, quality, and performance.

The references **[113],** include a list of some of the earlier studies that employed the Taguchi technique as a tool for designing experiments in a variety of fields, including metal cutting. In order to detect non-significant variables as soon as feasible, as many components as possible should be included. Taguchi divided components and parameters into two categories: fixed factors and changeable factors.

2.8 Friction stir welding Application

FSW is regarded as the most important advancement in metal joining in the past ten years. The primary benefit of FSW is that it is a "green" technique because it is environmentally friendly and energy-efficient, using just around 2.5 percent of the energy required for laser/electron beam welding and Since FSW avoids melting and re-solidification, solidification flaws are minimized **[114].** Numerous industries, such as aerospace, shipbuilding, railroads, automobile, etc., have used FSW. Incorporating as many elements as feasible would allow for the identification of non-significant variables at the earliest opportunity.

2.8.1 Stainless steel for heat exchanger

An iron alloy that resists corrosion and rusting is called stainless steel. In order to get additional desired qualities, it may also incorporate non-metals such carbon and at least 11% chromium. When exposed to oxygen, stainless steel's chromium forms a passive coating that can protect the material and cause it to self-heal its resistance to corrosion **[115].**

These days, heat ex-changers come in a variety of materials. The function and service life are determined by the choice of material. Because of this, it needs to be given particular consideration right away. Here, stainless steel has shown itself to be an especially dependable and long-lasting material. Stainless steel heat ex-changers are especially resistant to corrosion, and they reduce the amount of limestone and other residue deposits. For more than 50 years, stainless steel has been the only material used in vessel heat ex-changers.

The melting point of stainless steel, like that of the majority of alloys, is not a single temperature but rather a range of temperatures **[116].** The range of temperatures is 1,400 to 1,530 °C. There are more than 150 recognized grades of stainless steel, with 15 being the most widely used. Stainless steel and other steels, including US SAE steel grades, are graded using a variety of processes **[117].**

The material utilized faces significant challenges from mechanical impacts such vibrations, steam hammers, and high pressure inside the devices. For instance, deposits and corrosion from limestone or other leftovers are very crucial **[118].**

If not taken into account, they raise the heat ex-changer's maintenance needs. Since every maintenance procedure is expensive and frequently results in the system's partial or whole failure, the maintenance interval should be shortened initially, and the most durable material should be selected.

2.8.2 Copper for heat exchanger

Copper provides a lot of advantageous qualities for long-lasting and thermally effective heat ex-changers. First and foremost, copper is a very good heat conductor. Heat may move through copper rapidly because of its high thermal conductivity. 231 Btu/ (hr-ft-F) is the thermal conductivity of copper. Except for silver, which is a precious metal, this is higher than any other metal. Compared to stainless steel, copper has over 30 times the heat conductivity and a 60% higher rating than aluminium **[119].**

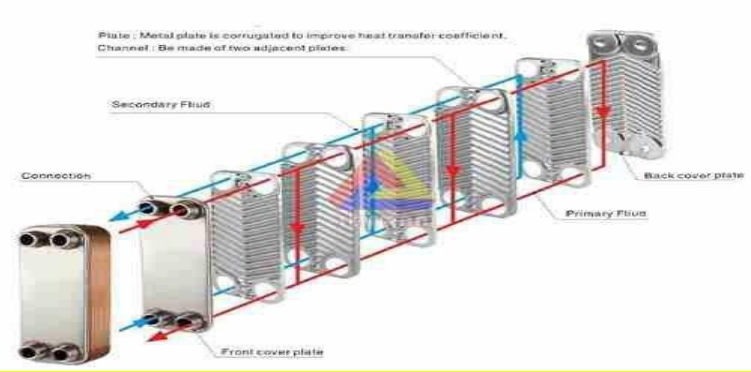

Fig. 2.7 Ss - Cu plate assembly through heat ex changer

Copper's combination of these qualities makes it suitable for use as heat sinks to cool computers, disc drives, televisions, computer displays, and other electronic devices, as well as heat ex-changers in industrial buildings, HVAC systems, and automobile coolers and radiators **[120].**

2.9 Application of FSW for heat exchanges

Many industries, particularly the cooling sector, have made extensive use of friction stir welding (FSW). FSW is frequently utilized in cooling applications to connect cooling plates and heat ex-changers, which are in charge of removing heat from machinery. The FSW technology may create robust, superior welds in cooling plates, which can lower energy consumption and improve cooling system efficiency. The ability to create welds with little distortion, which guarantees that the cooling plates keep their homogeneity and flatness, is one of the fundamental advantages of employing FSW in cooling applications.

Expermental process parameter flow chart of SS - CU FSW process

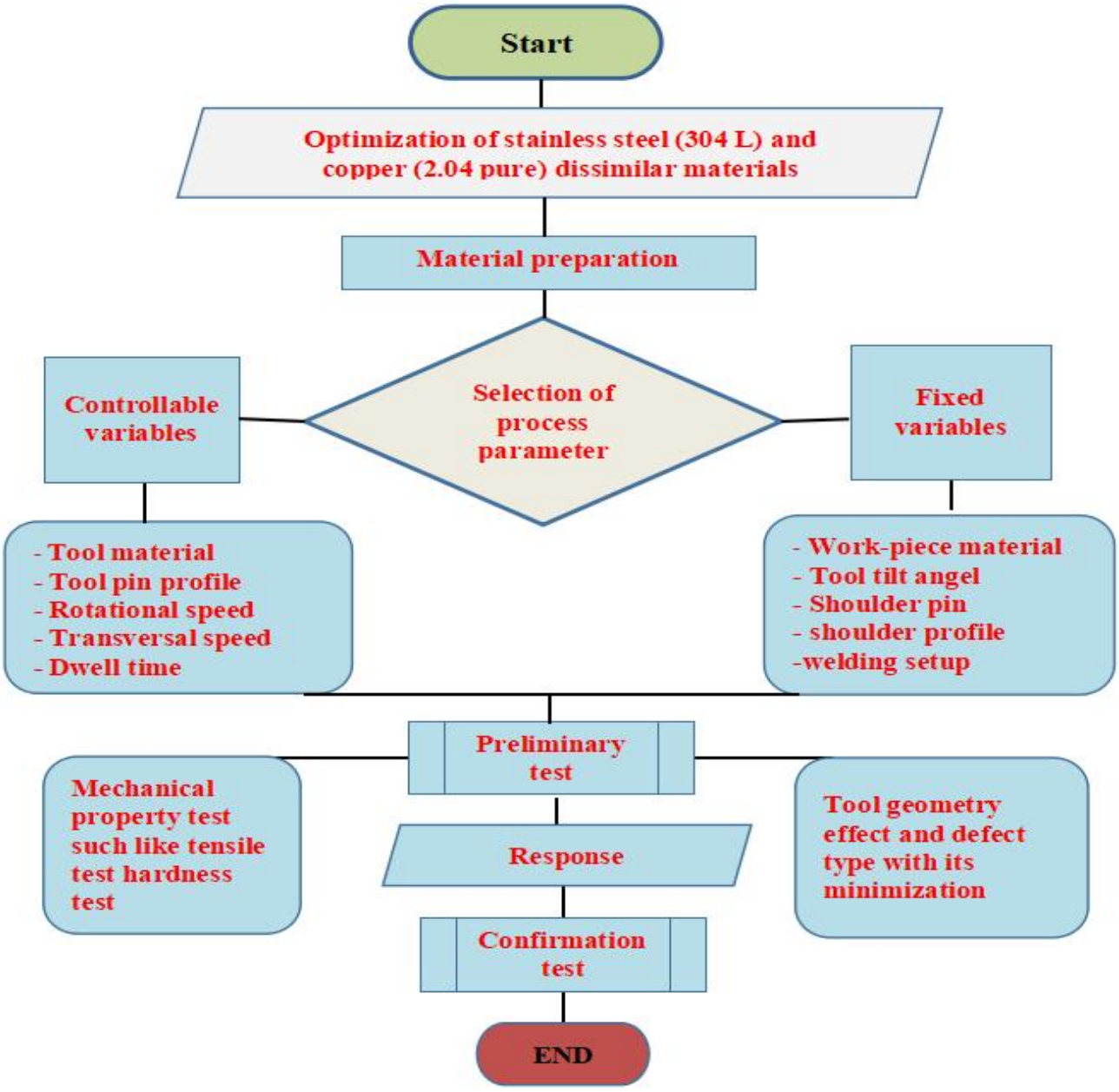

Figure 2.8 process parameter flow chart of SS - CU FSW process **[121]**

2.10 Reviewed Gap on the similar research title

In this study, gaps in the present research are identified requiring further research as follows:

- Due to the metallurgical difference in dissimilar metals like SS - CU during FSW its difficult to join them so, to maximize the weld-ability of those metals pre heat treatment process should be under go before the welding process The impact of heat treatment conditions before welding on the mechanical characteristics of FSW joints has not been extensively studied. This experimental investigation can be expressed in terms of it's relevance, as it will give a piece of information for future study.

- According to some other studies with similar thesis most review shows that travel speed, rotational speed and other process parameters where examined for SS-304L & CU-2.041 of dissimilar metals but, the effects of dwell time with the comparison in between experimental with software analysis was not validated adequately studied.

- Only a few studies on the optimization of FSW on SS-304L AND CU2.04 alloys in the form of pipe and rood structure have been found, However, in this instance, the study focused on plate type structure with but joint configuration, so in order to improve the FSW process parameters, this research will further examine and evaluate them.

- Finding an environmentally acceptable production choice is crucial because emissions and smoke from fusion welding have been shown in recent research to contaminate and warm the environment. These days, environmental pollution and global warming are major concerns. Friction stir welding is therefore one of the greatest methods for connecting materials.

CHAPTER THREE
MATERIALS AND METHODS

3.1 Research methodology

The following conceptual frameworks are used in the thesis structures to accomplish the predetermined objectives of this chapter, which offers comprehensive details on the tools and materials.

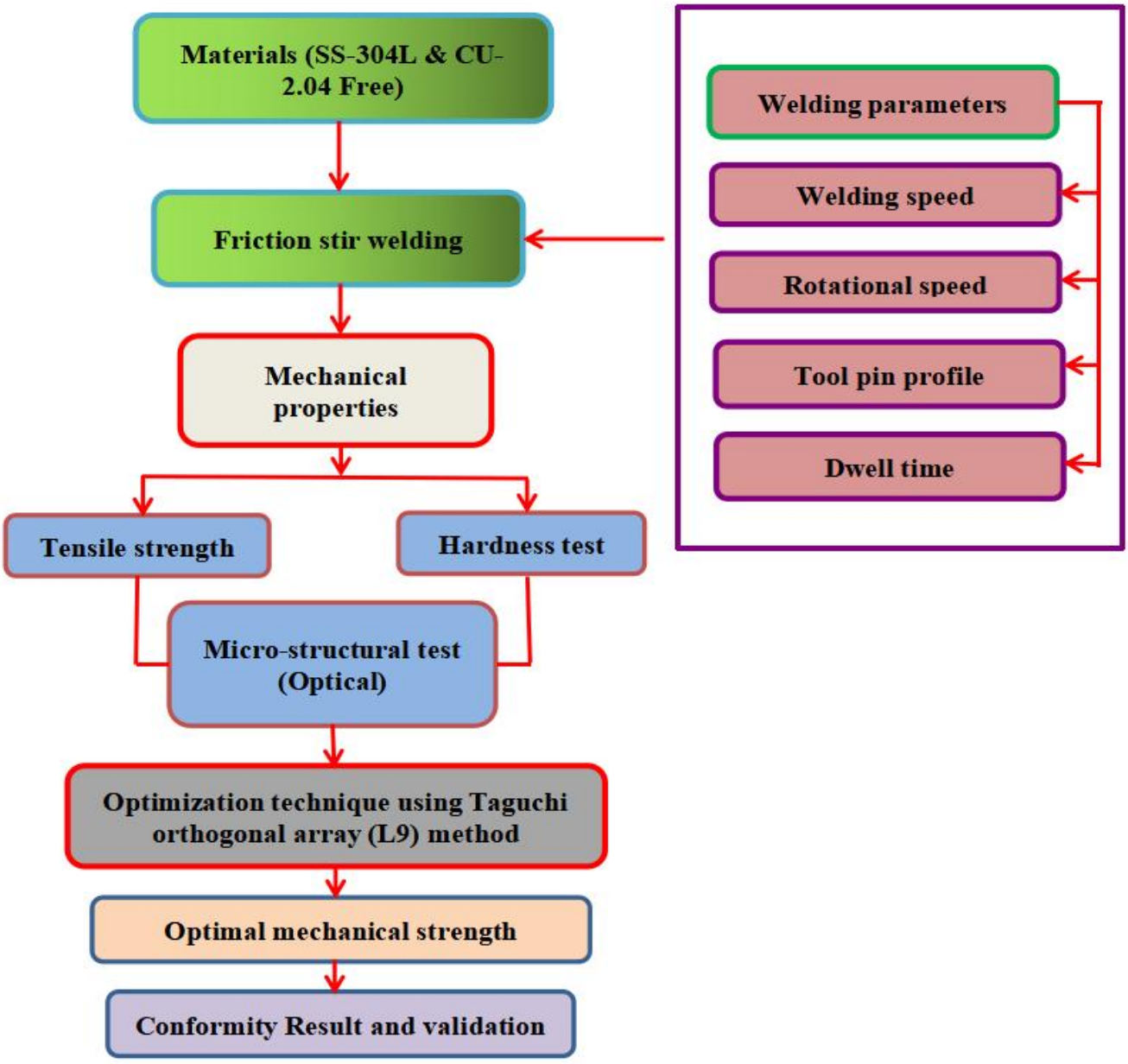

Figure 3.1 Research methodology process parameter

3.1.1 Experimental Work

According to the introduction part, the materials for the experiment which was selected, pure copper 2.04 alloy and stainless steel 304 L nickel chromium alloy sheet are utilized in a butt joint configuration. all specimens were cut off at the same 110 mm x 50 mm dimensions using grinder cutter and manual hacksaw.

To improve mechanical interlocking, the SS-304L plate was always placed on the advancing side and the CC-2.04 plate was on the retreating side during the experiment. A mechanical test was prepared in accordance with ASTM E8-04 guidelines after the specimen was welded, and the transient temperatures during FSW were measured with oC. The materials used in this work for joining trials were cut to plate size, each measuring 110×50×5mm, and the backing plate was placed at the bottom of the pleat. The experimental setup is shown in Figure 3 below:

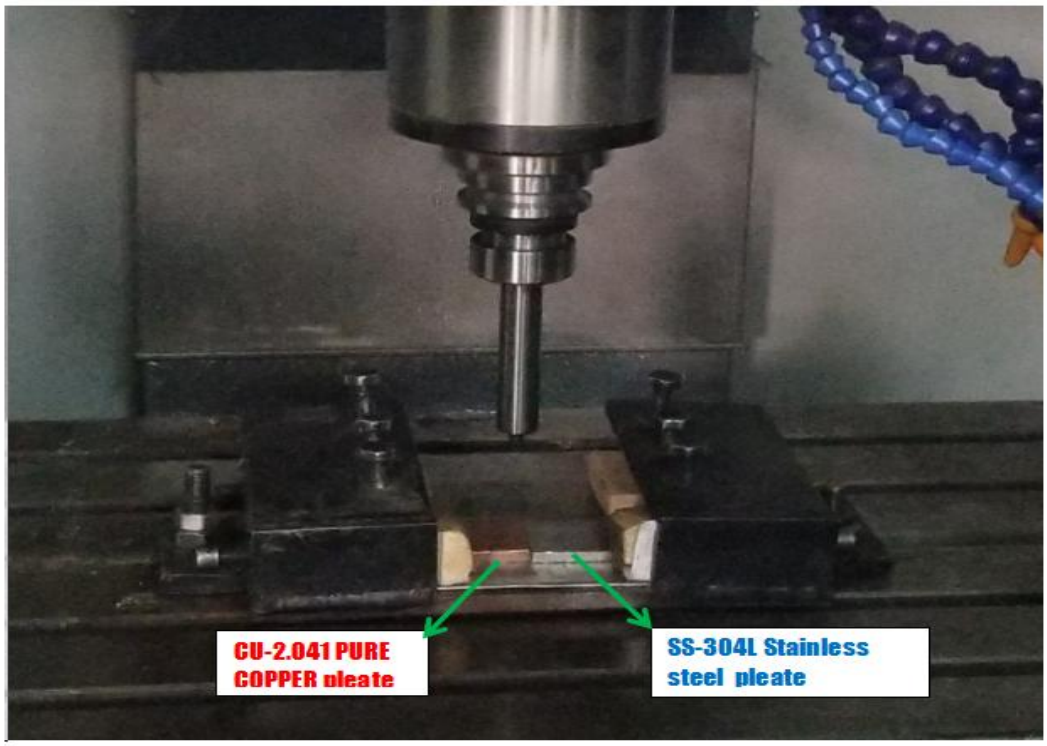

Figure 3.2 Experimental set-up

3.1.2 Work-piece Fixture

To guarantee that work-pieces are orientated and positioned precisely in the machine tool's working space during FSW operation, the fixture work-piece system must have a high static and dynamic rigidity. Fixtures are used to direct the force flow from the cutting edge into the machine tool structure on the work-piece side. Consequently, the general behaviour of machine tools is directly impacted by the mechanical characteristics of fixtures. The many parts that make up the fixture work-piece system are often joined by mechanical joints. The location and type of the structure's joints have a major effect on its dynamic and static stiffness. In FSW, a fixture is typically the most intricate and important part of the welding procedure. In order to withstand the side and perpendicular forces that are created during the welding process, the work parts need to be fastened to a sturdy, smooth backing plate. In order to stop blank movement during the welding process, the FSW backing plate is permanently fixed on the table of the vertical milling machine and supports work components.

During welding process their was a temperature reading taken from the solid state of SS-304L and CU-2.041 welding zone from the total 9 experimental three sample of welding zone selected randomly based on the temperature reading **376.25**, **849.37** and **964.21** in degree centigrade was recorded respectively with 4, 8 and 12 seconds of dwell time.

Figure 3.3 Actual work-piece fixture

3.1.3 CNC Milling Machine

Materials like metal, plastic, wood, and other solid objects can be shaped and cut with a vertical milling machine. Its spindle axis is upright and perpendicular to the work-piece. This can be accomplished by changing pressure, cutter head speed, and direction on one or more axes. The two distinct materials in this thesis were welded together using CNC milling machine. CC-2.04 and SS-304L The FSW machine is not found in any of Ethiopia's academic institutions or manufacturing sectors. Therefore, Computer Numerical Controlled (CNC) three-axis milling machine is used as an FSW machine in this study.

Table 3.1 XHS7145 CNC milling machine specification **(From machine manual)**

№	Part Name	Unit	Specification
1	Table working surface	mm	800 X 450
2	Max. Spindle Speed	rpm	8,000
3	Spindle Motor	HP, KW	7.4, 5.5
4	NC Controller	Type	Fanuc-0i MD
5	Tool Shank	Type	MAS-403 BT-40 Opt.: CAT-40

Figure 3.4 XHS7145 CNC milling machine or Vertical milling machine

3.2 FSW welding materials properties

FSW welding materials Pure Cu Grade B (2.041 99.8%) and stainless steel (Ss-304L) alloy were chosen to be welded using a but joining configuration, so the SPECTROMAX machine was used to detect the metal's chemical composition. Table 3 summarizes the findings and presents them. The mechanical properties of the alloys are influenced not only by their chemical composition but also by their condition, such as Annealed, cold worked, or precipitation hardened.

Figure 3.5 Sample of chemical composition of the metal was detected using SPECTROMAX

3.2.1 stainless steel (Ss-304L) plate with its dimension

An iron alloy with corrosion and rust resistance is called stainless steel. At least 11% of it is chromium, and other non-metals and carbon may be added to get other desirable qualities.

Different materials are used to make heat ex changers these days. Choosing the right material is essential for both function and longevity. It needs to be given extra consideration from the beginning because of this. Here, it has shown to be an especially dependable and long-lasting material.

Stainless steel heat ex-changers are especially resistant to corrosion, and they reduce the amount of limestone and other residue deposits. For more than 50 years, vessel heat ex-changers have exclusively been constructed of stainless steel.

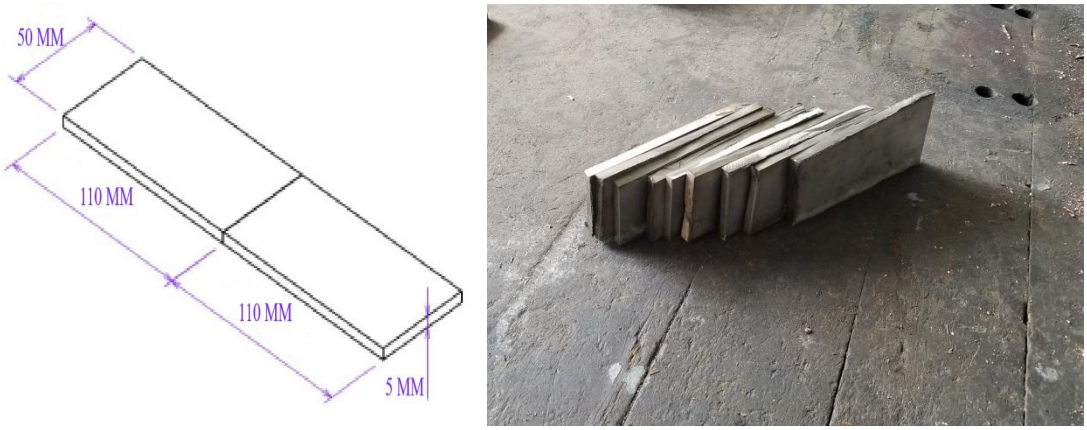

Figure 3.6 Stainless steel 304 L plate with its dimension

3.2.2 copper (CU-2.04) plate with its dimension

For heat ex-changers, copper offers a number of advantageous qualities, including durability and thermal efficiency. Copper is first and foremost a great heat conductor. This indicates that heat may move through copper swiftly due to its high thermal conductivity. The thermal conductivity of this substance is 231 Btu/ (hr-ft-F).

With the exception of silver, a precious metal, this is higher than any other metal. Copper is over 30 times more thermally conductive than stainless steel and has a 60% higher rating than aluminium. Its compatibility with other plating and coating techniques allows copper plating to be utilized as part of a dual system. In heat ex-changers, copper's resistance to corrosion, bio-fouling, maximum permissible stress, internal pressure, creep rupture, and other characteristics are also desirable**.**

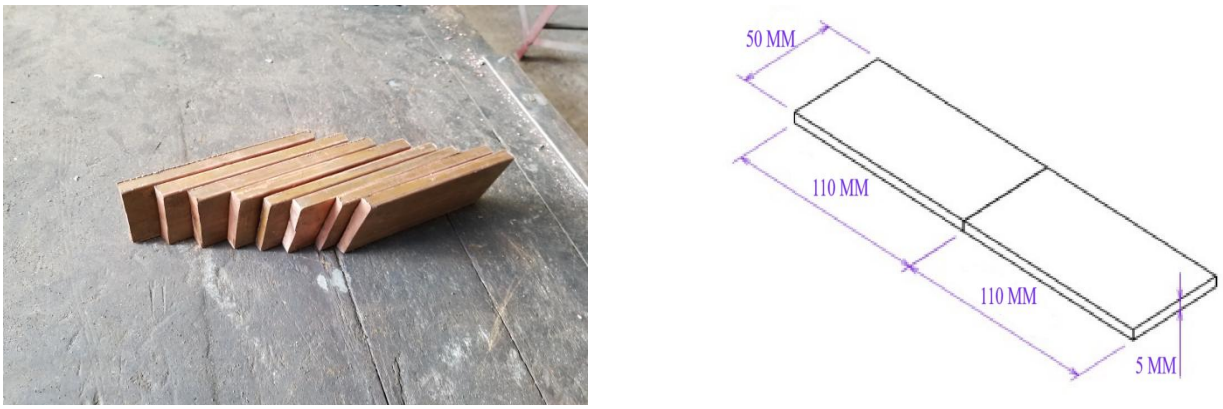

Figure 3.7 Pure copper steel 2.04 plate with its dimension

3.2.3 chemical composition for SS-304L stainless steel and CU-2.04 (pure copper)

Based on the result that detected using SPECTROMAX the chemical composition of SS-304L and CU-2.041 metals will illustrated on the below table for better look go to the appendix part and then there are direct results

Table 3.2 Chemical composition of SS-304L Stainless steel alloy (From Appendices 120)

Stainless steel Alloy	Si	Fe	Cu	Mn	Ni	Cr	C	Mo	Co	Al
SS-304L	<.0050	72.9	0.0932	0.949	7.53	18.0	0.0200	0.137	0.279	0.0030

Table 3.3 Chemical composition of Pure copper CU-2.04 alloy (From Appendices 121)

Pure Copper Alloy	Si	Fe	Cu	Mn	Ni	Cr	Zn	Pb	Co	Al
CU-2.04	0.0030	0.0432	99.86	0.0053	0.0030	0.0210	0.0100	0.0250	0.0123	0.0020

3.2.4 Mechanical property for Ss-304L stainless steel and Cu-2.04 (pure copper)

Table 3.4 Mechanical property for Ss-304L stainless steel and Cu-2.04 **[122]**

Properties	Units	SS-304L	CU-2.04
Ultimate tensile strength	MPa	330	210
Hardness, Vickers	HV	72.7	51.5
Yield tensile strength	MPa	210	33.3
Modulus of elasticity	GPa	193 - 200	110
Elongation at break	%	40	60
Charpy impact	J/cm3	216	48

3.2.5 Thermos-physical property for Ss-304L stainless steel and Cu-2.04 (pure copper)

Table 3.5 Thermos-physical property for Ss-304L stainless steel and Cu-2.04 **[122]**

Material type	Density [G/cm^3]	Melting point [^{o}C]	Thermal conductivity [W/m-k]	Elastic module Gpa
SS-304L	8.1	1450	398	193
CU-2.04	8.95	1083	391	117

3.3 Selection of welding tool materials

FSW advances to the point where it is currently welding a high-strength material when the performance demonstrated by this approach is impressive. As a result, one of the most crucial aspects of welding high-strength materials like copper and stainless steel (Ss-304L & Pure Cu-2.04) is choosing the appropriate FSW tools. Tool steel and tungsten (W)-based tool selection standards are frequently utilized for high strength materials. Pure tungsten (cp-WC), which is utilized commercially as a medium for titanium alloys and FSW steel, has low toughness and wears more quickly at room temperature than it does at high temperatures. Because it can tolerate temperatures as high as 1650 HV and abrupt temperature swings, tungsten carbide (WC) is an excellent material. It is also one of FSW's favoured materials because it is inexpensive and readily available. It is mentioned in the **[122]** article.

In addition to its Hardness HRa 92.0 and TRS of ≥3500 MPa, the drawing of the tungsten carbide cobalt content 10% (WC-Co 10%) with Grade 9008/C2 Grain Size of Sub-Micron Diameter Tolerance (h6) The next figure shows the material's dimensions and drawing.still

Figure 3.8 Tungsten Carbide steel

Table 3.6 Tungsten Carbide Castle bar specification

Material	Tungsten Carbide, carbide **[123]**
Brand	Castle bar
Item dimension	5.91 x 0.79 x 0.79 inches L x W x H
Shape	Round Rod
Item Diameter	20 Millimetres

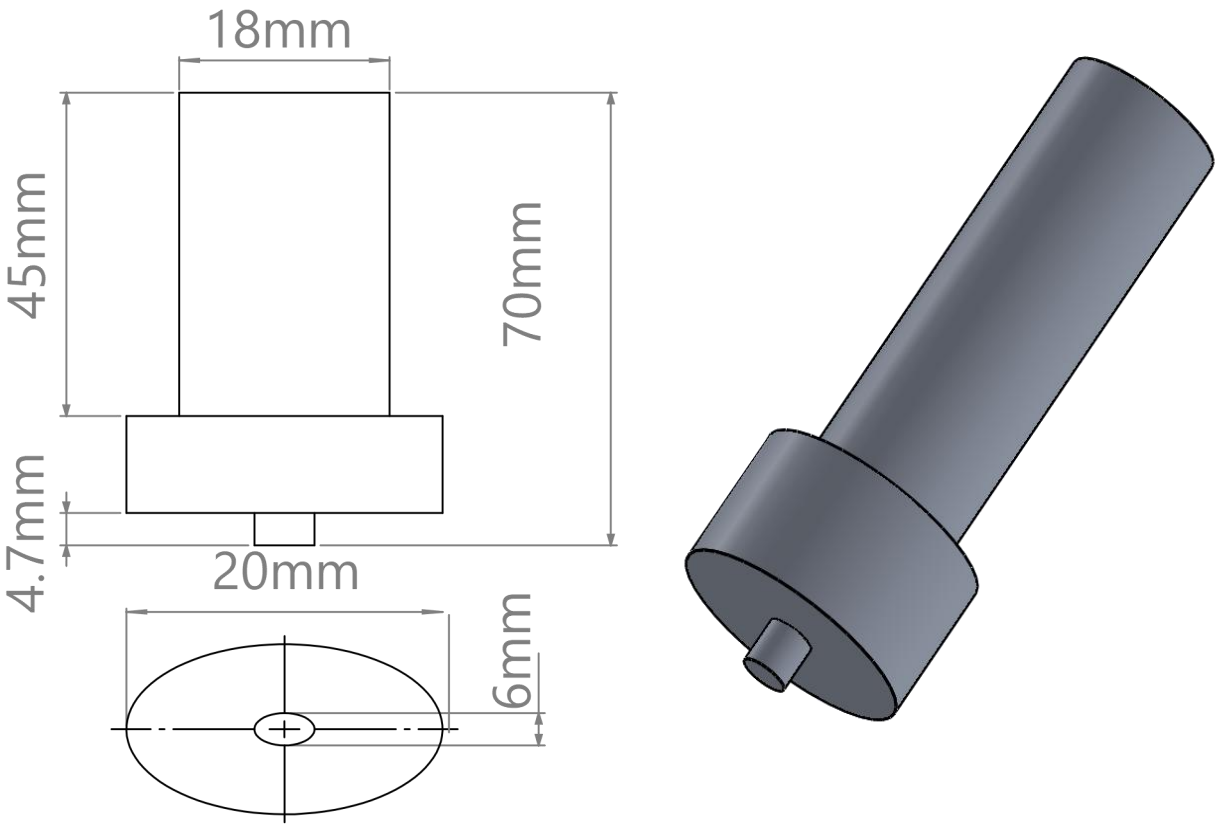

The FSW tools that are used to perform all the welds are fabricated with the help of additional attachments on the lathe machine with dimensions, based on a different review of litterateurs This tool consists of two main components: shoulder and pin after selection of friction welding tool material examining of their property is crucial and helpful during welding process.

Table 3. 7: Dimensions of the tool

Tool material	Tool profile	Probe diameter (mm)	Pin length (mm)	Shoulder Diameter (mm)
Tungeston carbide (WC-CO)	Cylindrical	6mm	4.7	18
	Conical	3 mm through 6 mm		
	Square	6 mm		

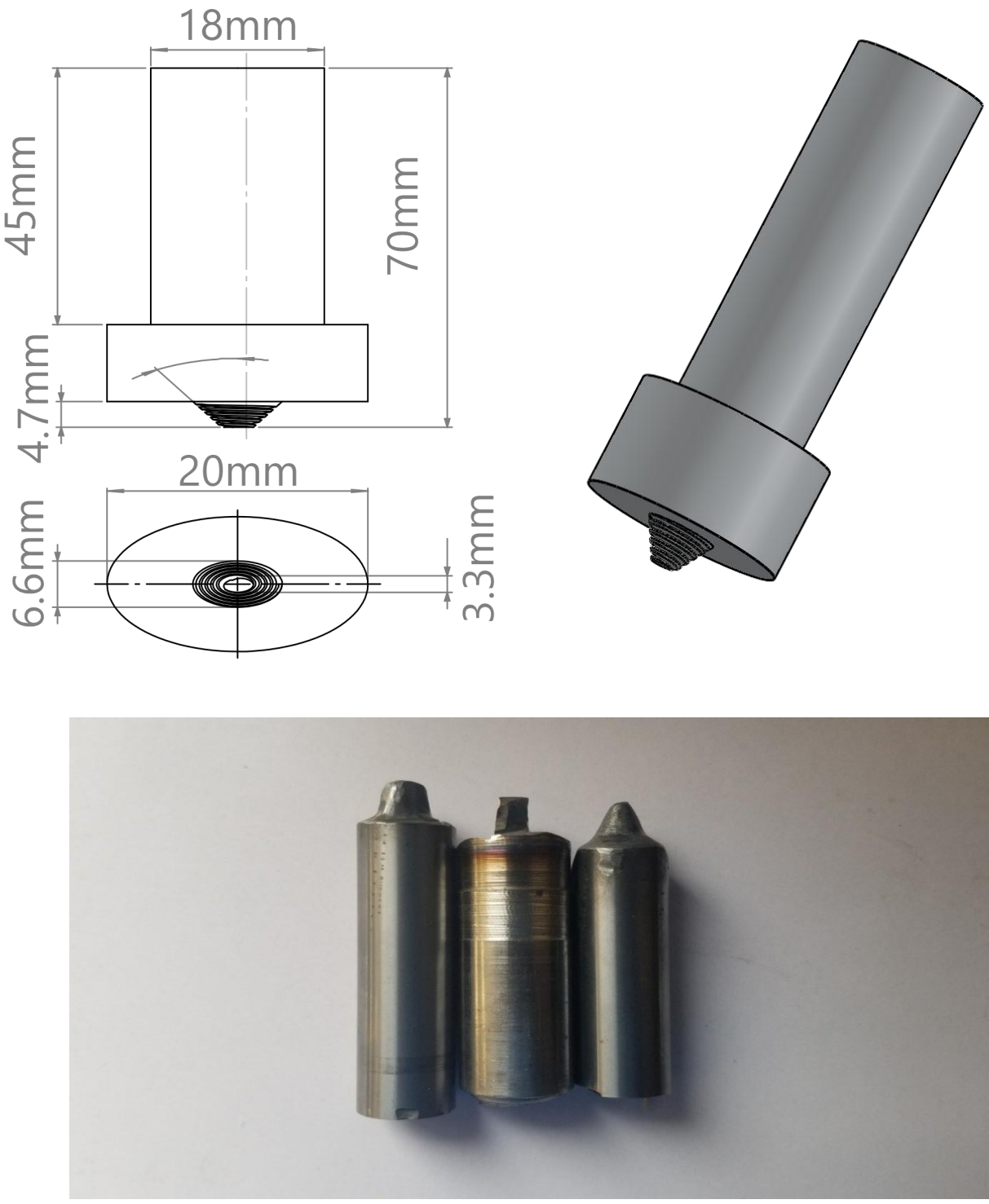

Figure 3. 9 Dimensions of welding tools 2D and 3D model for pin profiles, Actual image of tool Profiles: Square, Cylindrical and Conical

3.3.1 Mechanical property of tungsten carbide welding tool

The composition of tungsten carbide is tungsten metal and carbon, usually in a weight ratio of 90% tungsten to 10% carbon. based on the well-written study on the composition of WC-CO **[124].** claimed that the composition ratio offers the best possible balance between wear resistance, toughness, and hardness. While a higher carbon percentage enhances toughness, Hardness and resistance to wear are enhanced by a higher tungsten concentration. The tungsten composition of common tungsten carbide grades ranges from 85 to 97%, with carbon making up the remaining portion. Cobalt 10% (WC-Co 10%) is present in the tungsten carbide tools used in this investigation, which have a grade of 9008/C2. The rest are composed of tungsten metal. Properties are also influenced by the composition of the cobalt binder. 3-12% cobalt is used as a binder in most grades.While toughness is increased by higher cobalt, hardness and heat resistance are decreased. The application determines the ideal composition of the binder. The tools have identical dimensions, and the table displays their mechanical characteristics and chemical makeup.

Table 3.8 Physical properties, Mechanical properties and Thermal properties of tungsten carbide cobalt content 10% (WC-Co 10%) with Grade 9008/C2 **[124]**

PHYSICAL PROPERTIES	
Colour	Gray
Density	15.7 g/cm3
Knoop Hardness	1670 (Mohs, 9 – 9.5)
MECHANICAL PROPERTIES	
Hardness	25000 HB
Tensile Strength	350 MPa
Compressive Strength	4780 MPa
Young modulus	530-700 Mpa
Poison ratio	0.31
THERMAL PROPERTIES	
Thermal conductivity	85 W/m.K 49 BTU/h-ft-°F
Coefficient of Thermal Expansion	5.9 µm/m-K
Melting Point	2,785°C
Specific Heat Capacity	280 J/kg-K

3.3.2 Chemical property of tungsten carbide welding tool

Better qualities can be obtained for a variety of applications by using different chemical compositions. The percentage of chemicals for tungsten carbide cobalt content is 10% (WC-Co 10%) among different scholars **[125].** stated on tungsten carbide tool steel alloy determination.

Table 3.9 Chemical compositions of tungsten carbide with Grade 9008/C2 **[125]**

Tungsten	Grade 9008/C2 Composition	
Level of %	WC	CO
MIN	90 %	10%
MAX	93.5%	6.5%

As shown from the above table, the mechanical properties of the tools are higher than that of the mechanical properties of the welding specimen. Therefore, the welding tool is safe for joining the given specimen without breakage and the tool wears.

3.3.3 Selection and reason for Tungsten carbide tool

As stated in the **[126]** article. The remarkable hardness of tungsten carbide is well-known, and abrasion resistance, making it a material that is highly beneficial in the industrial sector. Low carbon steels might be easily fused using standard fusion welding techniques. Nevertheless, fusion connecting these steels causes issues with metal melting and weld tool solidification. Low carbon steel plate friction stir welding (FSW) was used in this investigation. To find out how welding parameters affect joint quality, use a tungsten alloy tool.

Tungsten carbide tool steel is classified as a hot working tool steel and the next significant alloying element of cobalt materials**.** The stresses imposed on the tool are determined by the work material's strength. The characteristics of the tool material affect how much heat is produced within the tool and, consequently, the temperatures reached. To attain particular characteristics in the final joint, factors like heat conductivity are then crucial when choosing the tool material.

The coefficient of thermal expansion determines the thermal stresses that a tool experiences. The choice of tool material may also be influenced by the work materials' reactivity, ductility, and hardness.

Tool steel alloy with tungsten carbide Additionally, it showed that material properties may be important for FSW. The work-piece, the necessary tool life, user preferences, and experience all influence the choice of tool material.

At high temperatures, the WC in WC-Co composite materials preserves the strength of the carbide particles. Because of its exceptional mechanical qualities, this composite is preferred for combining hard materials. According to Liu et al., adding CrC2 to WC-Co has a lowering effect. The likelihood of FSW/P of titanium alloys and steels is increased by WC-based tools. With a hardness of roughly 1650 HV, WC offers exceptional toughness. Additionally, during welding trials, it was demonstrated that this material is insensitive to abrupt temperature and stress changes.

Table 3.10 Tool materials and suitable weld metals

Tool Material	Suitable weld material
Tool steels	Al alloys, aluminium metal matrix composites (AMCs) and copper alloys
WC -Co	Aluminium alloys, mild steel
Ni-Alloys	Copper alloys
WC composite	Aluminium alloys, low alloy steel and magnesium alloys, Ti-alloys
W-alloys	Titanium alloys, stainless steel and copper alloys
PCBN	Copper alloys, stainless steels and nickel alloys

3.3.4 Reason for Selection of cylindrical tool

One of the most used tools in FSW is the cylindrical tool, which offers superior material transportation and doesn't pulse while welding employing these profiled tools to achieve the highest possible tensile and hardness strength.

3.3.5 Reason for Selection of squire type tool

Additionally, several researchers have used these profiled tools, such as and the tool imparts the highest tensile strength and hardness from the other tools. The following are some advantages of using a squire-type instrument for welding:

- The dispersion of particles is extraordinarily uniform.
- Joint hardness has a positive correlation with grain size.

3.3.6 Reason for Conical Tapered Tool Selection

Conical tapered tools improve the downward auguring motion, reduce welding force, and facilitate the flow of plasticized material. Additionally, the tool's travel speed was doubled by conical tapered tool pins. compared to the prior design. This tool was chosen in accordance with the aforementioned viewpoint.

3.3.7 Determination of Shoulder diameter size and its length

According to **[127],** their analysis shows that they used a D/d ratio of 3 to find good mechanical properties. The tool diameter was previously established to be 6 mm based on this study; thus, an 18 mm shoulder diameter was used in order to obtain a D/d ratio of 3. The tool's therm-mechanical environment, traverse force, torque, and rate of heat generation are all impacted by its geometry. The tool's geometry, as well as its rotational and linear motion, influence the flow of plasticized material within the work-piece. Important aspects include pin geometry, including size and shape, shoulder diameter, shoulder surface angle, and the type of tool surfaces.

The torque's two components are presented in Fig. for different shoulder diameters to help identify the ideal tool shape. The sticking torque rises, reaches a maximum, and then falls as the shoulder diameter grows. First, as the temperature rises, the material's strength, or shear stress, reduces because the shoulder diameter increases.

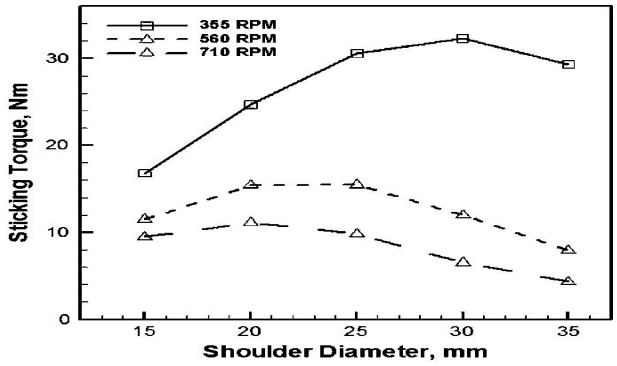

Figure 3.10 Shoulder Diameter VS Torque

First, the strength of the material, shear stress because the shoulder diameter increases as the temperature rises. Second, the area to the larger contact area. With the increase in diameter of the shoulders For large shoulder diameters, even when the sticking torque drops, the total torque keeps rising.

3.3.8 Selecting of Pin diameter and its length

The joint surfaces are deformed and heated by friction when friction stirring pins are used. The purpose of the pin is to transfer material behind the tool, shear material in front of the tool, and disturb the work piece's fried, or contacting, surfaces. Furthermore, the pin design controls the tool travel speed and depth of deformation. Other research indicates that in order to control undercut faults during welding, the pin's length should be less than 0.3 mm of the thickness of the base material.

As a result, the tool pin length was created taking into account the study mentioned above. The formula for the maximum outer pin diameter is 0.8 * plate thickness (mm) + 2.2. As a result, the pin diameter is 0.8*5 mm + 2.2 = 6.2 mm, and the tool length is 4.7 mm. However, the market does not carry tools with a pin diameter of 6.2 mm, thus 5 mm is utilized instead.

3.3.9 Material composition measuring device

It is crucial to first and foremost investigate the material composition of the welding tool and work-piece in order to achieve a better outcome and an acceptable welding process. A spectrometer is a very sophisticated analytical tool that is essential to the accurate determination of the chemical makeup of metals. The SPECTROMAX is a help full equipment.

The optical emission spark spectrometer is used by this device. method. Distinguish between different elements, such as nickel (Ni), molybdenum (Mo), copper (Cu), iron (Fe), and so on. Among its benefits are: Non-destructive characteristics: The test has no effect on the alloy. Safety, accurate and timely research, and more.

Figure 3.11 Spectrometer chemical composition of metals testing machine

3.4 Testing and Inspection

3.4.1 Tensile strength test

One of engineering's most basic tests, tensile testing yields important details about a material and its related characteristics. The samples were 220 mm × 15 mm × 5 mm, and their size varied according to machine capability and standards. ASTM E8 standards stated that the samples were already machined to the correct dimensions needed for the test. The HUT-600 type of Bairoe computer-controlled electron-hydraulic universal testing machine was used for the test. The test was evaluated three

periods and use the average outcome. Both the universal testing machine requirement and the specimen geometry standard **[128]** were followed in the preparation of the test samples. Figure 3 illustrates this

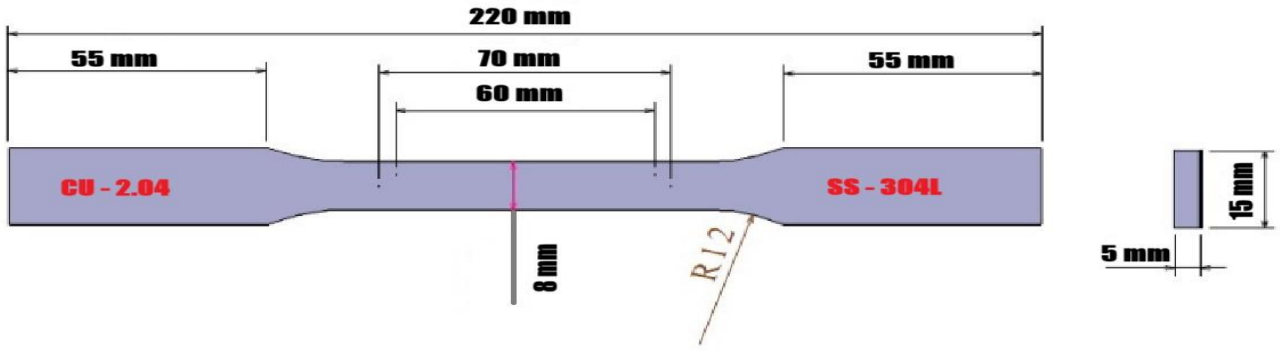

.

Figure 3. 12 Size of the tensile specimen (ASTM E8-04) **[128]**

Figure 3.13 Ss -304L & Cc - 2.04 welding sample preparation for testing

Figure 3.14 Before and after the tensile test

Figure 3. 15 Tensile test machine

3.4.2 Hardness test

The hardness test's objective is to ascertain how resistant a material is to long-term deformation from wear, scratch, abrasion, and indentation. The purpose of a hardness test is to demonstrate the connection between material qualities and hardness. This test is recommended due to its non-destructive nature, simplicity, and simple.

3.4.2.1 Vickers hardness test

Vickers hardness test is an indentation hardness test that involves forcing a square-based pyramidal diamond indent-er with specific face angles into the surface of the material being tested. The diagonals of the resulting impression are then measured after the force is removed. Three weld cross-sections were taken in order to examine the hardness strength. between tangents, applying a minor load of 20 kg and a main load of 80 kg for a 15-second duration. In accordance with scale H, measurements were made with a 1 mm gap between tangents, applying a minor load of 20 kg and a main load of 80 kg for a 15-second duration.

Figure 3.16 Rockwell hardness testing machine

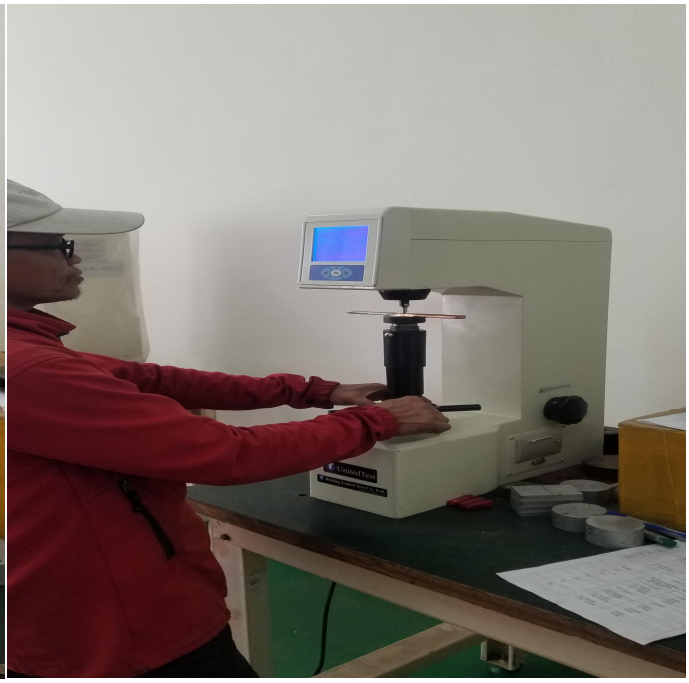

Figure 3.17 Hardness test of the specimen

3.4.3 Micro-structure Observation

Micro-structure observation is used to determining grain size and, shape, and distribution of various phases and inclusions was important as these effects of the mechanical properties of the metal. This process follows some procedures in order observe the structures. The specimen preparation of sample to examine micro-structure was cutting of specimen, grinding, polishing, etching, and observing micro-structure optical microscopy. For this thesis the micro-structure observation is mounting done for both Ss - 304L & Cc - 2.04 welding joint material.

Figure 3.18 Microstructural test machine

3.4.3.1 Sample preparation

After UTS and HV results, create three samples of the specimen that has the best mechanical properties then, Cutting the specimen precisely to the necessary testing size from the sample is the first stage in a micro-structural test. Each sample is chopped into a two-centimeters-long specimen using a consumable high-speed rotating disc abrasive cutter.

3.4.3.2 Grinding and Polishing of Specimen

All specimens underwent two grinding procedures. First, silicon carbide paper is used for rough grinding, and then the RP-2B grinder polisher machine is used for an intermediate grinding operation. First, the specimen was smiled for roughly two minutes on silicon carbide paper with a granularity of 400. Once more, the carbide papers with grit sizes of 800, 1200, and 2000, respectively, made me smile.

3.4.3.3 Etching

This is the last stage of specimen preparation that allows the sample to display numerous metal structural features. To do this, the polished surface is exposed to chemical activity through the use of a suitable reagent. In addition to marbles reagent copper sulphate (4 mg), hydrochloride acid (20 ml), and water (20 ml), all samples were etched using nitric acid (5 ml), hydrofluoried acid (1 mm with 48%), and water (44 mm). The etching process takes 30 seconds for every sample. Ultimately, The magnification ranges for optical microscopy are 50, 100, 200, 500, and 1000. The scanning area is 104 x 102 mm. 20 micrometre labels are used to observe micro-structural characteristics.

3.5 Optimization Techniques

An effective method for achieving the ideal set of operating conditions and the intended design parameters is optimization. This would direct the experimental activity and lower the operating and design risk and expenses**.**

3.5.1 Taguchi method

Taguchi experimental designs are a collection of fractional factorial designs that focus on main effect estimation while ignoring interaction. The most well-liked collection of Taguchi designs is produced by this process. The Taguchi method's crucial stage for attaining high quality without raising costs is process parameter optimization. The Taguchi technique analyses the outcomes using signal-to-noise (S/N), a statistical performance metric. This S/N ratio is used as a metric to select control settings that are most effective at sound. For the purpose of creating and enhancing product quality, the Taguchi method is a methodical use of experimental procedure design. This method's limitations are entirely philosophical; there is no mathematical component, it only provides the ideal value at any level that the experimenter specifies, and it cannot predict the future course of the best answer in the tests **.**

3.5.2 Taguchi Orthogonal Array (OA) design

One kind of generic fractional factorial design is the Taguchi Orthogonal Array (OA) design. Based on a design matrix put forth by Dr. Genichi Taguchi, this highly fractional orthogonal design enables you to take into account a specific subset of combinations of several factors at several levels. To guarantee that every level of every factor is taken into account equally, Taguchi orthogonal arrays are balanced. Consequently, the elements can be assessed separately from one another even though the design works.

Taguchi suggested that there should be three steps involved in the optimization of a process or product:
System design: This stage involves the synthesis and conceptualization of a process or product to be used, and it incorporates new knowledge, concepts, and concepts from the domains of technology and science. Finding the right design factor levels to reduce the system's sensitivity to different uncontrollable noise factors is known as **parameter design.** This improves the product's performance and lowers the customer's loss. **Tolerance design** is the process of creating items or processes with the goal of minimizing the total cost of their manufacturing and lifetime.

According to **[129],** the two main instruments utilized in resilient design are orthogonal arrays, which allow for flexibility, and the signal to noise ratio, which assesses quality with a focus on variance. numerous design elements at once. According to the article of **[130],** the Taguchis approach is entirely based on statistical experiment design, which may cheaply meet the needs of problem solving and product or process design optimization.

Examination of the Findings The procedures used to analyse data with interactions are the same as those used in the absence of interactions. Finding the ideal situation, determining the specific impact of each component, and estimating performance under ideal conditions are the same goals.

The way the optimum levels of factors are determined is slightly altered for the optimum state by interactions. A typical L9 (3x3) or (3x4) orthogonal array was employed as the fractional factorial design in this experiment, which has three components at three levels each. In the conventional L9 (3x3) or (3x4) orthogonal array that was examined in the article of factors A, B, C, and D are positioned in columns 1, 2, 3, and 4, respectively.

3.6 Experiments of design

Table 3.11 Standard Taguchi orthogonal array experiential design

Experiment runs	Control Factors and levels			
	A	B	C	D
1	1	1	1	1
2	1	2	2	2
3	1	3	3	3
4	2	1	2	3
5	2	2	3	1
6	2	3	1	2
7	3	1	3	2
8	3	2	1	3
9	3	3	2	1

A= rotational speed B = transverse speed C = dwell time D = pin profile

Levels-Factor	Number of experiment runs	Orthogonal array type
2^3	4	L_4
2^7	8	L_8
2^5		
2^3		
3^4	9	L_9
3^3		
4^5	16	L_{16}
2^{15}		
$2^1 \times 3^7$	18	L_{18}
$2^2 \times 3^6$		
3^7		
$2^1 \times 3^6$		
2^1x3^4		
2^1x3^3		
3^3	27	L_{27}

The basic Taguchi L9 (3^4) orthogonal array 3 Level and 4 Factor process parameter

3.6.1 Selection of Orthogonal array

This orthogonal array was selected due to the minimal number of experimental trials that it required. One trial was represented by each row in the matrix. Nevertheless, those experiments were conducted in a random order. Each factor had three levels, which were assigned in the L9 (3x4) orthogonal array as shown in the table. based on the material's roughing and semi-finishing characteristics.

Table 3.12 Taguchi orthogonal array experiential design

No	Tool material [Type]	Dwell time [Sec.]	Traverse speed [mm/min]	Rotational speed [RPM]	Tool shape [Type]
1	WC - CO	4	45	1200	Cylindrical
2	WC - CO	4	55	1400	Taper
3	WC - CO	4	65	1600	squire
4	WC - CO	8	45	1200	Taper
5	WC - CO	8	55	1400	squire
6	WC - CO	8	65	1600	Cylindrical
7	WC - CO	12	45	1200	squire
8	WC - CO	12	55	1400	Cylindrical
9	WC - CO	12	65	1600	Taper

It is well known that figuring out the ideal welding circumstances is one of the main duties. Tool shape, dwell time, traverse speed, and rotation speed are the characteristics chosen for this study.Additionally, three levels were chosen for every parameter. As a result, the mixed L9 orthogonal array is a suitable design for the levels and characteristics mentioned above. Experimental runs were carried out at night using this orthogonal array.

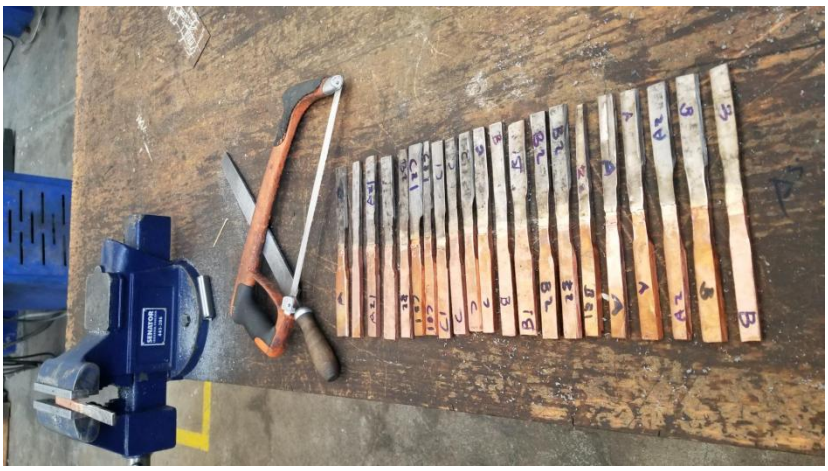

Figure 3.19 Welding sample for Ss - Cu before testing

3.7 Methods of FSW

3.7.1 Determination of Working Limits of Parameters

Table 3.13 Review and result to determine process parameter

No	Parameter with % contribution					Reference
	T.T.S	T.R.S	T.T.A	T.P.P	Error	
1	33	41	-	-	5	(Elatharasan and Kumar, 2013) **[131].**
2	14	47	-	-	1	
3	12.693	57.56	22.97	-	6.77	
4	30.18	52.6	-	-	3.61	
5	3.14	6.29	-	-	25.66	
6	13.5	67.2	15	-	4.3	
7	31.97	41.2	-	-	1.06	
8	81.25	7.58	-	-	4.88	
9	4	13	-	10	5	
10	31.05	44.33	-	19.55	5.06	
11	-	77.17	6.89	15.85	0.09	
12	6.67	15.58	10.58	-	7.03	
Average	23.768	39.209	13.86	15.13		

*TS – Traverse speed; TRS – Tool Rotational Speed; TPS Tol pin profile; TSD – Tool Shoulder diameter; PD – Plunge Depth; TTA – Tool Tilt Angle; D/d - Shoulder diameter-to-pin diameter ratio

The remaining levels of magnitudes are selected based on magnitudes highly closer to the selected RPM magnitude. The process parameters that are statistically significant can be found using the Analysis of Variance, or ANOVA, whereby parameter affects the response of the study **[132].**

3.7.2 Determination of Working Limits of levels

A review of the existing literature that is like a study of FSW on dissimilar metals was conducted to select the appropriate rotational and traverse speeds for the target materials which is SS-304L & CC-2.04, the levels were chosen based on their frequency.

3.7.3 Determination of RPM levels

Table 3.14 Selection of tool rotational speeds selected from different scholar

No.	Title	Material type	Initial rpm	Optimized RPM selected at	Result	Ref.
1	Friction welding of dissimilar joints copper-stainless steel pipe consist of 0.06 wall thickness to pipe diameter ratio	copper (ETP-Cu) and stainless steel (SS) of grade 304 L	250, 300, 350 and 400	350 @ 35	217 M Pa 85 HV	[133]
2	Welding Equality and Mechanical Properties of Aluminium Alloys Joints with copper Prepared by Friction Stir Welding	Cu - 2.04 and AA7075-T6 aluminium 4 mm	700, 1000, 1400	1400 @ 46	225 Mpa 98 Hv	[134]
3	Micro-structures and mechanical properties of copper-stainless steel butt-welded joints by FSW	Ss-304L and Pure copper 3mm	1000, 1200	1000 @ 30	129 MPa 98.6 HV	[135]
4	The Joining of Copper to Stainless Steel by Solid-State Welding Processes: A Review	Ss-316l and Copper c7100 5mm	1000, 1100, 1200	1200 @ 42	175 MPa 73.8 HRB	[136]
5	Improving friction stir welding between copper and 304L stainless steel	Ss-304l and Copper c10100 5mm	1400, 1600	1600 @ 56	247 MPa 112 HV	[137]

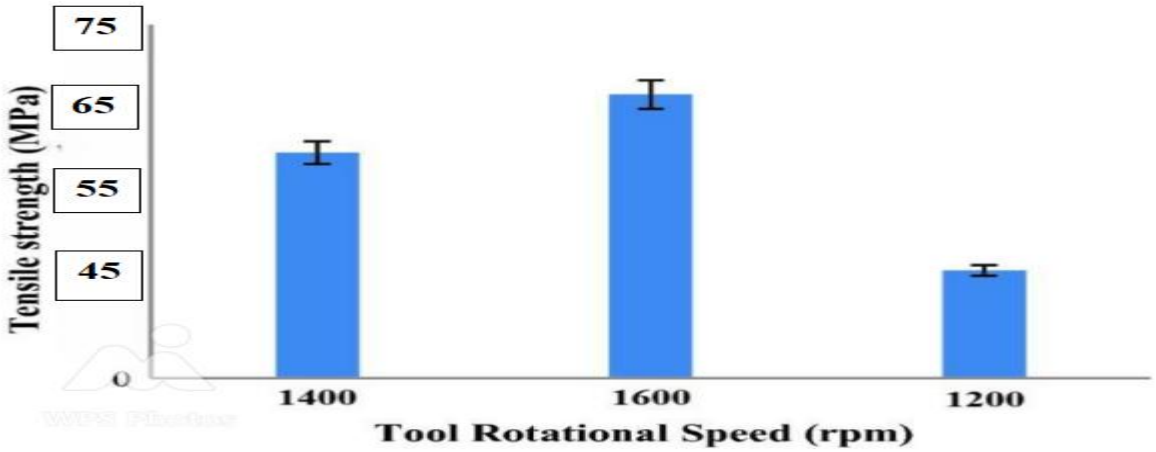

Figure 3.20 Tensile strength VS Tool rotational speed

The magnitude of parameters is selected based on the frequency of the scholars most used. which is shows the parameters selected for this thesis work.

Table 3.15 Selected tool rotational speed

RPM	Tensile Test	Hardness	Frequency	Rank
350	217 Mpa	85 Hv	1x	**5**
1400	225 Mpa	98 HV	1x	**2**
1000	129 Mpa	98.6 HV	1x	**4**
1200	175 MPa	73.8 HV	3x	**3**
	168 Mpa	-		
	186 Mpa	-		
1600	247 Mpa	112 HV	2x	**1**

Based on the above table it is possible to select 1200, 1400, or 1600 rpm as the rotational speed magnitude for welding of dissimilar SS-304L & CC-2.04 materials. The first magnitude gap is different from the second and third. The reason for this is that most scholars achieve maximum tensile strength at a rotational speed of 1600 rpm for dissimilar metals and achieve maximum tensile strength at 1200 rpm or 1400 rpm.

3.7.4 Determination of Traverse speed levels

The selection of level magnitudes of traverse speed is based on the selected rpm magnitudes.

Table 3.16 Selection of Transverse Speed

No	Title	Material type	Initial traverse speed	Optimized traverse speed at selected rpm	Result	Ref.
1	Improving friction stir welding between copper and 304L stainless steel	SS-304L and CU-2.04	14, 20, 28, 40, 56 and 112	56 @ 1000	160.6 Mpa 80 HV	**[138]**
2	Friction Stir Welding of Austenitic Stainless Steel by PCBN Tool and Its Joint Analyses	AISI-316 with PCBN welding tool	16, 25, 45	45 @ 1100	255 MPa 64 HV	**[139]**
3	Effect of Welding Speed on Mechanical Properties of Friction Stir Welded Copper and stainless steel	CU-2.04 & SS-316L	25, 31.5 and 45	25 @ 900	168Mpa 74 HV	**[140]**
4	Friction stir welding of dissimilar Al 6013-T4 To X5CrNi18-10 stainless steel	Al 6013-T4 & X5CrNi18-10 stainless steel	40, 55, 65, 80	65 @ 1300	186 MPa 100 HV	**[141]**
5	characterization and processing of friction stir welding on copper with AL & SS welds	CU with AL & SS different alloy	20, 40, 55 and 80	55 @ 1120	197Mpa 81 HV	**[142]**

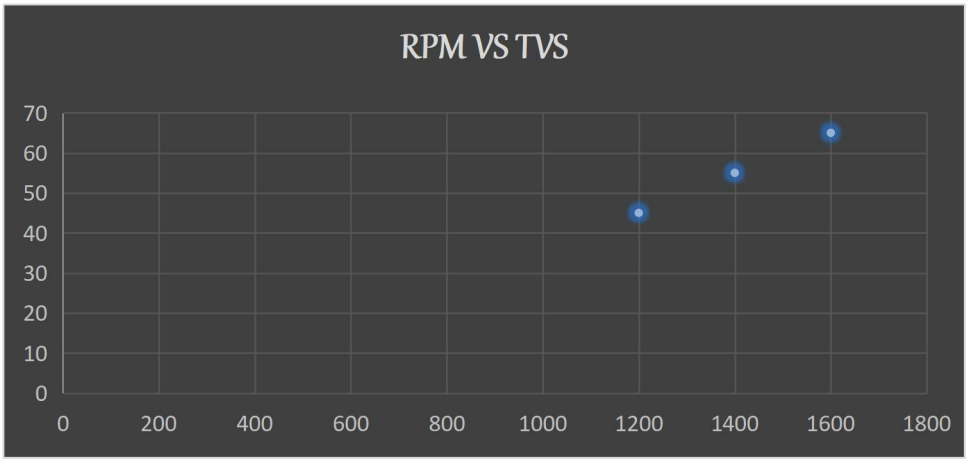

Figure 3.21 RPM Vs Traverse speed

Table 3.17 Selected traverse speed from reviewed

Traverse speed, [mm/min]	Tensile Mpa	Hardnes Hv	Frequency	Rank
65	200 Mpa	-	2x	**3**
	186 Mpa	100 HV		
55	197 Mpa	81 HV	1x	**2**
45	255 Mpa	64 HV	1x	**1**

Traverse speed (mm/min)	Rotational Speed (rpm)
45	1200
55	1400
65	1600

The traverse speed (45, 55 and 65 mm/min) was selected based on the above RPM. Table 3: Summary of Selected tool rotational speed and traverse speed.

3.8 Fabrication of tool pin profiles

The FSW process tool was created using a modified hand grinder on a lathe. The alloy tungsten carbide (WC-CO) was chosen for this experiment's welding tool. Along with greater toughness, it has a very high hardness and good resistance to wear [148]. In the workshop of the AAiT School of Mechanical and Industrial Engineering, there is no practical way to construct the desired tool pin profile according to the chosen dimensions and sheep using a round bar tool pin profile working tool, such as a cutting tool. Round bar tungsten carbide (WC-CO) with a length of 150 mm and a diameter of 20 mm can be handled or clamped by designing and fabricating a simple attachment on the griping tool post. Then, using a hand grinding machine with a cutting disc, then the tool material to be grind into a cylindrical, squire and taper conical shape, as illustrated in figure 3.22.

Figure 3.22 Tool pin profiles Fabrication

3.9 Grey relational analysis Taguchi approach

The current environment of rapid manufacturing and cost reduction with maximum utilization necessitates the use of numerous multi-response optimization techniques since complex processes have multiple quality characteristics **[143].** Numerous scholars have studied the FSW process optimization using a variety of statistical approaches. Several engineering issues can benefit from the Taguchi approach, which is a helpful method for single response optimization studies.

To compute the S/N ratio, the Taguchi technique offers three options: greater is better, nominal is best, and smaller is better. However, choosing a suitable S/N ratio requires some competence, process knowledge, and practical experience. as well as the use of Taguchi-based gray relational analysis in this thesis as shown in the figure 3.20. Finding the increased hardness and tensile strength that correlate to improved welding performance is the goal of this study. Consequently, a larger is better S/N ratio was chosen. The following formula was used to calculate it **[144].**

The Taguchi method's goal is to identify the optimal combinations of controllable factors and create goods and procedures that exhibit the least amount of change when non-controllable factors are present. This approach is predicated on an orthogonal array of experiments **[145].** The two primary elements of the Taguchi approach are orthogonal arrays and Signal/Noise (S/N) ratios. Testing time and expense are decreased by using an orthogonal array. In order to determine the factors' relative significance being examined, Taguchi promoted the S/N ratio as a single indicator that simultaneously and jointly takes into account the average value and standard deviation of test results. Three sorts of S/N ratios can be distinguished: nominal, bigger, and smaller. Response characteristics determine the best S/N ratio to use.

Designing orthogonal array matrix and conducting experiments:

The Taguchi method requires extra approaches for gray relationship creation in a multi-response setup. One of these strategies is gray relational analysis. Grey relational analysis normalizes experimental data between 0 and 1. We refer to this process as gray relational generation. In gray connection analysis, data normalization can be divided into three categories.

Grey relational generation:

Additional techniques are required for the Taguchi method to work with a multi-response design. One of these strategies is Grey relational analysis. Grey relational analysis normalize experimental data between 0 and 1. We refer to this process as grey relational generation **[146].** The three methods of data normalization used in Gray relation analysis are closer to the target value, smaller-the-better, and smaller-the-better

Data normalization is the first stage in the GRA technique, which changes the original sequence to produce a comparable one. The normalization range for the experimental results is zero to one. When the target's direction in the sequence changes or the arrangement scatter range is excessively wide, the procedure is required **[147].**

The next step is to use the following formula to determine the Grey relationship coefficient, ξi (k), from the normalized data. The correlation between the comparability sequence and the reference sequence is described by the GRC **[148].**

Table 3.18 Standard L9 orthogonal array

Experimental run	Control factors and levels		
	Rotational speed(rpm)	Transverse speed (mm/min)	Tool pin Shape
1	1200	45	Squire
2	1400	55	
3	1600	65	
4	1200	45	conical
5	1400	55	
6	1600	65	
7	1200	45	cylindrical
8	1400	55	
9	1600	65	

3.10 Reviews pre or post-welding heat treatment on FSW on dissimilar joints

In order to reduce the metal consumption of machines and structures, increase their service life and reliability, it is necessary to improve the quality of metal products. to form the mechanical properties of metal, heat treatment and plastic deformation are used in practice, generating structural and phase transformations in the system. heat treatment has been studied in detail and practically exhausted. Further progress in solving this problem can be achieved by applying promising deformation methods.

The impact of heat treatment conditions before and/or after welding on the mechanical characteristics of FSW joints has not been extensively studied. The combined effects of rotational speed and pre- and post-heat treatment of (T6) on the mechanical characteristics and micro-structure of semi-solid A356 butt joints were investigated by Boonchouytan et al. **[149].**

Figure 3.23 Heat treatment metal furnace machine

Nevertheless, a higher carbon concentration also makes the steel less weldable. L grades' low carbon content is specifically intended to improve weld ability. To prevent inter-granular corrosion, low-carbon stainless steels like SS304L are frequently utilized **[150].**

Steel is an inexpensive, high-strength structural material **[151].** The most widely used true stainless steel, SS304L, is well known for having remarkable strength and resilience to corrosion. In terms of strength and metallurgical properties, the mechanical joining of stainless steel (SS304L) with dissimilar materials like titanium, ferritic stainless steels, Incone l600, and titanium with nickel interlayer has been extensively studied by Anandaraj et al **[152].**

Figure 3.24 picture of annulling heat treatment in the furnace

results of the annealed Al–Cu alloy's ultrasonic testing. Only welds produced at greater rotational and transverse speeds 1000 rpm and 45 mm were deemed acceptable. The penetration percentages varied widely, and welds with penetration percent ages less than 70% were deemed undesirable. As a result, regardless of transverse speed, very harmful penetration was achieved at low rotating speed (630 rpm).

It is important to note that appropriate welds should exhibit a penetration rate of 90% or higher; a 100% penetration percentage is not anticipated because the pin length was selected to be 2 mm less than the welded plate thickness.

3.11 Thermal simulation

Complex continuous problems can be solved using the Finite Element Method (FEM), which breaks them down into a number of straightforward, connected problems. A geometry is created in ANSYS Design Modeller for simulation purposes based on the dimensions of the experimental setup. The material's mechanical and thermal reactions during the friction stir welding process are examined using finite element simulations. A transient thermal solver workstation is chosen for this investigation in order to verify the experimental welding temperature. The temperature distribution simulation during a friction stir welding process was examined in the current study using finite element program ANSYS 21.R2.

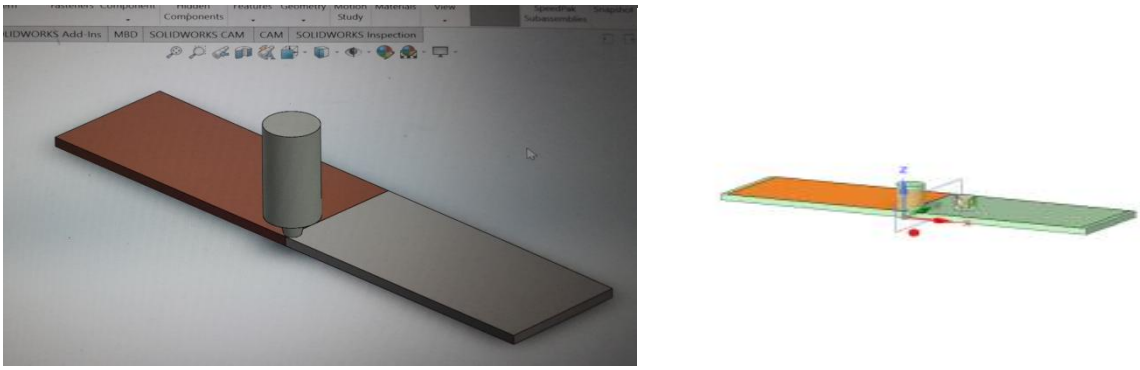

Figure 3. 25: 3-D modeling of the work-piece

To facilitate the solution process, the model was discreetness hexa-hedral elements using ANSYS

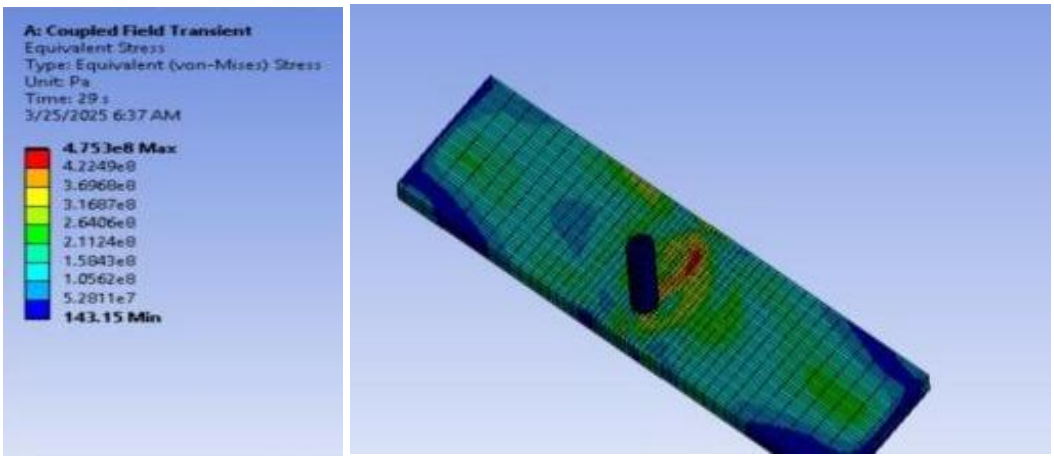

Figure 3. 26: Finite Element meshing of the work-piece

- ✓ The discretion joint surface of the plates to be welded was exposed to a moving heat source with a time step of 4, 8 and 12 seconds.
- ✓ Using the tool's axial force constant then vary rotating speed, and dwell time , the heat source was computed using the heat generation equation.
- ✓ Based on experimental setup dimensions a geometry for the simulation purpose is drawn in ANSYS design modeler the size is 220 mm x 50 mm x 5 mm modeling is designed.
- ✓ The model was discretized mush into 100,000 hexahedral elements to help the solution process using body sizing of element size 0.001m in ANSYS meshing.
- ✓ During the material type and property input standard material mechanical property chemical property and others taken from the material file manager
- ✓ Among the three pin profile cylindrical pin profile is selected for both Ansys and baques simulation result

CHAPTER FOUR

RESULTS AND DISCUSSION

4.1. Introduction

In this work, the optimization of FSW parameters on the selected quality characteristics has been examined using the primary effects plots based on the obtained data from the experiments. This chapter gives the overall results of the experiments using the application of Taguchi and Grey relational analysis method. The experiment was conducted to find the optimum response of hardness and tensile strength of SS-304L & CU-2.04 Plates with butt joint configuration.

4.2. Experimental results

The experiments were carried out in order to investigate the impact of process parameters over the output response characteristics of hardness and tensile strengths. A series of welding tests were performed to find out how welding factors affect the hardness and tensile strength of SS-304L & CC-2.04 material. Experimental results of the hardness and tensile strength of SS-304L & CC-2.04 materials with different process parameters are presented.in Table 4.1 average

Table 4.1 Experimental result

NO.	**Tool material [Type]**	**Dwell time [Sec.]**	**Traverse speed [mm/min]**	**Rotational speed [RPM]**	**Tool shape [Type]**	**UTS [MPa]**	**UTS [MPa] Average**	**Hv [HRH]**	**Hv [HRH] Average**
1	Wc-Co	8	45	1200	Square	216	**239**	87.3	**94.5**
2	Wc-Co	8	45	1400		217		105.6	
3	Wc-Co	8	45	1600		284		90.4	
4	Wc-Co	12	55	1200		177		92.4	

5	Wc-Co	12	55	1400	Conical	279	**251**	109.3	**104.3**
6	Wc-Co	12	55	1600		297		111.1	
7	Wc-Co	12	65	1200	Cylindrical	267	**265**	79.9	**79.0**
8	Wc-Co	12	65	1400		202		69.7	
9	Wc-Co	12	65	1600		326		87.5	
10	Wc-Co	4	55	1400	Conical	261	**256**	100.7	**93.5**
11	Wc-Co	4	55	1600		312		79.1	
12	Wc-Co	4	55	1200		196		100.9	
13	Wc-Co	4	65	1400	Cylindrical	257	**252**	64.6	**78.0**
14	Wc-Co	4	65	1600		277		87.3	
15	Wc-Co	4	65	1200		222		82.7	
16	Wc-Co	8	45	1400	Square	264	**280**	88.1	**81.9**
17	Wc-Co	8	45	1600		294		79.3	
18	Wc-Co	8	45	1200		281		78.5	
19	Wc-Co	12	65	1600	Cylindrical	267	**235**	98.5	**89.5**
20	Wc-Co	12	65	1200		196		85.7	
21	Wc-Co	12	65	1400		242		84.2	

22	Wc-Co	8	45	1600	Square	248	**237**	107.1	**98.5**
23	Wc-Co	8	45	1200		226		97.5	
24	Wc-Co	8	45	1400		237		91.0	
25	Wc-Co	4	55	1600	Conical	272	**241**	76.1	**83.7**
26	Wc-Co	4	55	1400		257		82.2	
27	Wc-Co	4	55	1200		194		92.8	

4.2.1. Tensile Strength

A UTM machine conducted a tensile test. It was found that three crucial elements of the friction stir welding process are tool geometry, traverse speed, and rotating speed. It is found that the most significant parameter among them is tool geometry. The UTS values of square tool geometry ar superior to those of conical and cylindrical tools.

The maximum tensile The highest stress a material can bear when being stretched or pulled is known as its ultimate strength which is before failure or fracture. The maximum tensile strength result was 280 MPa obtained from Squire pin profile tool at a rotation speed of 1600 rpm with a traverse speed of 45.5 mm/min. At 8 second Correspondingly, The lowest tensile strength test result was, 235 MPa, observed at a rotational speed of 1200 rpm, traverse speed of 65 mm/min, dwell time of 4 seconds with Cylindrical tools. When using Pure CU-2.041 and SS-304L separately, the FSW weld joint's tensile strength was 65.84% and 47.13%, respectively. The weld joint's ultimate tensile strength of 280 MPa indicates that, with a square pin profile and 1600 rpm 45.5 mm/min, the weld joint is 65.84% efficient to the weak base metal. This indicates that when the welded area zone result of tensile strength grows, with respect to the traverse speed minimizes and its rotational speed increases because the lower traverse speed and higher rotational speed produce adequate heat for joining the base metal and gives higher tensile strength.

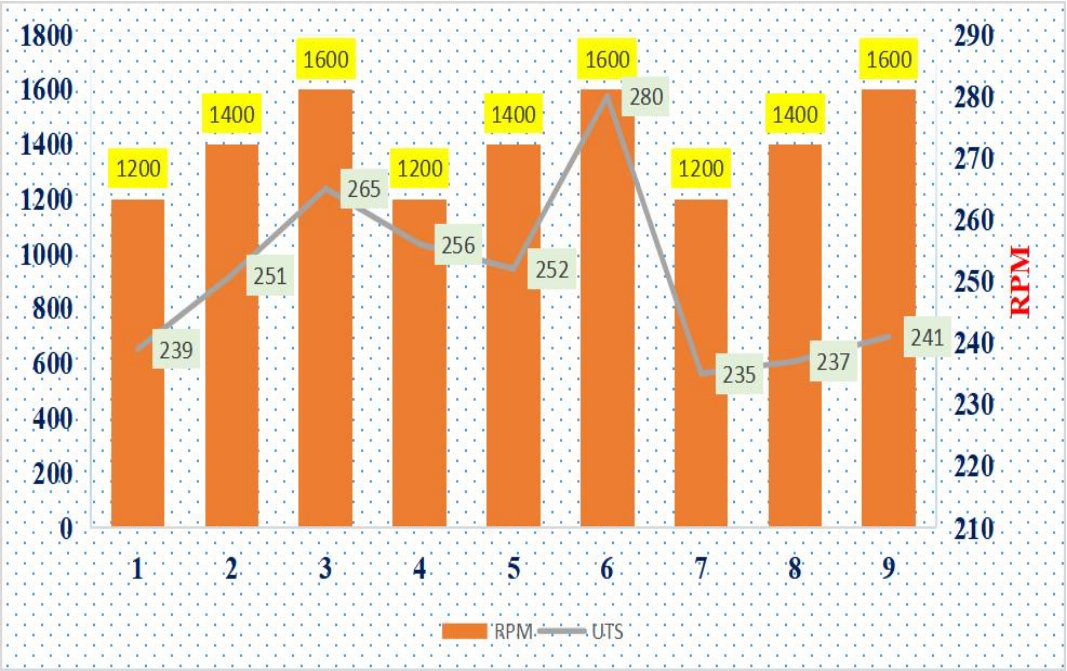

Figure 4. 1: RPM VS Tensile strength

The graph shows that the tensile strength was increased at a combination setting of the higher rotational speed and the lower traverse speed.

4.2.2. Hardness

The application of hardness testing enables you to evaluate a material's properties, such as strength, ductility and wear resistance, and so helps you determine whether a material or material treatment is suitable for the purpose you require

The hardness of the joint was measured three times at the nugget zone. The higher hardness value of total 9 samples is 104.3 HRF was obtained at a rotational speed of 1600 rpm, traverse speed of 55 mm/min and taper conical tool pin profile. Similarly, the minimum hardness value at sample 5, was 78 HRF was recorded at a rotational speed of 1200 rpm, traverse speed of 65 mm/min and cylindrical tool pin profile. The higher rotational speed with a combination of a taper conical tool pin provides the highest hardness. The rotational speed with a combination of traverse speed and tool shape contributes a great influence on the hardness of the joint.

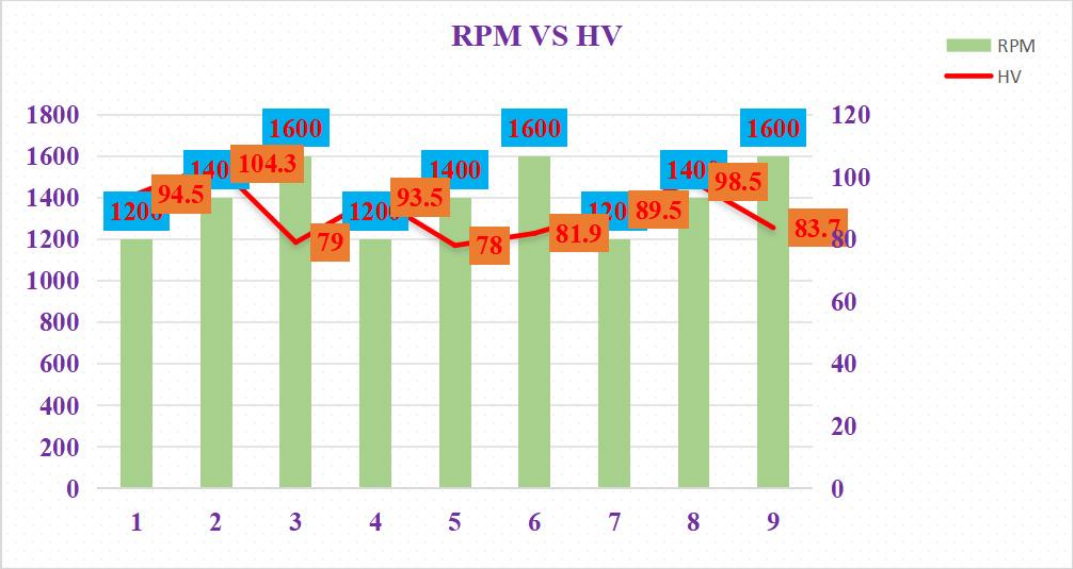

Figure 4.2 Relationship B/N RPM and HV

According to the graph, the target material achieves its maximum hardness at a Conical tool pin profile compered to other welding tool pin profile. due to the fact that the quantity of heat generated during the churning operation determined the joint's hardness.

4.2.3 Microscopic Examination

The stir zone or nugget zone (SZ), the base metal, the heat affected zone (HAZ), and the thermos-mechanical heat affected zone (TMAZ) are the four different metallo-graphic zones of friction stir welding. The regions' significant deformations during tool movements cause the grains to recrystallize. Re-crystallization causes the formation of fine or tiny grains in the stir zone. The size and form of the grains changed in TMAZ. The heat-affected zone that follows TMAZ is where precipitation affects the zone's characteristics. The base metal is the final region, and its micro-structural and physical characteristics remain unchanged **[148].** Smaller grains generally lead to increased strength and hardness due to more grain boundaries that hinder dislocation movement. After UTS and HV results, create three samples of the specimen that has the best mechanical properties then, Cutting the specimen precisely to the necessary testing size from the sample is the first stage in a micro-structural test. Each sample is chopped into a two-centimeters-long specimen using a consumable high-speed rotating disc abrasive cutter.

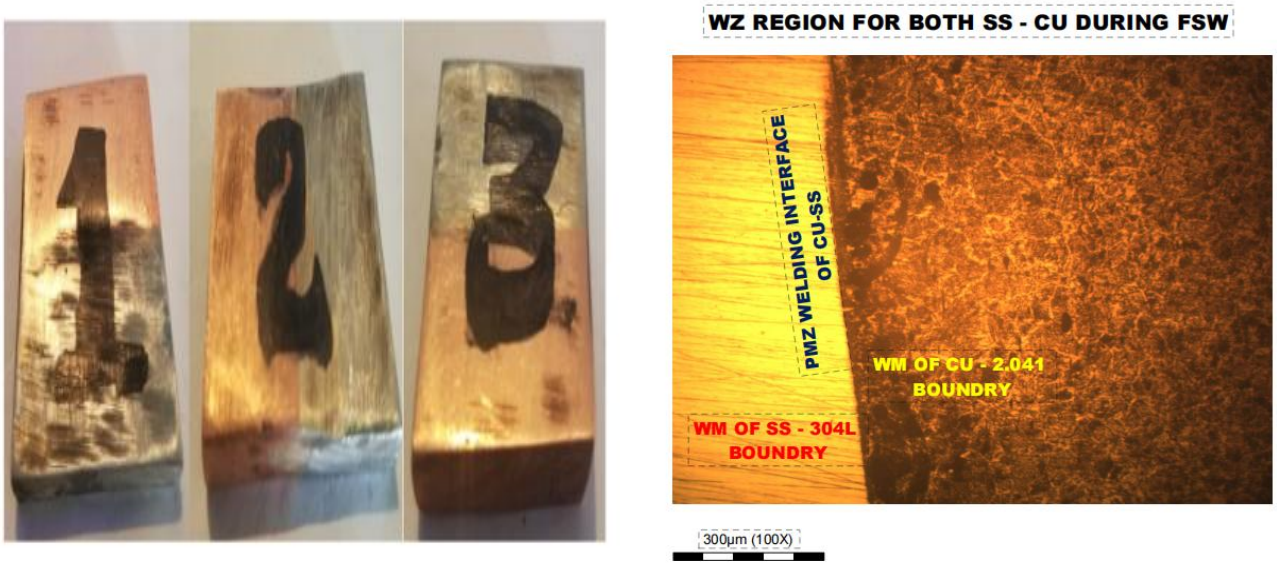

Figure 4.3 Optical micro-structural sample preparation and WZ observation

Micro-structural test sample preparation and selection where done from their best results of UTS and HV welded joints by different welding parameters. The welded joints were obtained by different welding parameters without grooving or preheating. Joints with excellent bonding was observed in the back of the joint. For micro-structures test, 3 samples were prepared with selected optimized parametric result. In terms of the micro-structural observational test result sample 2, show low Void defect level due to the low RPM input parameter from all three samples.

- ✓ Sample 3, show sound weld with Good Phase boundaries and inter-phase due to the squire pin profile welding tool among others.
- ✓ Smaller grains generally lead to increased strength and hardness due to more grain boundaries that hinder dislocation movement.
- ✓ Result shown that at 300 micro meter with x 100 magnification optical microscope welding zone interface
- ✓ Due to different microscopic resolution observation two distinct micrometer optical view

  A. Microscopic observation 60 micrometer with 500 magnification of welding zone and HAZ

  B. Microscopic observation 150 micrometer with 200 magnification of welding zone and HAZ

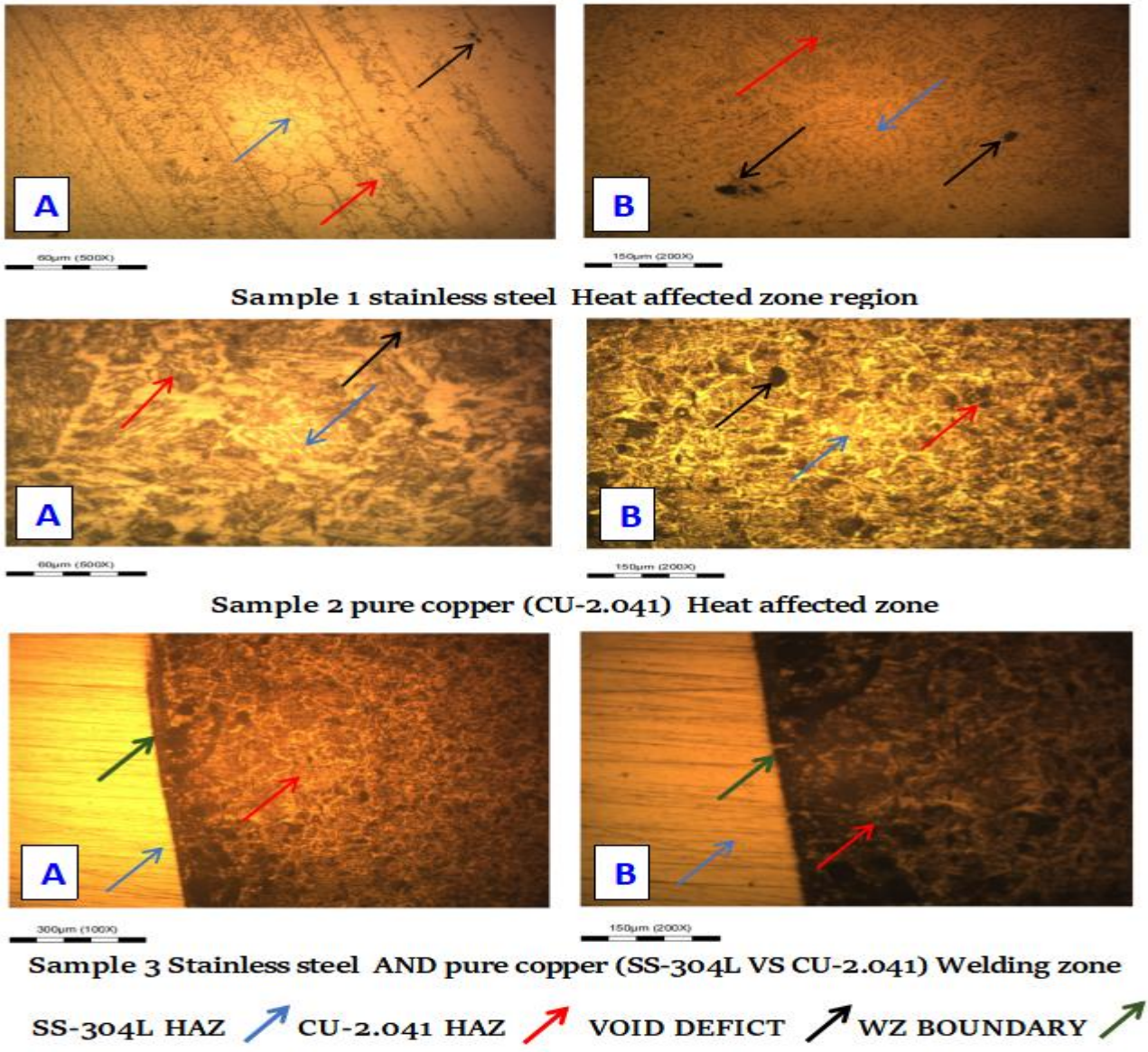

B.

Figure 4.4 Optical micro-structural observation HAZ,BM,WZ, welding interfaces

On figure displays the weld zone micro-structures at the three joints. There is a greater quantity of CU melting as the joints transition from welding FSW. Consequently, there was a notable improvement in the weld's SS content. The MST examination revealed that the optical observation of their welding interface between SS-CU HAZ levels in the weld joints 1, 2, and 3 Conducted, respectively indicated in The coarsening copper grain was therefore visible in the weld zone of joint 1, which was made up entirely of the copper phase, as illustrated in Fig. 4.4. There were two separate phases in the weld as the CU content increased.

4.3 Results for pre -welding heat treatment on FSW of SS304l - CU2.041

In the FSW final result, the joint in SS304L Normal condition will be harder or more difficult to weld than the material's pre-heat treated strength because the heat treatment pre-welding solution greatly enhanced the smoothness and weld-ability of SS304L condition joints. Also examined were the effects of FSW and pre-welding heat treatment on the properties of different materials.

Heat treatment prior to welding in dissimilar SS304L and CU2.041 FSW joints. The plates underwent annealing, FS welding, pre-welding control, and testing. When paired with the pre-welding heat treatment, the joints had a tensile strength and hardness of 82–86% of the SS304L – CU2.041.

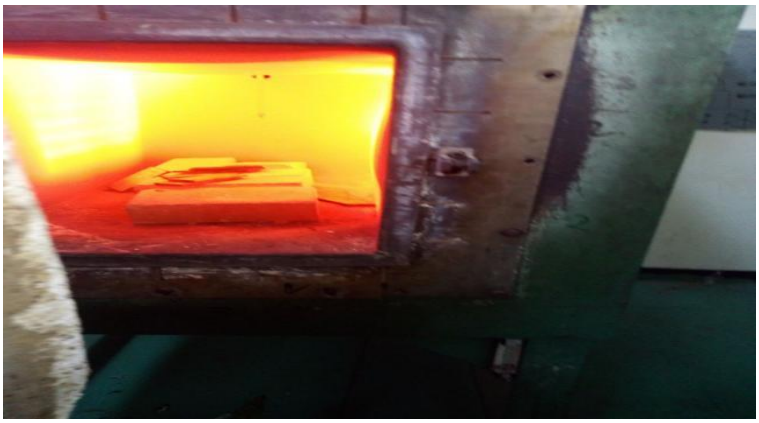

Figure 4.5 Heat treatment process

The microstructure and mechanical characteristics of an SS304L/CU2.041 dissimilar friction stir welded alloy were examined in relation to the impact of heat treatment (pre-weld). In solution-treated, solution-treated and aged, and pre-weld heat treatment circumstances, optical analysis of the dissimilar friction stir-welded SS304L/CU2.041 joints showed welds absence of defects. Additionally, different zones—namely, the base material (BM), heat affected zone (HAZ), and thermomechanical affected zone—were noted throughout the weld region.

Due to the production of the strengthening precipitates, the SS304L/CU2.041 dissimilar friction welds with varying heat treatment conditions indicated exceptional mechanical properties. Conversely, the condition's mechanical properties were the most presumably as a result of the strengthening precipitates dissolving

during friction welding. The SS304L/CU2.041 dissimilar friction weld circumstances were found to fail at the SS304L side's HAZ, away from the weld interface. This suggests that the weld region was stronger than the weakest base metal (CU2.041) in the different joints.

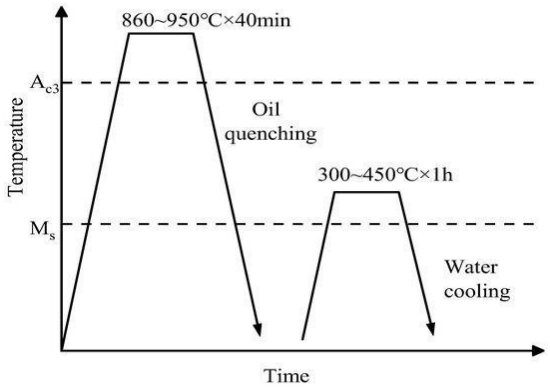

Figure 4.6 Temperature VS Time Heat treatment process graph

Because of their superior mechanical performance at higher temperatures, austenitic stainless steels are widely employed in petrochemical and nuclear settings. These steels are also resistant to oxidation and corrosion. These steels are categorised according to their carbon content as "L," "straight," or "H" grades. The carbon content of the L grades is 0.03%, that of the straight grades is 0.03–0.08%, and that of the H grades is 0.04–0.10%. H grades are more tougher and more wear-resistant due to their high carbon content.

The H grades are appropriate for high-temperature applications because of their increased carbon content, which allows them to maintain their strength and hardness at higher temperatures. Nevertheless, a higher carbon concentration also makes the steel less weldable. L grades' low carbon content is specifically intended to improve weldability. SS304L and other low-carbon stainless steels are frequently used to prevent inter-granular corrosion.

The dissimilar SS304L/CU2.041 welds in this investigation were prepared utilizing the continuous friction stir welding process. The influence of heat treatment on the micro-structural and mechanical properties was evaluated under different conditions.

- ✓ Defect-free dissimilar SS304L/CU2.041 welds with no solidification cracking, fissure cracks, or imperfect bonding could be attained using the continuous friction welding process.
- ✓ The macro-structure of dissimilar SS304L/CU2.041 welds revealed a higher flash on the SS304L side and less flash on the CU2.041 side, owing to a sharp reduction in flow stress in the SS304L at high temperatures.
- ✓ Among all the weldments, the dissimilar SS304L/CU2.041 weldment in the condition showed a higher strength and lower elongation. This could be attributed to the formation of strengthening precipitates.
- ✓ To obtain the best combination of mechanical properties, while keeping the practical difficulties of welding large components in mind, a dissimilar SS304L/CU2.041 friction stir welded joint should be welded in a solution-treated condition and subjected to post-weld heat treatment

To summarize, in addition to processing parameters, the effect of pre - heat treatment only on joint quality for different alloys. the effect of pre-heat treatment conditions alone on the properties of FSW joints of SS304L – CU2.041 alloy and the role of the pre-welding heat treatment on reducing strength loss and consequently reducing the need for pre-welding heat treatment. Pre welding heat treatment processes are usually used to eliminate the variation in material properties in the weld regions, specifically, strength recovery. The complexity of pre welding processes lies in the need for the additional and sometimes customized and costly facilities, set-ups, and equipment to treat welded structures. Therefore, reducing the complexity or eliminating the need for pre-welding heat treatment will lead to lower welding processing costs. The research question at hand is whether a specific pre-welding heat treatment of a selected plate SS304L – CU2.041 will result in better FSW joint quality better penetration percentage and mechanical properties, mainly hardness and wear rate hence eliminating or reducing the need for costly and complex pre-welding heat treatment. In addition, copper particles were used to increase the alloy's strength and hardness as well as to make it heat treatable.

4.4. Transient thermal simulation Result

ANSYS Workbench 21.R2 software has been used to simulate the Friction Stir Welding process using a shoulder diameter model moving heat source. The thermal behaviour during the friction stir welding of SS-304L and CU-2.041plates is the sole topic of the current simulation. Transient thermal analysis was used to simulate the temperature distribution curves for the simulation.

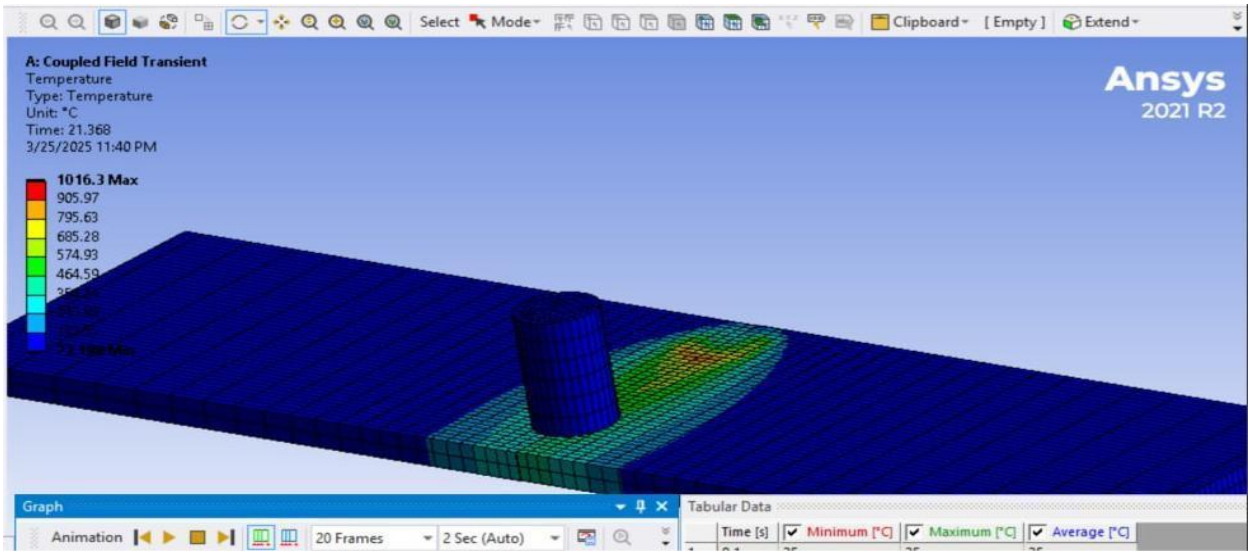

Figure 4.7 Coupled field transient of SS-304L with CU-2.041and simulation

The temperature contours that were simulated in SS-304L and CU-2.041 plates at a rotational speed of 1600 and a constant axial force are depicted in the above Figure . Changing the welding parameters of rotating speed and dwell duration allows for the plotting of all temperature contours.

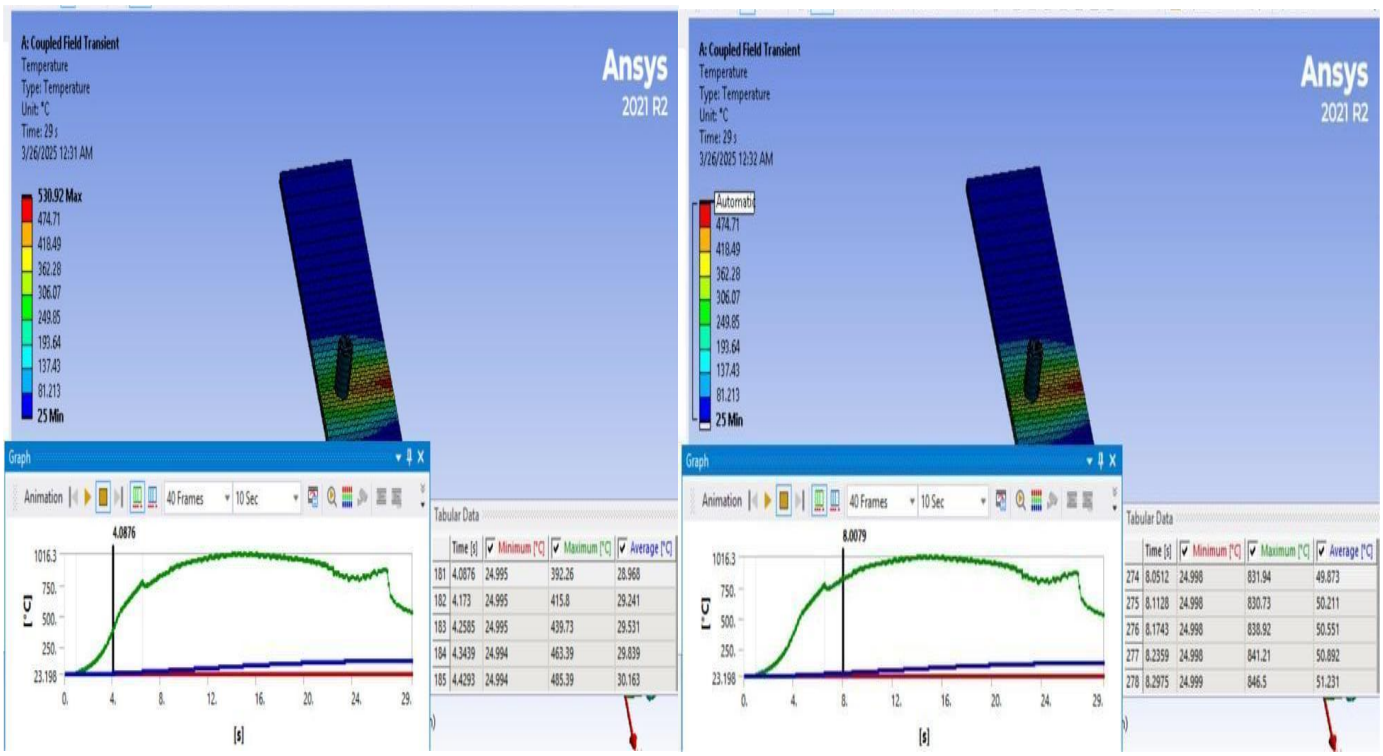

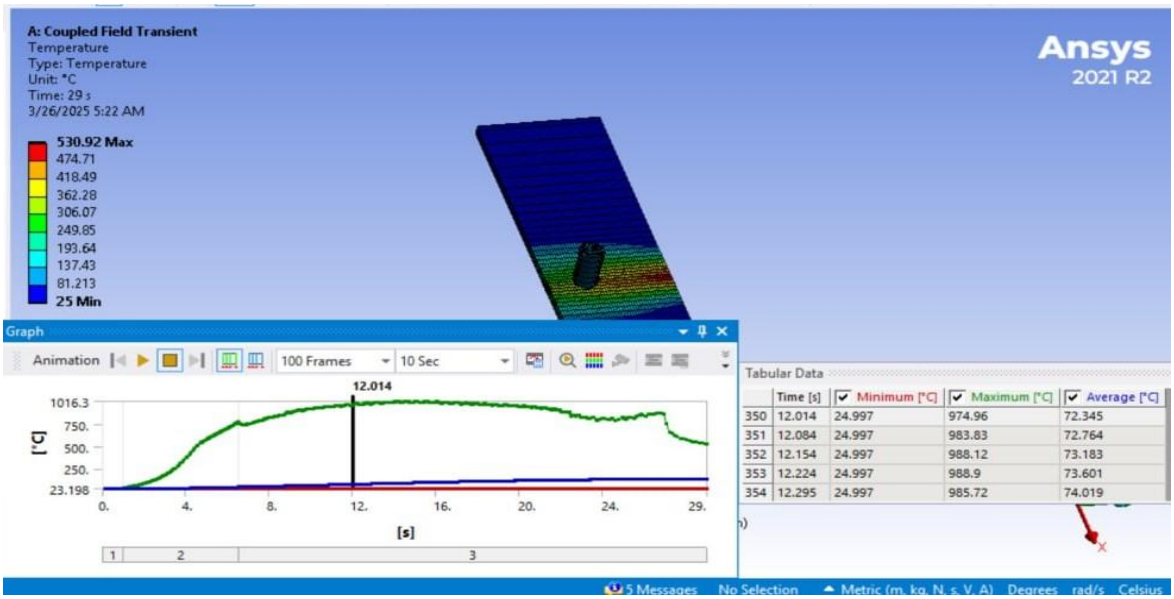

Figure 4.8 Temperature contour of SS-304L and CU-2.041 at various positions

The highest temperature of 1016.3 was reached at a Dwell time of 12 second and a rotational speed of 1600 rpm. At a combination of rotational speed and dwell duration of 1200 rpm and 4 second, respectively, the lowest temperature of 243.6 was also recorded. Based on the simulation figures above, slight temperature variations between 0 and 22 oC have been generated on the experimental work in comparison to the simulation results. Furthermore, the modelling and experimental data show a temperature difference, which is shown below the table.

NO. sample	Dewll Time in seconds	Max. Temp. on FSW Experment [°C]	Max. Temp. on Ansys Simulation [°C]	Experimental Temp. VS Simulated Temp Assessment %
1	4	376.25	392.26	0.042
2	8	849.37	831.94	0.021
3	12	964.21	974.96	0.012

Table 4.2 Experimental Temp. VS Simulated Temp assessment in %

The experimental temperature was slightly different from the modelling results, which vary from 0 to 22 o C, according to the above table. Furthermore, the welding zone area temperatures in the simulation findings are identical. In summary, the simulated results and the experimental temperature result are more similar. This indicates that there hasn't been any temperature measurement inaccuracy. Thus, during the welding process, the experimental temperature results are precise and safe.

Recently, some researchers have simulated FSW using FEM and studied the influence of process parameters and tool geometry on material flow, welding time, and temperature and strain distributions during friction stir processing.

In this work, a finite element model (FEM) is established to study the different temperatures in simulated vs time during friction stir welding (FSW) evolution of SS304L/CU2.041 alloy. To this aim, first, the RPM at different temperatures and strain rates were carried out. Next, a continuum based coupled Transient thermal simulation FEM model was proposed in Deform-3D software to simulate the FSW of SS304L/CU2.041 alloy. To evaluate temperature distribution of the weld zone a model is proposed based on the combination of software and experimental result.

Results: Temperature distribution, strain distribution and welding zone are achieved through the effects of rotational speed and dwell time on the difference of mechanical properties

Conclusion: There is a good agreement between results of numerical models and experiments in the aspects of welding RPM, temperature record and dwell time which was taken during the experimental process of FSW of SS304L/CU2.041.

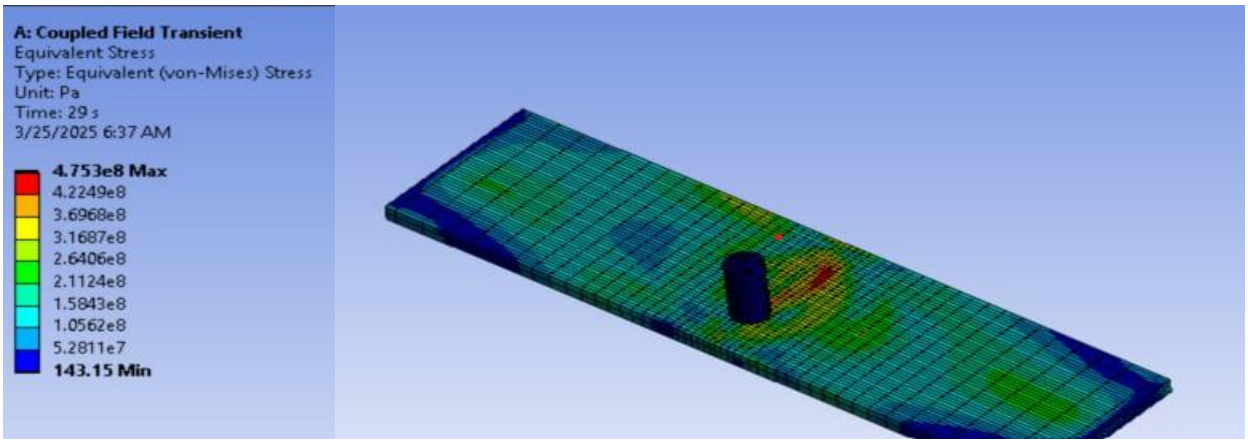

Figure 4.9 Mush of SS-304L and CU-2.041 at various positions

In this work, a finite element model is established to study the temperature distribution evolution during FSW of SS304L/CU2.041 alloy. The hardening parameter, the recovery parameter, and the strain rate sensitivity, required for the model, are investigated according to flow stress results.

Results show that the simulated temperature distribution of the weld zone has a good agreement with that of the experiments. The proposed model can simulate the dynamic re-crystallization process during friction stir welding and predict the grain size and micro-structure of the weld zone precisely. The Simulated temperature distribution under different process parameters reveals that by increasing the RPM and welding time parameter. When welding time is increased drastically from 4 second to 29 seconds The temperature is increased directly with the same 1600 RPM The combination of high temperature, as a result of frictional heat, and high strain rate, due to the severe proper welding tool geometry to come-up with better plastic deformation, leads to generation of semi- recrystallized grains in the stir zone.

Welding temperature obtained by numerical simulation are approximately 18% - 20% higher than experimental temperature, which means that the FSW process can be successfully simulated with FEM.

We can conclude that the largest maximum experimental measured values of the temperature are obtained in the first 3 points of the experimental plan where the dominant factor is the diameter of the shoulder of the tool of 18 mm. In the central points of the experimental plan where the diameter of the shoulder is 16 mm, small temperature values are obtained, where the average temperature at a distance of 10 mm from the joint line is 392.26 ◦C, and at a distance of 27 mm from the first edge of the joint, is 831.94 ◦C in the upper zone.

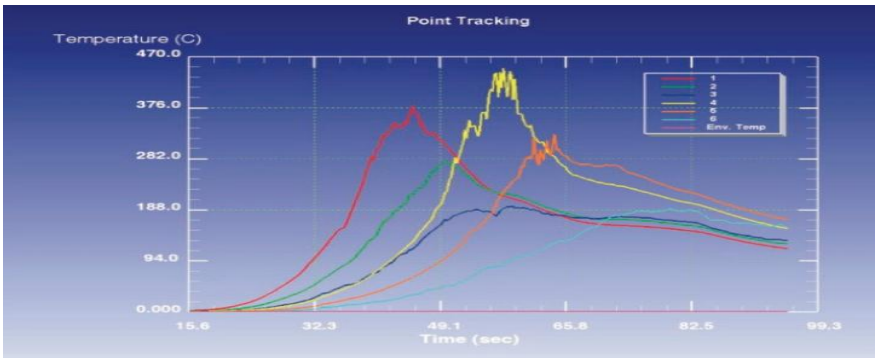

Figure 4.10 The resulting temperature diagram

The resulting temperature diagram numerical simulations at the First selected point of the experimental plan. Next 2nd and 3rd temperature diagram numerical simulations will be followed up

In the points of the experimental plan from 12 to 20 mm, where the smaller diameter of the tool 15 mm, a significantly lower temperature value is obtained. The numerical simulations also distinguish three temperature regions in which the temperature values are analogous to the experimental results.

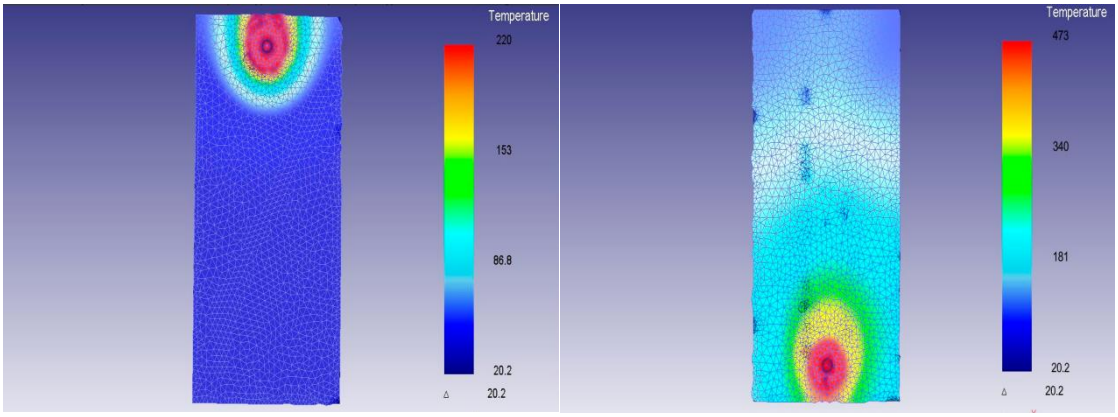

Figure 4.11 Distribution of temperature fields: (a) At the end of the first phase of FSW process; (b) at the end of the second phase of FSW process.

A comparison of experimentally obtained temperature values with the values obtained by numerical simulation shows a relatively good agreement with the difference below 0% - 20%. This allows the conclusion that heat generation and temperature distribution within the work-piece in the FSW process can be successfully simulated by FEM.

For the defined measurement positions of the work piece temperature in the micro-structural zones in the Point Tracking sub-module, the results for the central points of the experimental plan are shown in Figure ,

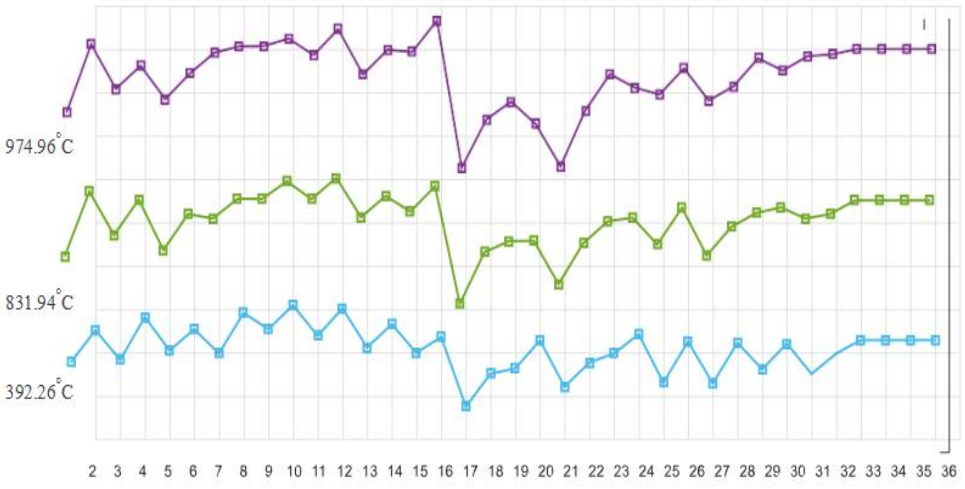

Figure 4.12 The Ansys temperature difference at starting at the middle and at the end diagram

Table 4.3 Point Tracking (Temperature ˚C)

No.	1	2	3	4	5	6
1.	392.26	219.31	170.23	371.82	263.51	161.90
2.	831.94	783.85	593.96	658.62	581.47	487.19
3.	974.96	878.42	693.17	745.10	828.03	687.62

Table 4.3 shows the maximum values of the received temperature values in the adopted measuring points for 4 and 8 and 12 seconds of the point for experimental plan.

Since point P_3 is closest to the joint line, at this point we have the highest values of the numerically generated temperature. The lowest value of the temperature at point P_1 is in the 1st simulation and is 392.26 ˚C. At point P_1 located in the lower zone and 10 mm from the joint line, from the selected dwell time for analytical comparison the highest temperature value was obtained in the P_3 is located in the upper zone at a distance of 27 mm simulation, which is 974.26 ˚C.

On the total of simulation for the points P1, P2, P3 and P4, The lowest temperature values were obtained from the point P1 of the upper zone, at a distance of 10 mm from the joint line is 392.26 ◦C. Point P4 is located in the upper zone at a distance of 32 mm from the joint line,which is the highest temperature of all obtained was in the final numerical simulation which is 1016.3 ◦C

4.5. Effect of welding parameters on the joint quality

Table 4.3: Effect of welding parameters on the joint quality

No	RPM	T.S	Strength property	Welding joint	Observation
1A	Welding tool Squire pin profile 1600	46.4	UTS = 280 HRF = 78.0	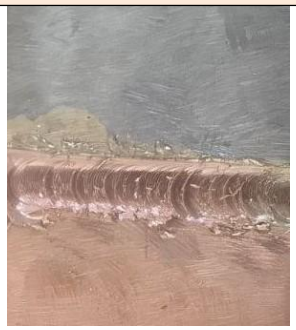	Name of the defect: Defect free (i) Location of the defect: Nil (ii) Reason for the defect: Nil
2B	Welding tool conical pin profile 1400	54.2	UTS = 251 HRF = 104.3		Name of the defect: Defect free (i) Location of the defect: Nil (ii) Reason for the defect: Nil
3C	Welding tool Cylindrical pin profile 1400	64.5	UTS = 265 HRF = 79.0		Name of the defect: Flash (i) Location of the defect: both at the A.S and R.S (ii) Reason for the defect: very high RPM **[153]**
4C	Welding tool Cylindrical pin profile 1200	46.4	UTS = 256 HRF = 93.5	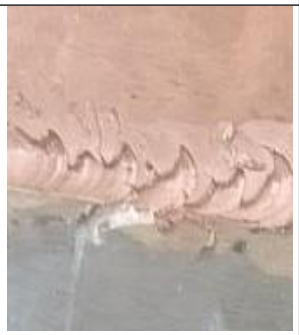	Name of the defect: Defect free (i) Location of the defect: Nil (ii) Reason for the defect: Nil

6C	Welding tool Squire pin profile 1200	54.2	UTS =228 HRF = 50		Name of the defect: Defect free (i) Location of the defect: Nil (ii) Reason for the defect: Nil
7A	Welding tool conical pin profile 1600	64.5	UTS = 252 HRF = 87.9		Name of the defect: Flash (i) Location of the defect: Retreating Side (ii) Reason for the defect: Very high RPM
9B	Welding tool conical pin profile 1600	46.4	UTS = 239 HRF = 94.5		Name of the defect: Defect free (i) Location of the defect: Nil (ii) Reason for the defect: Nil **[153]**

T.S- Tensile strength [MPa] and HRH- Rockwell Hardness in scale F

Despite having flash defects on the retreating and advancing sides, Experiments 1A, 1B, 2C, 3B, 4A, and 6A have the highest hardness and tensile strength compared to the other experiments because of their lower traverse speed and higher RPM. However, there are some cavity and void flaws in the stir zone in Experiments 2B, 3C, 4B, 4C, 6C, 7A and 9B.

Table 4.4: Experimental results of UTS & HV

Sample No.	Rotational Speed (rpm)	Welding speed (mm/min)	Dwell time	Tool pin profile	Ultimate Tensile Strength (MPa)	Hardness value (HV)
1	1200	45	8	Square	239	94.5
2	1400	55	4	Conical	251	104.3
3	1600	65	12	Cylindrical	265	79.0
4	1200	55	4	Conical	256	93.5
5	1400	65	12	Cylindrical	252	78.0
6	1600	45	8	Square	280	81.9
7	1200	65	12	Cylindrical	235	89.5
8	1400	45	8	Square	237	98.5
9	1600	55	4	Conical	241	83.7

4. 6 Taguchi - based Grey analysis

Finding the increased hardness and tensile strength that correlate to improved welding performance is the goal of this study. It is necessary to compute the signal-to-noise ratio in order to identify those tests. Consequently, To determine the signal-to-noise (S/N) ratio, the Taguchi technique offers three options: greater is better, nominal is best, and smaller is better. Nevertheless, choosing a suitable S/N ratio requires some experience, practical knowledge, and process comprehension. Consequently, a larger is better S/N ratio was chosen. The following formula was used to calculate it **[154].**

$$\frac{S}{N}(\eta) = -10 \log 10 \frac{1}{n} \sum_{i=1} \frac{1}{y^2_{ijk}}^n \quad (1)$$

Where *n* is the number of replications and *yijk* is the ith performance characteristic's response value at the kth trial of the jth experiment. The results of UTS, Hv and their S/N ratios are given in Table 4.

Table 4.5 : Experimental results with its S/N ratio

Sample No.	Ultimate Tensile Strength (MPa)	Hardness value (HV)	S/N UTS	S/N HV
1	239	94.5	47.5680	39.5086
2	251	104.3	47.9935	40.3657
3	265	79.0	48.4649	37.9525
4	256	93.5	48.1648	39.4162
5	252	78.0	48.0280	38.8798
6	280	81.9	48.9432	37.8419
7	235	89.5	47.4950	39.0365
8	237	98.5	47.4214	39.8687
9	241	83.7	47.6403	38.4545

4.6.1 Grey relational analysis

Grey relational analysis (GRA) is a useful technique for multi-response condition optimization. This analysis technique was employed to resolve the complex relationships between the multi-objective replies. For the purpose of optimizing numerous responses, GRA contains seven steps **[155].**

The steps listed below were taken in this study: Mono-objective optimization, or the Taguchi method's use to optimize just one parameter, is one of its disadvantages. It is simple and efficient to optimize several parameters when Taguchi is combined with a Grey relational analysis method **[156].**

Steps of Grey relational analysis to optimize multiple responses

- ✧ Start
- ✧ Normalize the S/N ratio data
- ✧ Derivation sequence
- ✧ Calculating grey relational grade
- ✧ Selecting optimum parameter from GRG rank
- ✧ perform analysis of variance
- ✧ Compare confirmatory experimental results and Predicted GRG values THEN END

4.6.2 Principal Component Analysis

PCA, or principal component analysis, has been utilized to eliminate the response correlation. This matrix consists of Eigenvalues, Eigenvectors and quality characteristics contributions. The array's components for the various performance attributes mentioned in Table 4.6- 4.8 represent the grey relational coefficient matrix and determine the corresponding Eigenvalue.

Table 4. 6: Eigen values and explained variation (Appendices 140)

Principal component	**Eigen values**	**Explained Variation (%)**
UTM	1.5823	79.1
Hv	0.4179	20.9

The principal component with the highest Eigenvalues is decided to substitute the initial answers for additional examination. In this case, the highest Eigenvalues were obtained in the UTS first principal component. Then, the contribution of each individual quality characteristic for the first principal components is shown in Table 4.7

Table 4. 7: The Eigenvectors for principal component (Appendices 140)

Quality characteristic	**Eigenvector**	
	1st principal	2nd principal
UTS	-0.707	-0.707
Hv	0.707	-0.707

Table 4. 8: Quality characteristic contribution

UTS	0.4999
Hv	0.4999

Therefore, the gray relational coefficients values are taken $\xi = 0.5$ is used.

4.6.3 Data normalization

On the Grey relational analysis method the first step finding the data normalization of s/n ratio for both ultimate tensile stress as well hardness so, it should have a process of conveying the original sequence to a comparable sequence. For which reason, the experimental results are normalized in the range between zero and one. The process is necessary when the sequence scatter range is too large, or when the direction of the target in the sequence are different **[157]**.

$$x^{(k)} = \frac{x_i^0(k) - \min x_i^0(k)}{\max x_i^0(k) - \min x_i^0(k)} \qquad (2)$$

If the response is to be maximized, then larger is better characteristics are intended for normalization to scale it into an acceptable range **[154].** The reference sequence, i = 1, 2, m; k = 1, 2..., n; m is the number of experiment and n is the number of experimental data.

4.6.4 Calculation of deviation sequences and Gray relational coefficients

The GRC is used to Describe how the reference sequence and the comparability sequence are related. The GRC (ξ) is calculated to integrate the data achieved from equations **[156]**. The next step is to calculate the Gray relational coefficient, ξi (k) from the normalized values

$$\Delta_{0i}(k) = \|x_{0*}(k) - x_{i*}(k)\| \qquad (3)$$

$$(x_{0*}(k), x_{0*}(k)) = \frac{\Delta_{min}(k) + \xi\Delta_{max}(k)}{\Delta_{0i}(k) + \xi\Delta_{max}(k)} \qquad (4)$$

it is necessary to calculate the deviation sequences before the calculation of the GRC. The deviation sequences are calculated using equation (3). Where $\Delta_{0i}(k)$ is the deviation sequence of the reference

sequence $x_0*(k)$ and comparability sequence $x_i*(k)$ and ξ is the defining factor that has a value between 0 and 1 and the value of ξ = 0.5 is taken from the calculation result.

Table 4. 9 Data normalization and Deviation sequence

Step 1: Data normalized			Step 2: Deviation sequence	
No	**UTM**	**HV**	**UTM**	**HV**
1	0.0963	0.6604	0.9037	0.3396
2	0.3759	1.0000	0.6241	0.0000
3	0.6857	0.0438	0.3143	0.9562
4	0.4885	0.6238	0.5115	0.3762
5	0.3986	0.4112	0.6014	0.5888
6	1.0000	0.0000	0.0000	1.0000
7	0.0484	0.4733	0.9516	0.5267
8	0.0000	0.8031	1.0000	0.1969
9	0.1438	0.2427	0.8562	0.7573

4.6.5 Calculation of gray relational grades

The gray relational grade represents the level of correlation between the reference sequence and comparability sequence. The gray relational grade is a weighted average

of the gray relational coefficients of multi-objective **[158].** It is determined as the following equation

$$\gamma(x_{0*}, x_{1*}) = \frac{1}{n}\sum_{i=1}^{n} wi\xi(x_{0*}(k), x_{i*}(k)) \quad (5)$$

Where $\gamma_i(x_{0*}, x_{1*})$ is the GRG for the i^{th} experiment, *wi* is the weighting value of the i^{th} performance characteristic and *n* is the number of performance characteristics.

Table 4. 10 Gray relational grades and Coefficient

Step 3: Grey relational Coefficient			Step 4: Grey relational grade and it is rank	
No	**UTM**	**HV**	**GRG**	**Rank**
1	0.3562	0.5955	0.4759	6
2	0.4448	1.0000	0.7224	1
3	0.6140	0.3434	0.4787	5
4	0.4943	0.5706	0.5325	3
5	0.4540	0.4592	0.4566	7
6	1.0000	0.3333	0.6667	2
7	0.3444	0.4870	0.4157	8
8	0.3333	0.7174	0.5254	4
9	0.3687	0.3977	0.3832	9
Average GRG = 0.5174				

4.7 Determination of the optimal level of each parameter

As shown in Table 4.11, which displays the average of each answer characteristic for each level of each factor, the main effect analysis of GRG is used to determine the response table for gray relational analysis. The highest minus the lowest average of each factor is the delta static. Based on delta values, Mini-tab ranks the optimal parameters; for example, rank 1 denotes the highest delta value, rank 2 denotes the second, and so forth. The mean response is the average value of the performance characteristic for each parameter at various levels, and these ranks show how important each element is to the response.

The ideal parameter combination for the various performance characteristics is the tool shape of the square pin profile welding tool, dwell time of 8 seconds, traverse speed of 45.5 mm/min, and rotational speed of 1600 rpm, as indicated by the highest GRG value for each parameter in Table 4 and the indicated points in Figure 4. The largest influence on the rotational speed is the welded joint's hardness and tensile strength, according to the results shown in Table 4.11.

Response Table for Means

Table 4.11 : Main Effects means of GRG

Level	Rotational speed [A]	Transversal speed[B]	Dwell time[C]	Welding tool profile[D]
1	0.4414	0.4747	0.5560 *	0.4386
2	0.5519	0.5681 *	0.5460	0.6016 *
3	0.5590 *	0.5095	0.4503	0.5122
Delta	0.1176	0.0934	0.1056	0.1630
Rank	**2**	**4**	**3**	**1**

*** Indicates the optimum value in each parameter**

Response Table for Signal to Noise Ratios

Larger is better

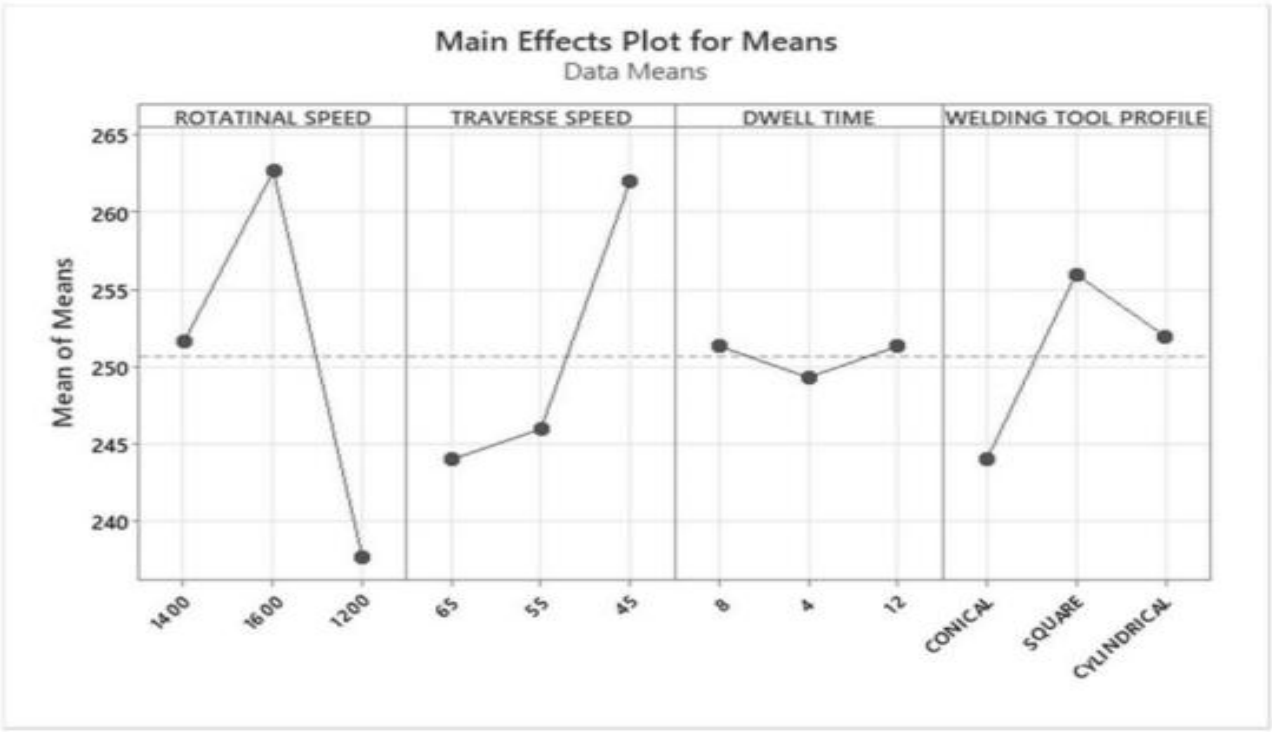

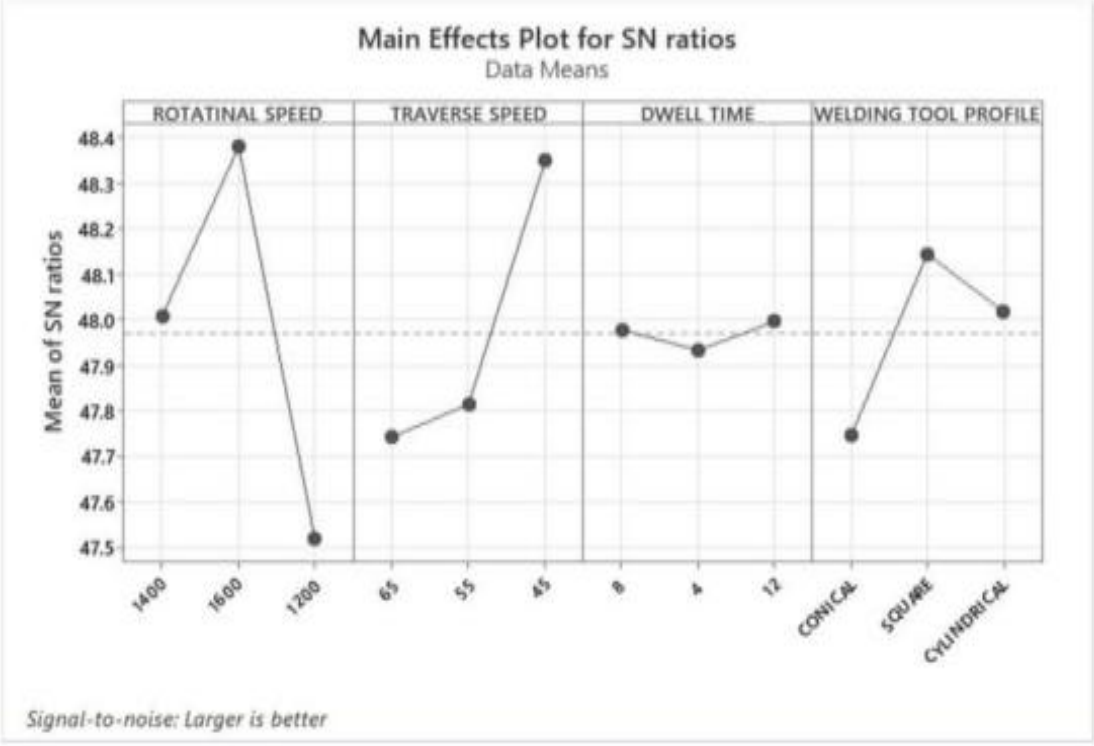

Figure 4.13 signal to noise rato for larber is better

4.8 Performing (ANOVA) Analysis of Variance

To identify important parameters, the Analysis of Variance (ANOVA) was performed. The impact of the factors on the gray relational grade was determined using the ANOVA results. A factor or parameter is deemed significant if the ANOVA table F-value is higher than the F-value reading from a standard table and the P-value for the factor falls below 0.01 at a 99% confidence level **[158].** To ascertain which parameter has a substantial impact on the performance characteristics, statistical software with the analytical method of ANOVA is utilized. Table 4.12 provides the ANOVA results for the gray relationship grades.

The ANOVA results show that the process factors under investigation have a considerable impact on the tensile strength and hardness of FSW joints. The effect is ranked as follows:1) The pin profile of the to ol; 2) The rotating speed of the tool; and 3) The duration of residence.

*DF- Degree of Freedom; SS-Sum of Square; MS-Mean Square; PC- Percentage contribution

Table 4. 12: Analysis of Variance results for GRG

Source	DF	Adj SS	Adj MS	F-Value	P-Value	PC-% Contribution	Remark
Rotational speed	2	0.12608	0.013038	26.4619	0.098	24.3042	Significant
Transversal Speed	2	0.07041	0.010206	13.2802	0.002	11.0761	Significant
Dwe11 time	2	0.10338	0.006690	18.1453	0.091	15.5548	Significant
Tool Pin Profile	2	0.28000	0.020001	68.3261	0.001	47.7176	Significant
Error	2	0.00247	0.00201			1.4474	
Total	10	0.58234				100%	

Each parameter's percentage contribution to the average GRG is computed and displayed. Table 4 illustrates this. The average GRG values were affected by the tool pin profile, tool rotational speed, dwell time and traverse speed by 47.7%, 24.3%, 15.5%, and 11% respectively. As a result, the most significant factor influencing the average GRG values was the tool pin profile. The P value values are Lower than 0.05, which indicates that tool pin profiles have statistical relevance on average GRG results at a 95% reliability level. The findings of the ANOVA show that the process parameters being studied have a substantial impact on the tensile strength and hardness of FSW joints.

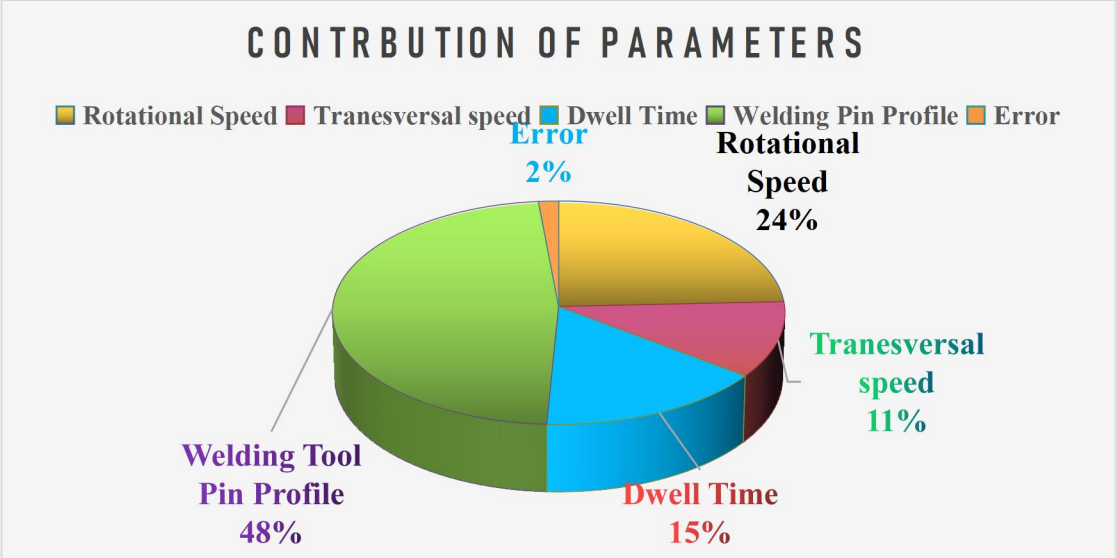

Figure 4.14: Contribution of each welding parameters in ANOVA

4.9 Confirmation Experiment

The confirmation test was carried out on three samples with average values of experiments result with each quality attribute of UTS as-well as HV under ideal FSW parameter setting conditions:

A_3 (rotational speed of 1600 rpm), B_2 (traverse speed of 45.5 mm/min), C_1 (dwell time of 8 seconds), , and , and D_2 (tool shape of square tool). Based on the confirmation experimental results, estimated values for multi-response optimization at the optimal level of parameter setting were validated. The confirmation experiments' 95% confidence interval must contain the average values of the response variables. on a confirmation test was calculated using the following equations **[158]**.

[158], $\mu A1B2 = \acute{\Gamma}GRG + (A1 - \acute{\Gamma}GRG) + (B2 - \acute{\Gamma}GRG) = A1 + B2 - \acute{\Gamma}GRG$

Where $\acute{\Gamma}_{GRG}$ is the overall mean of gray relational grade = 0.6442, $\acute{\Gamma}_{GRG}$ is equal to the overall mean of gray relational grade = 0.6442. A_1 and B_2 are the mean values of gray relational grade with parameters at optimum levels.

$$\mu A3B2C1D2 = 0.5590 + 0.5681 + 0.5560 + 0.6016 - 3 * 0.5174 = \mathbf{0.7327}$$

The confidence interval (CI) for the expected mean on a confirmation run is computed using the following equation [208], which estimates the predicted mean of the grey relational grade in the confirmation test.

Where F ; $(1, fe) = F_{0.05}; (1, 3) = 10.13$ (F-Table in the Appendices 141)

α = Risk = 0.05

N = Total number of experiments = 9

DOF = 3 (F-Table in the Appendices 147)

Ve = Error adjusted mean square (Table 4.12) = 0.00201

n_{eff} = Effective number of replications

r = Number of replications for confirmation experiment = 3

Also the effective number of replications (*neff*) is calculated by:

$$neff = \frac{T}{1+Ts} \qquad \frac{9}{1+2} = 3$$

Where *neff* = is expressed in mathematical,

Tn = Total number of experiments = 9

Ts = the sum of the total degree of freedom of significant factors. Therefore, the calculated CI is

$$CI = \mu \pm \sqrt{F\ Ve * \left(\frac{}{neff} + \frac{}{r}\right)}$$

$$0.7327 \pm \sqrt{10.13 * 0.00201 \left(\frac{}{3} + \frac{}{3}\right)} = 0.11650$$

The 95% confidence interval of the predicted optimal gray relational grade is:

$$(\mu - CI) < \mu < (\mu + CI) \quad \ldots\ldots \quad (9)$$

*

$$= (0.7327 - 0.11650) < 0.7327 < (0.7327 + 0.11650)$$

$= 0.61620 < 0.7327 < 0.84920$

Table 4. 13: Results of confirmation tests

Optimal combination	**The response of quality characteristics**			
A3B2C1D2	**HR**	**HRS/N**	**UTS**	**UTSS/N**
Replication 1	98.3	39.3657	251	51.9935
Replication 2	78.0	37.8419	280	53.4649
Replication 3	89.5	36.0365	235	52.4950
Average	90.6	**113.24**	255.3	**159.95**
Mean of GRG for confirmation test = 0.70797				

The expected GRG under ideal conditions is between 0.61620 and 0.84920 at 95% confidence. The effectiveness of the ideal condition can be guaranteed if the many performance metrics' anticipated and observed GRG values are near to one another. Experiments were carried out Three times under ideal conditions to test the projected outcomes. Hardness and tensile strength were 280 MPa and 78 HV, respectively, and the experiment's gray relational grade was 0.70797, falling within the 95% confidence interval. Thus, the experiment is the safest, according to the findings of the confirmatory experiment testing.

Table 4. 14: Results of the confirmation tests

	Optimal parameters		**Experiment**
	Predicted optimal value (GRG)	Predicted confidence intervals at 95% confidence level	Actual value (Avg. of 3 confirmation test)
Setting levels	**ABCD**	**CI: 0.61620 < μ < 0.84920**	**ABCD**
Tensile strength			280 MPa
Hardness			78 HV
Grey relational grade	**0.7327**		**0.70797**

CHAPTER FIVE

CONCLUSION AND RECOMMENDATIONS

5.1. Conclusion

Most dissimilar metals can be welded using a variety of welding mechanisms, according to various studies. The most recent and best method is FSW. Following the welding process, a combination of the Taguchi method and Grey relational analysis was used to determine the ideal parameters for FSW in order to examine the impact of combined factors, such as UTS and Hv, on mechanical strength. The two dissimilar Ss plates (304l and Cu 2.04) are joined using FSW. The plates are successfully welded, and samples of the welded area are tested using a standard testing machine to measure the welded dissimilar welding metals at room temperature.

- ✧ The number of welding tests in the experiment was determined using the Taguchi L9 orthogonal array. An experimental design based on the L9 orthogonal array was carried out, and GRA was used to analyse the data obtained from the experiments. Testing is done to determine the best possible combination of parameters and how they affect the hardness and tensile strength of the welded joints. Ultimately, the following findings were reached.
- ✧ At a rotating speed of 1600 rpm, traverse speed of 45.5 mm/min, tool shape of square pin profile, and dwell period of 8 seconds, the maximum tensile strength of 280 MPa were attained at sample 6.
- ✧ Similarly, At a rotating speed of 1200 rpm, traverse speed of 65 mm/min, tool shape of Cylindrical pin profile, and dwell period of 4 seconds, the minimum tensile strength of 235 MPa were attained at sample 7.
- ✧ The hardness of the joint was measured three times at the nugget zone. The higher hardness value is found at samples 2, 104.3 HRF was obtained at a rotational speed of 1600 rpm, traverse speed of 55 mm/min and taper conical tool pin profile with 12 second.
- ✧ Similarly, the minimum hardness value at sample 5, was 78 HRF it recorded at a rotational speed of 1200 rpm, traverse speed of 65 mm/min and cylindrical tool pin profile with 4 second.

- ✧ The experiment and ANOVA show that the hardness of the stir zone, the creation of defects, and ultimately the tensile strength of friction stir SS 304L & CU 2.04 materials are significantly influenced by the rotating speed, traverse speed, tool shape, and dwell time.

- ✧ In contrast to cylindrical and tapered conical welding Tool, a square welding tool pin profile with a traverse speed of 45.5 mm/min and a rotation speed of 1600 rpm produces a sound weld for Ss-304L materials at sample 6.

- ✧ Welding temperature is influenced by dwell duration, traverse speed, and rotating speed. The welding temperature climbed and reached its maximum hardness and tensile strength as the rotational speed and dwell duration increased. The welding temperature, dwell time, and rotational speed all have an indirect relationship with traverse speed. Furthermore, the joint strength had a significant impact on the tool profiles. The maximum temperature of 635°C was recorded at the Square tool pin profile, which is 14.34% lower than the cylindrical tool pin profile liquid temperature of Ss-304L (965°C).
- ✧ The results of ANOVA indicate that the RPM, traverse speed, tool shape, and dwell duration are significant features at a 99% confidence interval.
- ✧ For hardness and tensile strength, the respective contributions of tool shape, traverse speed, dwell duration, and rotating speed were 47.7%, 24.3%, 15.5%, and 11.0%.

In conclusion, distinct process parameters produce distinct outcomes, and a mix of controlled and uncontrolled parameters yields noteworthy outcomes. The hardness and tensile strength of SS-304L and CU-2.04 material were found to be more significantly influenced by the parameters of rotational speed, traverse speed, tool shape, and dwell duration. For FS welding of SS-304L and CU-2.04 material, controllable factors/parameters yield a superior result over uncontrolled / noise factors.

5.2. Recommendations

- ✓ Its highly difficult to prepare welding tool pin profile by using conventional machine so, before having the experiment welding tool should be ready with requested design and fully manufactured from upgraded welding tool company.
- ✓ The gripper on the tensile testing apparatus makes it challenging to hold the specimens. The welded specimens preparation should be taken into consideration before beginning because of the machine gripper's holding space diffidence in position and space.
- ✓ At the moment, Ethiopia does not have access for advanced CNC milling machine with an axial load-controlled so, axial load is not regulated in CNC milling machines currently therefore, utilize such as the most recent CNC machine with a force controller helps to investigate the axial force.
- ✓ Different shoulder characteristics and a range of shoulder diameters on the tool aid in achieving the right temperature and stirring action. It should be noted that a laboratory instrument is an issue that requires resolution.
- ✓ It's also very difficult to find diverse testing equipment like UTS testing machine and also CNC milling machine. Higher education institutions would be better off considering importing the equipment to further researching their manufacturing, optimization, and mechanical testing studies.

5.3. Future Research Direction

People are always trying to develop more and more modified techniques that are successful, stunning, and effective. The following research gaps were identified by interested authors and may need further investigation:

- ✓ This thesis is used tungsten carbide as a welding tool , but it can be applied for other tools which will give upgraded result as well-as characteristics of the welding.
- ✓ Only UTS and HV where examined in mechanical property's in the future it can be included other mechanical properties.
- ✓ The adequate heating during the stirring operation will be enhanced by the use of tools with features on the shoulder and the pin. To optimize the stirring instrument, this research scenario can be expanded to execute FSW for ferrous metals.

Reference

[1]. Asadi, Mohammad Kazem Besharati Givi and Parviz. 2014. Advances in Friction Stir Welding. Wood head Publishing. 2014. Advances in Friction Stir Welding and Processing. london: Wood head Publishing. 8**,** 2493-2498.

[2] W. M. Thomas, E. D. Nicholas, C.N. James, S. Walden, M. G. Murch, P. Temple-Smith, C. J, Dawes, Friction welding, Weld. J. (Miami, Fla). 78 (1991) 56.

[3] K.N. Zaman, A.N. Siddiquee, Z.A. Khan, Friction Stir Welding: Dissimilar Aluminium Alloys, 2017. 31**,** 395-404.

[4] Zhou H., Lee J., Kang M., Kim H., Lee H., In J. Bin. All Laser-Based Fabrication of Microchannel Heat Sink. Mater. Des. 2022;221:110968. doi: 10.1016/j.matdes.2022.110968.Davis, Joseph R., ed. (1994). Stainless Steels. ASM Specialty Handbook. Materials Park, OH: ASM International. ISBN 9780871705037. Archived from the original on 14 April 2021. Retrieved 8 March 2020.2**,** 69-75.

[5] Gibsona, B.T.; Lammlein, D.H.; Prater, T.J.; Longhurst, W.R.; Cox, C.D.; Ballun, M.C.; Dharmaraj, K.J.; Cook, G.E.; Strauss, A.M. Friction stir welding: process, automation and control. Journal of Manufacturing Processes 2014, 16(1)

[6] Z. Zhang, H.W. Zhang, Numerical studies on controlling of process parameters in friction stir welding, Journal of Materials Processing Technology 209/1 (2019)

[7] Y Zhang, Y S Sato, H Kokawa, et al. Stir zone microstructure of commercial purity titanium friction stir welded using PCBN tool. Mater. Sci. Eng.-Lausanne- A, 2008, 488(1–2): 25–30

[8] Chen C, Zhang H, Zhao S, Ren X. Effects of sheet thickness and material on the mechanical properties of flat clinched joint. Front Mech Eng 2021. https://doi.org/ 10.1007/s11465-020-0618-y.

[9] Mubiayi, M.P.; Akinlabi, E.T. Friction stir welding of materials between steeliness steel alloys and copper-An overview. In proceedings of the world congress on engineering, London, U.K, July 2013. 978-988.

[10] Nandan, T. DebRoy and H. K. D. H. Bhadeshia: 'Recent advances in friction stir welding – process, weldment structure and properties', Prog. Mater. Sci., 2008, 53, 980–1023.

[11] A. Esmaeili, M. K. Besharati-Givi and H. R. Zarei Rajani: 'A metallurgical and mechanical study on dissimilar friction stir welding of aluminum 1050 to brass (CuZn30)', Mater. Sci. Eng. A, 2011, 528, 7093–7102

[12] Schmidt, H.N.B.; Dickerson, T.L.; Hattel, J.H. Material flow in butt friction stir welds In AA2024-T3. Acta Mater. 2006, 54, 1199–1209.

[13] NOOR ZAMAN KHAN, A. N. S. A. Z. A. K. 2017. Friction Stir Welding: Dissimilar Aluminium Alloys, CRC Press. 38**,** 544-554.

[14] Arun Kumar N., Srinivasan V., Krishna Kumar P., Analysing the strength of unidirectional fibre orientations under transverse static load, International Journal of Applied Engineering Research, v7749-7754, 2014. 11**,** 12258-12261.

[15] Akos meilinger and imre torok, The importance of friction stir welding Tool, Production Processes and Systems, vol. 6, 2013, no. 1, Pp. 25-34.

[16] Epstein, N., Heat Exchanger Theory and Practice. In Heat exchangers, J. Taborek and G. ewiĴ (Eds.), 1983. In Heat Exchanger Theory and Practice: McGraw-Hill. Incorporea, F., D. Dewitt, T. Bergman, and A. Lavine. 2011. Fundamentals of heat and mass transfer, 7th ed. New York: Wiley. 231**,** 571-583.

[17] Steinhagen, R., H. Müller-Steinhagen and K. Maani, Problems and costs due to heat exchanger fouling in New Zealand industries. Heat Transfer Engineering, 1993. 14(1): pp. 19–30.

[18] Hoang, T.A., H.M. Ang and A.L. Rohl, Effects of temperature on the scaling of calcium sulphate in pipes. Powder Technology, 2007. 179(1): pp. 31–37.

[19] KUMAR, S. R. K. R. A. P. 2016. Optimization of Process Parameters of Friction Stirs Welding of Aluminum Alloys (6061) Using Taguchi Method. International Journal of Science and Research, 5, 1988-1994.

[20] K.V.P.P CHANDU, E. V. R., A.SRINIVASA RAO AND B.V.SUBRAHMANYAM 2014. The Strength of Friction Stir Welded Aluminium Alloy 6061. International Journal of Research in Mechanical Engineering & Technology, 4, 119-122.

[21] MFX MUTHU, JAYABALAN V. Tool travel speed effects on the microstructure of friction stir welded aluminum–copper joints [J]. J Mater Process Technol. 2015; 217:105–113.

[22] ERICSSON M, SANDSTRÖM R. Influence of welding speed on the fatigue of friction stir welds, and comparison with MIG and TIG. Int J Fatigue. 2003;25(12):1379–1387

[23] Abdollah-zadeh A, Saeid T, Sazgari B. Microstructural and mechanical properties of friction stir welded aluminum/copper lap joints. J Alloys Compd. 2008; 460(1):535–538.

[24] T. Ding, H.-g Yan, J.-h Chen, W.-j Xia, B. Su, Effect of welding speed on microstructure and mechanical properties of Al—Mg—Mn—Zr—Tialloy sheet during friction stir welding, Trans. Nonferrous Met. Soc. China 31 (2021) 3626–3642.

[25] G. Nagesh, Nageswara Rao, K. Kkanishk, K.M. Anurag, N. Abhinav, Investigation of mechanical properties on non-ferrous alloys of copper and brass joints made by friction stir welding, IOP Conf. Ser. Mater. Sci. Eng. 1057 (2021), 012062.

[26] K.P. Mehta, V.J. Badheka, Influence of tool pin design on properties of dissimilar copper to aluminum friction stir welding, Trans. Nonferrous Met. Soc. China 27 (2017) 36–54

[27] R. Beygi, M. Zarezadeh Mehrizi, A. Akhavan-Safar, S. Safaei, A. Loureiro, L.F.M. da Silva, Design of friction stir welding for butt joining of aluminum to steel of dissimilar thickness: heat treatment and fracture behavior, Int. J. Adv. Manuf. Technol. 112 (2021) 1951–1964.

[28] K. Praneetha, M. Apoorva, T. Prasanna Laxmi, S. Ravi Sekhar, S. Sravan Sashank, Experimental investigation on aluminium alloy AA6082 and AA2014 using the friction stir welding, Mater. Today Proc. 62 (2022) 3397–3404.

[29] S. Jannet, P. Mathews, R. Raja, Comparative investigation of friction stir welding and fusion welding of 6061 T6–5083 O aluminum alloy based on mechanical properties and microstructure. Bulletin of the Polish Academy of Sciences, Tech. Sci. 62 (2014) 791–795

[30] R.S. Mishra, Z.Y. Ma, Friction stir welding and processing, Mater. Sci. Eng. R Reports. 50 (2005) 1–78.

[31] KHAN, N. Z., SIDDIQUEE, A. N., AL-AHMARI, A. M. & ABIDI, M. H. 2017. Analysis of defects in clean fabrication process of friction stir welding. Transactions of Nonferrous Metals Society of China, 27, 1507-1516.

[32] S.L. J, G. Bharathiraja, V. Jayakumar, A review on Friction Stir Welding in Aluminium Alloys, IOP Conf. Ser. Mater. Sci. Eng. (2020) 15. https://doi.org/10.1088/1757- 899X/954/1/012007.

[33] Zhang Dawei, Zhang Qi, Fan Xiaoguang and Zhao Shengdun. 2018. "Review on Joining Process of Carbon Fiber-Reinforced Polymer and Metal." Methods and Joining Process 47 (12).

[34] Aritoshi M, Okita K. Friction welding of dissimilar metals. Weld Int 2003;17:271–5. https://doi.org/10.1249/01.mss. 0000538518.76078.fa.

[35] Joon-Tae Yooa, Jong-HoonYoona, Kyung-Ju Mina and Ho-Sung Lee. 2015. "Effect of Friction Stir Welding Process Parameters on Mechanical Properties and Macro Structure of Al-Li alloy." Procedia Manufacturing 2: 325 – 330

[36] Chirag G. Dalwadi, Anjal R. Patel, Jaydeep M. Kapopara, Dhrupal J. Kotadiya, Nikul D. Patel, H. G. Rana. 2018. "Examination of Mechanical Properties for Dissimilar Friction Stir Welded Joint of Al Alloy (AA-6061) to PMMA (Acrylic)." Materials Today 5: 4761–4765.

[37] Ponte M., Adamowski J., Gambaro C. and Lertora E. (2005) 'Low Cost transformation of a conventional milling Machine into A Simple FSW Work Station' Advanced Manufacturing Systems and Technology, CISM Courses and Lectures No.486, Springer Wien New York.

[38] Siddiqui M.A, Jafri S.A.H., Bharti P.K and Kumar P., (2014) 'Friction Stir Welding as a Joining Process through Modified Conventional Milling Machine' A Review, International Journal Of Innovative Research & Development July, Vol 3 Issue 7.

[39] SHAH, P. H. & BADHEKA, V. J. 2017. Friction stir welding of aluminium alloys: An overview of experimental findings–Process, variables, development and applications. Proceedings of the Institution of Mechanical Engineers, Part L: Journal of Materials:

[40] Mishra, R.S.; Mahoney, M.W. Friction stir welding and processing; ASM international, 2007

[41] Davis, Joseph R., ed. (1994). Stainless Steels. ASM Specialty Handbook. Materials Park, OH: ASM International. ISBN 9780871705037. Archived from the original on 14 April 2021. Retrieved 8 March 2020.

[42] Thomas W.M., Staines D.G., Norris I.M., De Frias R., 'Friction stir welding tool and developments' The Welding Institute, TWI Ltd (UK).

[43] Esmaeili, A., et al., The role of rotation speed on intermetallic compounds formation and mechanical behavior of friction stir welded brass/aluminum 1050 couple. Intermetallics, 2011. 19(11): p. 1711-1719.

[44] Galvão, I., et al., Influence of tool offsetting on the structure and morphology of dissimilar aluminum to copper friction-stir welds. Metallurgical and Materials Transactions A, 2012. 43(13): p. 5096-5105.

[46]. Mehta, K.P. and V.J. Badheka, A review on dissimilar friction stir welding of copper to stillness steel: process, properties, and variants. Materials and Manufacturing Processes, 2016. 31(3): p. 233-254.

[47]. Singh, V.P., et al., Recent research progress in solid state friction-stir welding of aluminium–magnesium alloys: a critical review. Journal of Materials Research and Technology, 2020. 9(3): p. 6217-6256.

[48]. Taheri, H., et al., Investigation of nondestructive testing methods for friction stir welding. Metals, 2019. 9(6): p. 624.

[49]. Xue, P., et al., Effect of friction stir welding parameters on the microstructure and mechanical properties of the dissimilar Al–Cu joints. Materials science and engineering: A, 2011. 528(13-14): p. 4683-4689.

[50]. Mehta, K.P. and V. Badheka, Experimental investigation of process parameters on defects generation in copper to AA6061-T651 friction stir welding. International Journal of Advances in Mechanical & Automobile Engineering, 2016. 3(1): p. 55-58.

[51]. Investigations on tunneling and kissing bond defects in FSW joints for dissimilar aluminum alloys. Journal of Alloys and Compounds, 648, 360-367.

[52]. Mishra RS, Mahoney MW, Sato Y, Hovanski Y (2016) Friction stir welding and processing VIII. Frict Stir Weld Process VIII 50:1–300

[53]. Investigations on tunneling and kissing bond defects in FSW joints for dissimilar aluminum alloys. Journal of Alloys and Compounds, 648, 360-367.

[54]. H. K. Mohanty, M. M. Mahapatra, P. Kumar, P. Biswas and N. R. Mandal, Effect of Tool Shoulder and Pin Probe Profiles on Friction Stirred Aluminum Welds – a Comparative Study, J. Marine Sci. Appl., 11: 200-207, DOI: 10.1007/s11804-012- 1123-4, 2012, Pp. 200-207.

[55]. H. K. Mohanty, M. M. Mahapatra, P. Kumar, P. Biswas and N. R. Mandal, Effect of Tool Shoulder and Pin Probe Profiles on Friction Stirred Aluminum Welds – a Comparative Study, J. Marine Sci. Appl., 11: 200-207, DOI: 10.1007/s11804-012- 1123-4, 2012, Pp. 200-207

[56]. A. Arora, A. De and T. Deb Roy, Toward optimum friction stir welding tool shoulder diameter, Acta Materialia Inc. Elsevier, doi:10.1016/j.scriptamat.2010.08.052, 2010, Pp-9- 12

[57]. K. Elangovan and V. Balasubramanian, Mater. Des. 29, 2008, Pp.362.

[58]. Beygi R., Mehrizi M.Z. and Verdera D. (2018) 'Influence of tool geometry on material flow and mechanical properties of friction stir welded Al-Cu bimetals' Journal of Materials Processing Tech. 255, 739–748.

[59]. Krasnowski K., Hamilton C. and Dymek S. (2015) 'Influence of the tool shape and weld configuration on microstructure and mechanical properties of the Al 6082 alloy FSW joints' archives of civil and mechanical engineering 15, 133 – 141.

[60]. Adesina A.Y., Gasem Z.M. and Al-Badour F.A. (2017) 'Characterization and evaluation of AlCrN coated FSW tool: A preliminary study' Journal of Manufacturing Processes 25, 432–442.

[61]. Aguiara T., Verdera D., Leitão C. and Rodrigues D.M. (2016) 'Tool assisted friction welding: A FSW related technique for the linear lap welding of very thin steel plates' Journal of Materials Processing Technology 238, 73–80.

[62]. Wanga F.F., Li W.Y., Shen J., Wena Q. and dos Santos J.F. (2018) 'Improving weld formability by a novel dual-rotation bobbin tool friction stir welding' Journal of Materials Science & Technology 34 135–139

[63]. Smith C. B., Hinrichs J. F. and Ruehl P.C. 'Friction Stir and Friction Stir Spot Welding - Lean, Mean and Green' Friction Stir Link, Inc. W227 N546 Westmound Dr., Waukesha, WI 53186.

[64]. Patel N., Bhatt K.D. and Mehta V. (2016) 'Influence of Tool Pin Profile and Welding Parameter on Tensile Strength of Magnesium Alloy AZ91 during FSW' Procedia Technology 23, 558 – 565.

[65]. Mugada K.K. and Adepu K. (2018) 'Influence of ridges shoulder with polygonal pins on material flow and friction stir weld characteristics of 6082 aluminum alloy' Journal of Manufacturing Processes 32, 625–634

[66]. Tarasov S. Yu., Rubtsov V.E. and Kolubaev E.A. (2014) 'A proposed diffusioncontrolled wear mechanism of alloy steel friction stir welding (FSW) tools used on an aluminium alloy' Wear 318, 130–134.

[67]. Eslami S., Ramos T., Tavares P.J. and Moreira P.M.G.P. (2015) 'Shoulder design developments for FSW lap joints of dissimilar polymers' Journal of Manufacturing Processes 20, 15–23.

[68]. NOOR ZAMAN KHAN, A. N. S. A. Z. A. K. 2017. Friction Stir Welding: Dissimilar Aluminium Alloys, CRC Press.

[69]. XUE P, NI D, WANG D, XIAO B, MA Z. Effect of friction stir welding parameters on the micro-structure and mechanical properties of the dissimilar Al−Cu joints [J]. Materials Science and Engineering A, 2011, 528(13): 4683−4689

[70]. TOLEPHIH M H, MAHMOOD H M, HASHEM A H, ABDULLAH E T. Effect of tool offset and tilt angle on weld strength of butt joint friction stir welded specimens of AA2024 aluminum alloy welded to commercial pure cupper [J]. Chemistry and Materials Research A, 2013, 3(4): 49−58

[71]. MEILINGER, Á. & TÖRÖK, I. 2013. The importance of friction stir welding tool. Production Processes and Systems, 6, 25-34.

[72]. RAJAKUMAR, S., MURALIDHARAN, C. & BALASUBRAMANIAN, V. 2011. Influence of

friction stir welding process and tool parameters on strength properties of AA7075-T6 aluminium alloy joints. Materials & Design, 32, 535-549.

[73]. ELANGOVAN, K. & BALASUBRAMANIAN, V. 2008. Influences of tool pin profile and tool shoulder diameter on the formation of friction stir processing zone in AA6061 aluminium alloy. Materials & design, 29, 362-373.

[74]. MARZBANRAD J, AKBARI M, ASADI P, SAFAEE S. Characterization of the influence of tool pin profile on micro-structural and mechanical properties of friction stir welding [J]. Metallurgical and Materials Transactions B, 2014, 45(5): 1887−1894.

[75]. KUMAR A, RAJU L S. Influence of tool pin profiles on friction stir welding of copper [J]. Materials and Manufacturing Processes, 2012, 27(12): 1414−1418

[76]. VIJAY S, MURUGAN N. Influence of tool pin profile on the metallurgical and mechanical properties of friction stir welded Al−10wt.% TiB 2 metal matrix composite [J]. Materials & Design, 2010, 31(7): 3585−3589.

[77]. PALANIVEL R, MATHEWS P K, MURUGAN N, DINAHARAN I.Effect of tool rotational speed and pin profile on micro-structure and tensile strength of dissimilar friction stir welded AA5083-H111 and AA6351-T6 aluminium alloys [J]. Materials & Design, 2012, 40: 7−16.

[78]. RAMACHANDRAN K, MURUGAN N, KUMAR S S. Effect of tool axis offset and geometry of tool pin profile on the characteristics of friction stir welded dissimilar joints of aluminium alloy AA5052 and HSLA steel [J]. Materials Science and Engineering A, 2015, 639: 219−233.

[79]. PADMANABAN G, BALASUBRAMANIAN V. Selection of FSW tool pin profile, shoulder diameter and material for joining AZ31B magnesium alloy–An experimental approach [J]. Materials & Design, 2009, 30(7): 2647−2656.

[80]. CHEN Y, NAKATA K. Effect of tool geometry on micro-structure and mechanical properties of friction stir lap welded magnesium alloy and steel [J]. Materials & Design, 2009, 30(9): 3913−3919

[81]. CHOWDHURY S, CHEN D, BHOLE S, CAO X. Tensile properties of a friction stir welded magnesium alloy: Effect of pin tool thread orientation and weld pitch [J]. Materials Science and Engineering A, 2010, 527(21): 6064−6075.

[82]. Y.N. Zhang, X. Cao, S. Larose, P. Wanjara, Review of tools for friction stir welding and processing, Can. Metall. Q.51 (2012) 250–261. https://doi.org/10.1179/1879139512Y.0000000015.

[83]. DUBOURG, L. & DACHEUX, P. Design and properties of FSW tools: a literature review. Proceedings of the 6th International Symposium on Friction Stir Welding, Saint Sauveur, Quebec, Canada, 2006.

[84]. KHALILABAD, M. M., ZEDAN, Y., TEXIER, D., JAHAZI, M. & BOCHER, P. The Influence of Tool Geometry on Mechanical Properties of Friction Stir Welded AA-2024 and AA-2198 Joints. 34th conference and exhibition icsoba, 2016.

[85]. VENKATESWARLU, D., MANDAL, N., MAHAPATRA, M. & HARSH, S. 2013. Tool design effects for FSW of AA7039. Welding Journal, 92, 41-47.

[86]. S.L. J, G. Bharathiraja, V. Jayakumar, A review on Friction Stir Welding in Aluminium Alloys, IOP Conf. Ser. Mater. Sci. Eng. (2020) 15. https://doi.org/10.1088/1757- 899X/954/1/012007.

[87]. POELMAN, L. 2012. Characterization of tools for friction stir welding of steels. Department of mechanical construction and production-Laboratory Soete, 6-p7.

[88]. MESHRAM, S. & REDDY, M. 2018. Influence of Tool Tilt Angle on Material Flow and Defect Generation in Friction Stir Welding of AA2219. Defence Science Journal, 68, 512-518.

[89]. SAUMIL K.JOSHI, J. D. G. 2015. Influence of Tool Shoulder Geometry on Friction Stir Welding: A Literature Review. IJRSI, III, 261-264

[90]. MFX MUTHU, JAYABALAN V. Tool travel speed effects on the microstructure of friction stir welded aluminum–copper joints [J]. J Mater Process Technol. 2015; 217:105–113.

[91]. ERICSSON M, SANDSTRÖM R. Influence of welding speed on the fatigue of friction stir welds, and comparison with MIG and TIG. Int J Fatigue. 2003;25(12):1379–1387

[92]. Abdollah-zadeh A, Saeid T, Sazgari B. Microstructural and mechanical properties of friction stir welded aluminum/copper lap joints. J Alloys Compd. 2008; 460(1):535–538.

[93]. Sahin M. Joining of stainless steel and copper materials with friction welding. Ind Lubr Tribol 2009;61:319–24. https://doi.org/10.1108/00368790910988435

[94]. RATHI, R. D. S. A. M. G. 2016. OPTIMIZATION OF FSW PROCESS PARAMETER TO ACHIEVE MAXIMUM TENSILE STRENGTH OF ALUMINUM ALLOY AA6061. International Research Journal of Engineering and Technology, 03, 936-943.

[95]. MURUGAN, R. & THIRUMALAISAMY, N. 2018. Experimental and numerical analysis of friction stir welded dissimilar copper and bronze plates. Materials Today: Proceedings, 5, 803-809

[96]. SHALIN, M. & HITEN, M. 2018. Experimental analysis on effect of tool transverse feed, tool rotational speed and tool pin profile type on weld tensile strength of friction stir welded joint of AA 6061. Materials Today: Proceedings, 5, 487-493.

[97]. GOMATHISANKAR M, G. M. A. P. P. 2018. A Novel Optimization of Friction Stir Welding Process Parameters on Aluminium Alloy 6061-T6. Materials Today: Proceedings, 5, 14397–14404.

[98]. HUSSAIN, M. A., KHAN, N. Z., SIDDIQUEE, A. N. & KHAN, Z. A. 2018. Effect Of Different Tool Pin Profiles On The Joint Quality Of Friction Stir Welded AA 6063. Materials Today: Proceedings, 5, 4175-4182.

[99]. KRISHNA, M., UDAIYAKUMAR, K., KUMAR, D. M. & ALI, H. M. Analysis on effect of using different tool pin profile and mechanical properties by friction stir welding on dissimilar aluminium alloys Al6061 and Al7075. IOP Conference Series:

[100]. SACHIN JAMBHALE, S. K. A. S. K. 2015. Effect of Process Parameters & Tool Geometries on Properties of Friction Stir Spot Welds: A Review. Universal Journal of Engineering Science, 3, 6-11.

[101]. GAOHUI LI, L. Z., WEILU ZHOU, XIAOGUO SONG AND YONGXIAN HUANG 2019. Influence of dwell time on micro-structure evolution and mechanical properties of dissimilar friction stir spot welded aluminium–copper metals. Journal of Materials Research and Technology, 8, 2613–2624.

[102]. KAI CHEN, X. L. A. J. N. 2016. EFFECTS OF PROCESS PARAMETERS ON FRICTION STIR SPOT WELDING OF ALUMINUM ALLOY TO ADVANCED HIGH-STRENGTH STEEL. Proceedings of the ASME 2016 International Manufacturing Science and Engineering Conference.

[103]. Rishikesh Arun Gite, Praveen Kumar Loharkar and Rajendra Shimpi. 2019. "Friction stir welding parameters and application: A review." Materials Today: Proceedings

[104]. Mojtaba Rezaee Hajideh, Mohammadreza Farahani and Navid Molla Ramezani. 2018. "Reinforced Dissimilar Friction Stir Weld of Polypropylene to Acrylonitrile Butadiene Styrene with Copper Nanopowder." Journal of Manufacturing Processes 32: 445–454.

[105]. DHAS, J. E. R. & DHAS, S. J. H. 2012. A review on optimization of welding process. Procedia engineering, 38, 544-554.

[106]. W.H. Yang, Y.S. Tarng, Design Optimisation of Cutting Parameters for Turning Operations Based on the Taguchi Method, Journal of Material Processing Technology 84 (1998), pp. 122-129.

[107]. Mishra RS, Mahoney MW, Sato Y, Hovanski Y (2016) Friction stir welding and processing VIII. Frict Stir Weld Process VIII 50:1–300

[108]. "What is the melting point of stainless steel?" Langley Alloys. Retrieved 23 March 2022.

[109]. Cobb, Harold M. (September 2007). "The Naming and Numbering of Stainless Steels". Advanced Materials & Processes. ASM International. **165** (9). Archived from the original on 27 June 2021. Retrieved 1 October 2021.

[110]. Galvao, I.; Leal, R.M.; Loureiro, A.; Rodrigues, D.M. Material flow in heterogeneous friction stir welding of aluminum and copper thin sheets. Science and Technology of Welding and Joining 2010, 15(8), 654-660. doi: 10.1179/136217110X12785889550109

[111]. Elrefaey, A.; Takahashi, M.; Lkeuchi, K. Preliminary investigation of friction stir welding aluminum/copper lap joints. Welding in the World 2005, 49(3/4), 93-101. doi: 10.1007/BF03266481

[112]. "Introduction". Copper properties and uses. SchoolscIence.co.uk.

[113]. Chung, DDL (2001). "Materials for thermal conduction" (PDF). Applied Thermal Engineering. 21 (16): 1593–1605. doi:10.1016/s1359-4311(01)00042-4

[114]. NOURANI, M., MILANI, A. S. & YANNACOPOULOS, S. 2011. Taguchi optimization of process parameters in friction stir welding of 6061 aluminum alloy: A review and case study. Engineering, 3**,** 144.

[115]. Cobb, Harold M. (September 2007) International Manufacturing Science and Engineering Conference.

[116]. S.K.Selvam, and Dr. T.Parameshwaran Pillai, "Comparison Of Heavy Alloy Tool In Friction Stir Welding," International Journal of Engineering Science and Technology (IJEST), vol. 4, no. 12, pp. 1-10,

[117]. Ronald W. Armstrong, The Hardness and Strength Properties ofWC-Co Composites, Materials 2011,

[118]. H.J. Liu, J.C. Feng, H. Fujii, K.Nogi, Wear characteristics of aWC–Co tool in friction stir welding of AC4AC30 vol%SiCp composite,International Journal of Machine Tools & Manufacture 45 (2005)

[119]. Bhadeshia and T. DebRoy, Review no friction stir welding tools, Science and Technology of Welding and Joining, (2011) VOL16.

[120]. R. Rai, A. De, H. Bhadeshia and T. Deb Roy, Review: friction stir welding tools, Institute of Materials, Minerals and Mining, Science and Technology of Welding and Joining, Vol.16, No.4, 2011.

[121]. ASTM E92-82, Standard Test Method for Vickers Hardness of Metallic Materials, ASTM Int. 82 (2004) 1–9.

[122]. R. Unal, E.B. Dean, Taguchi approach to Design optimization for Quality and Cost: an Overview, Proceeding of the International Society of Parametric Analyst 13 th Annual (May 21-24, 1991)

[123]. E.M. Trent, Metal Cutting, 3rd. Edition, Butterworth Heinemann, London, 1991.vol. 3, no. 12, pp. 1-10

[124]. ELATHARASAN, G. & KUMAR, V. S. 2013. An experimental analysis and optimization of process parameter on friction stir welding of AA 6061-T6 aluminum alloy using RSM. Procedia Engineering, 64, 1227-1234.

[125]. CELIK, S. & CAKIR, R. 2016. Effect of friction stir welding parameters on the mechanical and micro structure properties of the Al-Cu butt joint. Metals, 6, 133.

[126]. Chen S, Huang J, Xia J, Zhang H, Zhao X. Microstructural characteristics of a stainless steel/copper dissimilar joint made by laser welding. Metall Mater Trans A Phys Metall Mater Sci 2013;44:3690–6. https://doi.org/10.1007/s11661-013- 1693-z.

[127]. Rajakumar S, Muralidharan C, Balasubramanian V. Influence of friction stir welding process and tool parameters on strength properties of AA7075-T6 aluminium alloy with copper (ETP-Cu) joints.

[128]. Bina, M.H., Dehghani, F., Salimi, M., 2013. Effect of heat treatment on bonding interface in explosive welded copper/stainless steel. Mater. Des. 45,

[129]. Aval, H.J. Micro-structural Evolution and Mechanical Properties of Friction Stir-Welded C71000 Copper–Nickel Alloy and 304 Austenitic Stainless Steel. Int. J. Miner. Metall. Mater. 2018, 25, 1294–1303. [CrossRef]

[130]. Takehiko Watanabe, Hirofumi Takayama, Atsushi Yanagisawa, "Improving friction stir welding between copper c10100 and 304L stainless steel, Journal of Materials Processing Technology 178 (2006) 342–349

[131]. Steel, S. Packer, (2011). "Improving friction stir welding between copper and 304L stainless steel". Proceedings of the Twenty-first International Offshore and Polar Engineering Conference. IV: 530-533.

[132]. Balasubramanian et al, (2010). Friction Stir Welding of Austenitic Stainless Steel by PCBN Tool and Its Joint Analyses" Materials and Design. 3: 4592–4600.

[133]. K. Okamoto, M. Doi, S. Hirano, K. Aota, H. Okamura, Y. Aono, and T.C. Ping., "characterization and processing of friction stir welding on copper with AL & SS welds Department of Mechanical Engineering), retrieved May 16, 2010, "A variation of FSW, called friction stir processing (FSP), uses the same general setup and tools as FSW, but is used to selectively modify the microstructure of materials to enhance specific properties."

[134]. Kamachi Mudali U, Ananda Rao BM, Shanmugam K, Natarajan R, Raj B. "Friction stir welding of dissimilar Al 6013-T4 To X5CrNi18-10 stainless steel. J Nucl Mater 2003;321:40–8.

[135]. Sterling, Colin J. (August 2004), "Effects of Friction Stir Processing on the Micro structure and Mechanical Properties of Fusion Welded 304L Stainless Steel" (PDF), Thesis (MSc) (Provo, UT, U.S.A.: Brigham Young University, CD-ROM]. Proc. 3rd Int. Symp.on Friction Stir Welding, Kobe, Japan, 2001, September 27-28

[136]. Yang, T., Chou, P., "Solving a Multiresponse Simulation-Optimization Problem with Discrete Variables Using a Multiple-Attribute Decision-Making Method", Mathematics and Computers in Simulation, 68: 9–21, (2005)

[137]. Dengiz, B., "Redesign of PCB Production Line with Simulation and Taguchi Design", Proceedings of the 2009 Winter Simulation Conference, 2197-2204, (2009).

[138]. Chang, C.Y., Huang, R., Lee, P.C., Weng, T.L., "Application of a Weighted GreyTaguchi Method for Optimizing Recycled Aggregate Concrete Mixtures", Cement & Concrete Composites 33:1038–1049,

[139]. Kabir, G., and Hasin, M.A.A., "Comparative Analysis of AHP and Fuzzy AHP Models for Multicriteria Inventory Classification", International Journal of Fuzzy Logic Systems (IJFLS) Vol.1, No.1,

[140]. Chang, D.–Y., Zhu, K.–J., Jing, Y., "A Discussion on Extent Analysis Method and Applications of Fuzzy AHP", European Journal of Operational Research, 116:450-456, (1999).

[141]. Kabir, G., and Hasin, M.A.A., "Comparative Analysis of AHP and Fuzzy AHP Models for Multicriteria Inventory Classification", International Journal of Fuzzy Logic Systems Vol.1, No.1, (2011)

[142]. K.N. Zaman, A.N. Siddiquee, Z.A. Khan, Friction Stir Welding: Dissimilar Aluminium Alloys, 2017.

[143]. W. Boonchouytan, T. Ratanawilai, P. Muangjunburee, Effect of pre/post heat treatment on the friction stir welded SSM356 aluminum alloys. Procedia Eng. 32, 1139–1146 (2012)

[144] Anandaraj, J.A.; Rajakumar, S.; Balasubramanian, V.; Petley, V. Investigation on mechanical and metallurgical properties of rotary friction welded In718/SS410 dissimilar materials. Mater. Today Proc. 2021, 45, 962–966. [CrossRef]

[145] GUPTA, S. K., PANDEY, K. & KUMAR, R. 2015. Multi-objective optimization of friction stir welding of aluminium alloy using grey relation analysis with entropy measurement method. *Nirma University Journal of Engineering and Technology (NUJET),* 3**,** 29-34.

[146] I. Abdulaziz, Albannai, Review The Common Defects In Friction Stir Welding, Int. J. Sci. Technol. Res. 9 (2020) 318–329. www.ijstr.org.

[147] KASMAN, Ş. 2013. Optimisation of dissimilar friction stir welding parameters with grey relational analysis. Proceedings of the Institution of Mechanical Engineers, Part B: Journal of Engineering Manufacture, 227**,** 1317-1324.

[148] VIJAYAN, S., RAJU, R. & RAO, S. K. 2010. Multiobjective optimization of friction stir welding process parameters on aluminum alloy AA 5083 using Taguchi- based gray relation analysis. Materials and Manufacturing Processes, 25**,** 1206-1212.

[149] SAMPATH KUMAR, R., ARUN KUMAR AND AMRISHRAJ 2016. Optimization of process parameters during Friction Stir Welding of dissimilar aluminium alloys using Grey relational analysis. Journal of Chemical and Pharmaceutical Sciences, 9**,** 16471653.

[150] N. D. GHETIYA, K. M. P. A. A. J. K. 2015. Multi-objective Optimization of FSW Process Parameters of Aluminium Alloy Using Taguchi-Based Grey Relational Analysis. The Indian Institute of Metals**,** 1-7.

[151] KUMAR, M. G. A. S. 2013. Multi-objective optimization of cutting parameters in turning using grey relational analysis. International Journal of Industrial Engineering Computations, 4**,** 547–558.

APPENDICES

Appendices 1: Chemical composition result

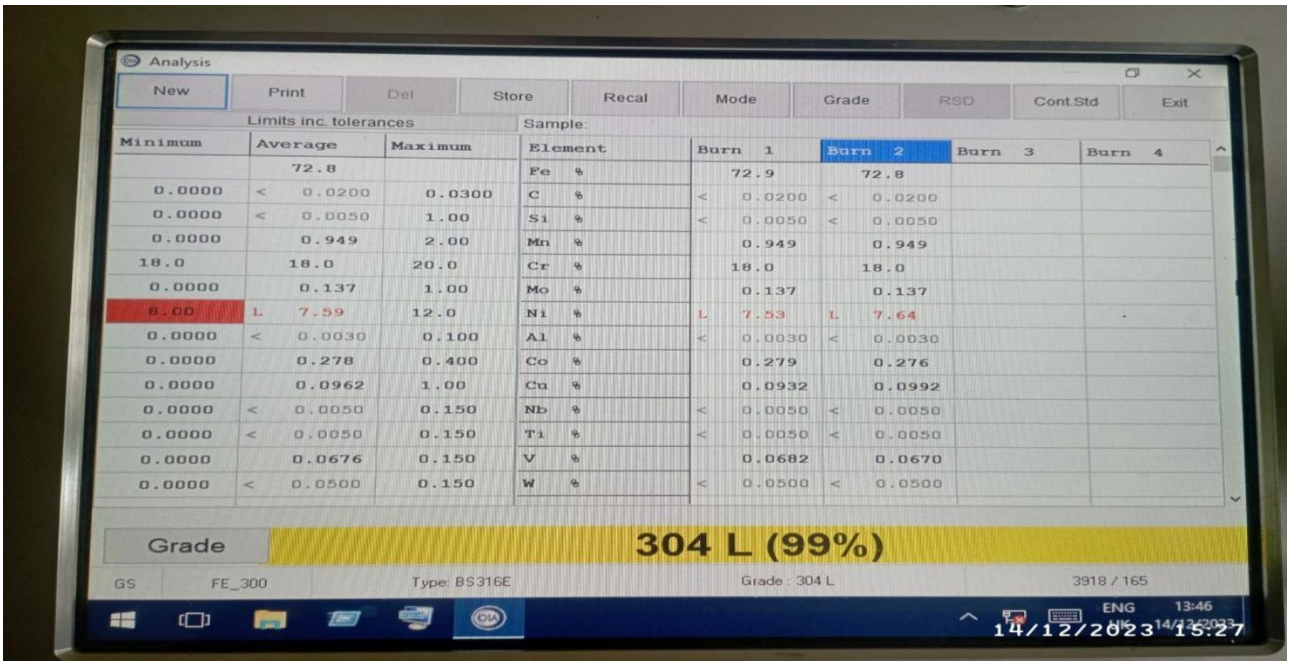

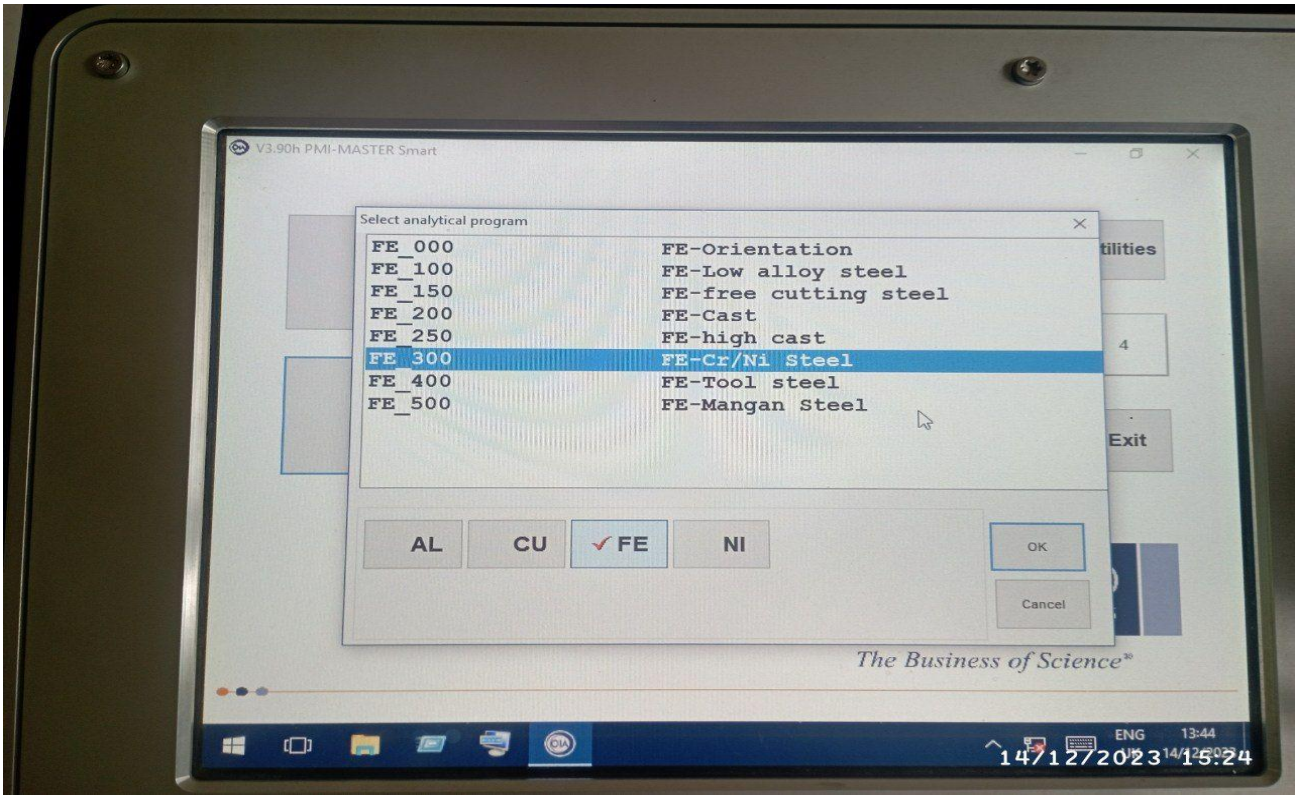

Appendices 2: Rockwell hardness scale of the machine

Table 1

Scale	Indenter	Initial test force	Totai test force(N)	Applications
HRA	Diamond indenter (BRALE)	98.07N (10Kg)	588.4(60Kg)	Hard alloy, carbide surface quenched
HRD			980.7(100Kg)	Steel sheet, surface quenched
HRC			1471(150.Kg)	Quenched steel tempered steel hard
HRF	Ball indenter1.5875mm (1/16 inch)		588.4(60Kg)	Cast iron aluminum magnesium alloy bearing alloy annealed copper alloy
HRB			980.7(100Kg)	Mild steel aluminum alloy copper alloy
HRG			1471(150.Kg)	Phosphoresced bronze beryllium
HRH	Ball indenter 3.175mm(1/8inch)		588.4(60Kg)	Aluminum zinc lead etc.
HRE			980.7(100Kg)	Bearing alloy tin hard plastics and other soft materials
HRK			1471(150.Kg)	

Table 2

Scales	Hardness range of the Standard blocks	Max. tolerance of displaying value
HRA	(20~75)HRA	±2HRA
	(>75~85)HRA	±1.5HRA
HRB	(20~45)HRB	±4HRB
	(>45~80)HRB	±3HRB
	(>80~100)HRB	±2HRB
HRC	(20~70)HRC	±1.5HRC
HRD	(40~70)HRD	±2HRD
	(>70~77)HRD	±1.5HRD
HRE	(70~90)HRE	±2.5HRE
	(>90~100)HRE	±2HRE
HRF	(60~90)HRF	±3HRF
	(>90~100)HRF	±2HRF

Rockwell						Rockwell Superficial				Brinell		Vickers	Shore	
A	B	C	D	E	F	15-N	30-N	45-N	30-T	3000 kg	500 kg	136		Approx Tensile Strength (psi)
60kg Brale	100kg 1/16" Ball	150kg Brale	100kg Brale	100kg 1/8" Ball	60kg 1/16" Ball	15kg Brale	30kg Brale	45kg Brale	30 kg 1/16" Ball	10mm Ball Steel	10mm Ball Steel	Diamond Pyramid	Sciero-scope	
86.5	---	70	78.5	---	---	94.0	86.0	77.6	---	---	---	1076	101	---
86.0	---	69	77.7	---	---	93.5	85.0	76.5	---	---	---	1044	99	---
85.6	---	68	76.9	---	---	93.2	84.4	75.4	---	---	---	940	97	---
85.0	---	67	76.1	---	---	92.9	83.6	74.2	---	---	---	900	95	---
84.5	---	66	75.4	---	---	92.5	82.8	73.2	---	---	---	865	92	---
83.9	---	65	74.5	---	---	92.2	81.9	72.0	---	739	---	832	91	---
83.4	---	64	73.8	---	---	91.8	81.1	71.0	---	722	---	800	88	---
82.8	---	63	73.0	---	---	91.4	80.1	69.9	---	705	---	772	87	---
82.3	---	62	72.2	---	---	91.1	79.3	68.8	---	688	---	746	85	---
81.8	---	61	71.5	---	---	90.7	78.4	67.7	---	670	---	720	83	---
81.2	---	60	70.7	---	---	90.2	77.5	66.6	---	654	---	697	81	320,000
80.7	---	59	69.9	---	---	89.8	76.6	65.5	---	634	---	674	80	310,000
80.1	---	58	69.2	---	---	89.3	75.7	64.3	---	615	---	653	78	300,000
79.6	---	57	68.5	---	---	88.9	74.8	63.2	---	595	---	633	76	290,000
79.0	---	56	67.7	---	---	88.3	73.9	62.0	---	577	---	613	75	282,000
78.5	120	55	66.9	---	---	87.9	73.0	60.9	---	560	---	595	74	274,000
78.0	120	54	66.1	---	---	87.4	72.0	59.8	---	543	---	577	72	266,000
77.4	119	53	65.4	---	---	86.9	71.2	58.6	---	525	---	560	71	257,000
76.8	119	52	64.6	---	---	86.4	70.2	57.4	---	500	---	544	69	245,000
76.3	118	51	63.8	---	---	85.9	69.4	56.1	---	487	---	528	68	239,000
75.9	117	50	63.1	---	---	85.5	68.5	55.0	---	475	---	513	67	233,000
75.2	117	49	62.1	---	---	85.0	67.6	53.8	---	464	---	498	66	227,000
74.7	116	48	61.4	---	---	84.5	66.7	52.5	---	451	---	484	64	221,000
74.1	116	47	60.8	---	---	83.9	65.8	51.4	---	442	---	471	63	217,000
73.6	115	46	60.0	---	---	83.5	64.8	50.3	---	432	---	458	62	212,000

73.1	115	45	59.2	---	---	83.0	64.0	49.0	---	421	---	446	60	206,000
72.5	114	44	58.5	---	---	82.5	63.1	47.8	---	409	---	434	58	200,000
72.0	113	43	57.7	---	---	82.0	62.2	46.7	---	400	---	423	57	196,000
71.5	113	42	56.9	---	---	81.5	61.3	45.5	---	390	---	412	56	191,000
70.9	112	41	56.2	---	---	80.9	60.4	44.3	---	381	---	402	55	187,000
70.4	112	40	55.4	---	---	80.4	59.5	43.1	---	371	---	392	54	182,000
69.9	111	39	54.6	---	---	79.9	58.6	41.9	---	362	---	382	52	177,000
69.4	110	38	53.8	---	---	79.4	57.7	40.8	---	353	---	372	51	173,000
68.9	110	37	53.1	---	---	78.8	56.8	39.6	---	344	---	363	50	169,000
68.4	109	36	52.3	---	---	78.3	55.9	38.4	---	336	---	354	49	165,000
67.9	109	35	51.5	---	---	77.7	55.0	37.2	---	327	---	345	48	160,000
67.4	108	34	50.8	---	---	77.2	54.2	36.1	---	319	---	336	47	156,000
66.8	108	33	50.0	---	---	76.6	53.3	34.9	---	311	---	327	46	152,000
66.3	107	32	49.2	---	---	76.1	52.1	33.7	---	301	---	318	44	147,000
65.8	106	31	48.4	---	---	75.6	51.3	32.5	---	294	---	310	43	144,000
65.3	105	30	47.7	---	---	75.0	50.4	31.3	---	286	---	302	42	140,000
64.7	104	29	47.0	---	---	74.5	49.5	30.1	---	279	---	294	41	137,000
64.3	104	28	46.1	---	---	73.9	48.6	28.9	---	271	---	286	41	133,000
63.8	103	27	45.2	---	---	73.3	47.7	27.8	---	264	---	279	40	129,000
63.3	103	26	44.6	---	---	72.8	46.8	26.7	---	258	---	272	39	126,000
62.8	102	25	43.8	---	---	72.2	45.9	25.5	---	253	---	266	38	124,000
62.4	101	24	43.1	---	---	71.6	45.0	24.3	---	247	---	260	37	121,000
62.0	100	23	42.1	---	---	71.0	44.0	23.1	82.0	240	201	254	36	118,000
61.5	99	22	41.6	---	---	70.5	43.2	22.0	81.5	234	195	248	35	115,000
61.0	98	21	40.9	---	---	69.9	42.3	20.7	81.0	228	189	243	35	112,000
60.5	97	20	40.1	---	---	69.4	41.5	19.6	80.5	222	184	238	34	109,000
59.0	96	18	---	---	---	---	---	---	80.0	216	179	230	33	106,000
58.0	95	16	---	---	---	---	---	---	79.0	210	175	222	32	103,000
57.5	94	15	---	---	---	---	---	---	78.5	205	171	213	31	100,000
57.0	93	13	---	---	---	---	---	---	78.0	200	167	208	30	98,000
56.5	92	12	---	---	---	---	---	---	77.5	195	163	204	29	96,000

Appendices 3: Test results of Hardness test

Hardnes test at the Nugget zone for 27 sample or 9 Run
Measured three times per sample and take the Average result

NO	TIME	TRIAL	RESULT	AVRAGE	
SAMPLE ORGINAL	1/14/2025 , 8:27	1	78.8 HRB	72.7 HRB	STAINLESS STELL (304 L) FIRST MATERIAL HARONES TEST AVRAGE RESULT
	1/14/2025 , 8:30	2	74.2 HRB		
	1/14/2025 , 8:33	3	65.3 HRB		

NO	TIME	TRIAL	RESULT	AVRAGE	
SAMPLE ORGINAL	1/14/2025 , 8:35	1	63.8 HRB	51.5 HRB	PURE COPPER (2.04) STELL FIRST MATERIAL HARONES TEST AVRAGE RESULT
	1/14/2025 , 8:38	2	48.1 HRB		
	1/14/2025 , 8:40	3	42.6 HRB		

NO	TIME	TRIAL	RESULT	AVRAGE		TIME	TRIAL	RESULT	AVRAGE		TIME	TRIAL	RESULT	AVRAGE
SAMPLE 1 A	1/14/2025 , 8:50	1	131.9 HRF	130.6 HRF	SAMPLE 4 A	1/14/2025 , 9:48	1	106.6 HRF	169.2 HRF	SAMPLE 7 A	1/14/2025 , 10:42	1	108.7 HRF	100.3 HRF
	1/14/2025 , 8:52	2	132.2 HRF			1/14/2025 , 9:50	2	111.2 HRF			1/14/2025 , 10:44	2	98.3 HRF	
	1/14/2025 , 8:55	3	127.7 HRF			1/14/2025 , 9:52	3	119.6 HRF			1/14/2025 , 10:47	3	94.1 HRF	
SAMPLE 1 B	1/14/2025 , 8:57	1	109.5 HRF	115.4 HRF	SAMPLE 4 B	1/14/2025 , 9:54	1	131.3 HRF	125.7 HRF	SAMPLE 7 B	1/14/2025 , 10:49	1	97.5 HRF	107.2 HRF
	1/14/2025 , 9:00	2	109.7 HRF			1/14/2025 , 9:57	2	119.7 HRF			1/14/2025 , 10:51	2	114.3 HRF	
	1/14/2025 , 9:03	3	126.9 HRF			1/14/2025 , 9:59	3	126.1 HRF			1/14/2025 , 10:53	3	109.8 HRF	
SAMPLE 1 C	1/14/2025 , 9:05	1	105.4 HRF	112.3 HRF	SAMPLE 4 C	1/14/2025 , 10:01	1	102.7 HRF	104.1 HRF	SAMPLE 7 C	1/14/2025 , 10:55	1	135.3 HRF	123.4 HRF
	1/14/2025 , 9:07	2	110.2 HRF			1/14/2025 , 10:03	2	100.5 HRF			1/14/2025 , 10:57	2	114.3 HRF	
	1/14/2025 , 9:10	3	121.3 HRF			1/14/2025 , 10:05	3	109.1 HRF			1/14/2025 , 11:00	3	120.8 HRF	
SAMPLE 2 A	1/14/2025 , 9:12	1	152.1 HRF	136.1 HRF	SAMPLE 5 A	1/14/2025 , 10:08	1	120.6 HRF	125.7 HRF	SAMPLE 8 A	1/14/2025 , 11:02	1	101.2 HRF	110.7 HRF
	1/14/2025 , 9:15	2	128.3 HRF			1/14/2025 , 10:10	2	131.1 HRF			1/14/2025 , 11:05	2	112.2 HRF	
	1/14/2025 , 9:17	3	128.0 HRF			1/14/2025 , 10:12	3	125.5 HRF			1/14/2025 , 11:07	3	118.7 HRF	
SAMPLE 2 B	1/14/2025 , 9:19	1	129.9 HRF	134.2 HRF	SAMPLE 5 B	1/14/2025 , 10:15	1	91.5 HRF	93.6 HRF	SAMPLE 8 B	1/14/2025 , 11:09	1	107.6 HRF	109.2 HRF
	1/14/2025 , 9:21	2	131.4 HRF			1/14/2025 , 10:17	2	95.8 HRF			1/14/2025 , 11:11	2	103.4 HRF	
	1/14/2025 , 9:24	3	141.5 HRF			1/14/2025 , 10:19	3	93.5 HRF			1/14/2025 , 11:13	3	116.7 HRF	
SAMPLE 2 C	1/14/2025 , 9:26	1	119.2 HRF	117.3 HRF	SAMPLE 5 C	1/14/2025 , 10:21	1	111.9 HRF	124.5 HRF	SAMPLE 8 C	1/14/2025 , 11:16	1	117.5 HRF	119.1 HRF
	1/14/2025 , 9:29	2	124.0 HRF			1/14/2025 , 10:23	2	132.9 HRF			1/14/2025 , 11:18	2	124.3 HRF	
	1/14/2025 , 9:31	3	108.9 HRF			1/14/2025 , 10:25	3	128.9 HRF			1/14/2025 , 11:20	3	115.7 HRF	
SAMPLE 3 A	1/14/2025 , 9:33	1	105.3 HRF	104.3 HRF	SAMPLE 6 A	1/14/2025 , 10:27	1	119.8 HRF	120.1 HRF	SAMPLE 9 A	1/14/2025 , 11:23	1	130.5 HRF	132.1 HRF
	1/14/2025 , 9:36	2	104.5 HRF			1/14/2025 , 10:29	2	119.6 HRF			1/14/2025 , 11:25	2	131.5 HRF	
	1/14/2025 , 9:38	3	102.5 HRF			1/14/2025 , 10:32	3	120.6 HRF			1/14/2025 , 11:27	3	134.3 HRF	
SAMPLE 3 B	1/14/2025 , 9:40	1	78.2 HRF	94.6 HRF	SAMPLE 6 B	1/14/2025 , 10:35	1	98.2 HRF	114.8 HRF	SAMPLE 9 B	1/14/2025 , 11:29	1	96.7 HRF	115.9 HRF
	1/14/2025 , 9:43	2	112.2 HRF			1/14/2025 , 10:37	2	127.1 HRF			1/14/2025 , 11:32	2	121.7 HRF	
	1/14/2025 , 9:45	3	93.6 HRF			1/14/2025 , 10:39	3	119.1 HRF			1/14/2025 , 11:35	3	129.4 HRF	
SAMPLE 3 c	1/14/2025 , 9:40	4	78.3 HRF	87.7 HRF	SAMPLE 6 C	1/14/2025 , 10:41	4	78.3 HRF	104.9 HRF	SAMPLE 9 C	1/14/2025 , 11:38	4	86.8 HRF	105.10 HRF
	1/14/2025 , 9:43	5	102.3 HRF			1/14/2025 , 10:43	5	117.2 HRF			1/14/2025 , 11:41	5	111.8 HRF	
	1/14/2025 , 9:45	6	85.7 HRF			1/14/2025 , 10:45	6	109.2 HRF			1/14/2025 , 11:44	6	119.5 HRF	

Appendices 4: Test results of tensile strength test

EN-02-Metallic materials-Tensile test-2

(Test data record sheet)

Sample No.		Test Standard	
Laboratory		Customer	
Temperature		Tester	
Humidity		Checker	
Test Date	14.01.2025		

No.	width	thickness	Lo	Fm	FeH	FeL	Fp0.2	Ft1.0	Lu
	mm	mm	mm	kN	kN	kN	kN	kN	mm
1	12	6	225	23.5	0.0	15.3	0.0	0.0	
No.	A	Rm	ReH	ReL	Rp0.2	Rt1.0			
	%	MPa	MPa	MPa	MPa	MPa			
1	100.0	326	0	213	0	0			

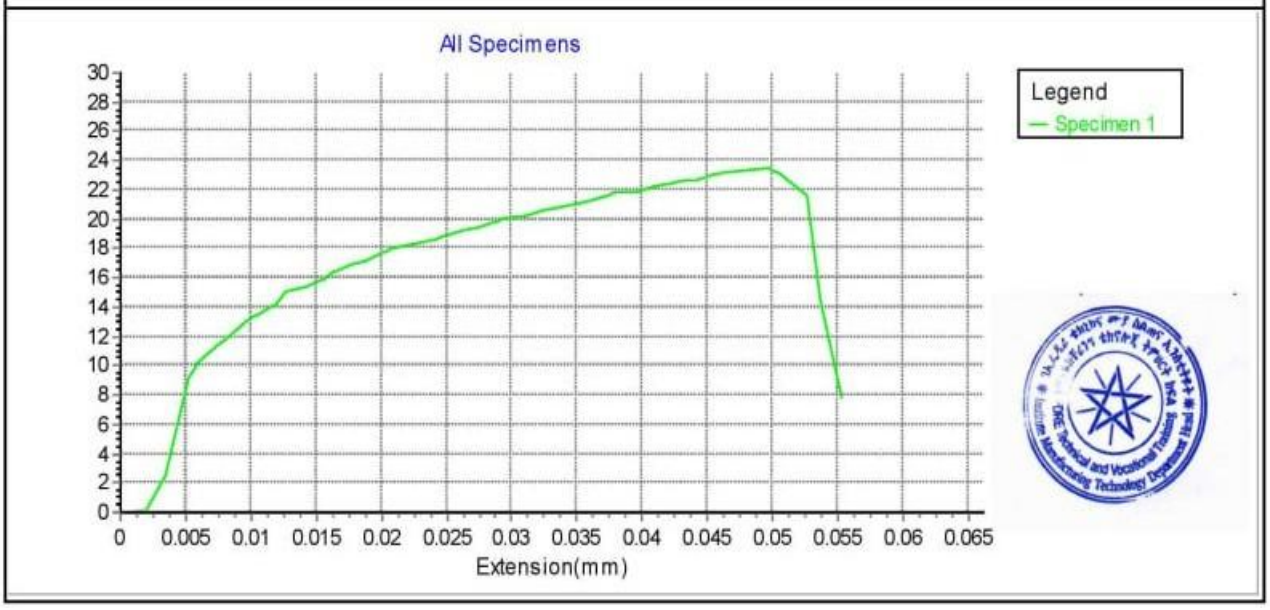

EN-02-Metallic materials-Tensile test-2

(Test data record sheet)

Sample No.		Test Standard	
Laboratory		Customer	
Temperature		Tester	
Humidity		Checker	
Test Date	14.01.2025		

No.	width	thickness	Lo	Fm	FeH	FeL	Fp0.2	Ft1.0	Lu
	mm	mm	mm	kN	kN	kN	kN	kN	mm
1	12	5.5	225	19.6	0.0	14.2	0.0	0.0	
No.	A	Rm	ReH	ReL	Rp0.2	Rt1.0			
	%	MPa	MPa	MPa	MPa	MPa			
1	100.0	297	0	215	0	0			

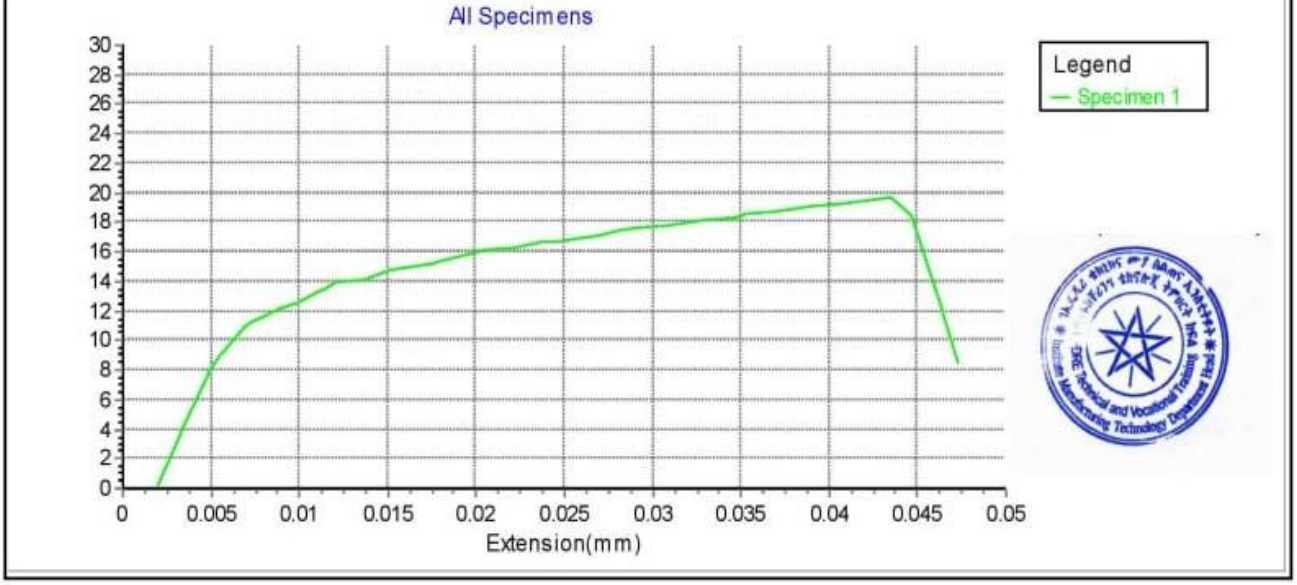

Appendices 5: Test results of tensile test Actual graph on the monitor.

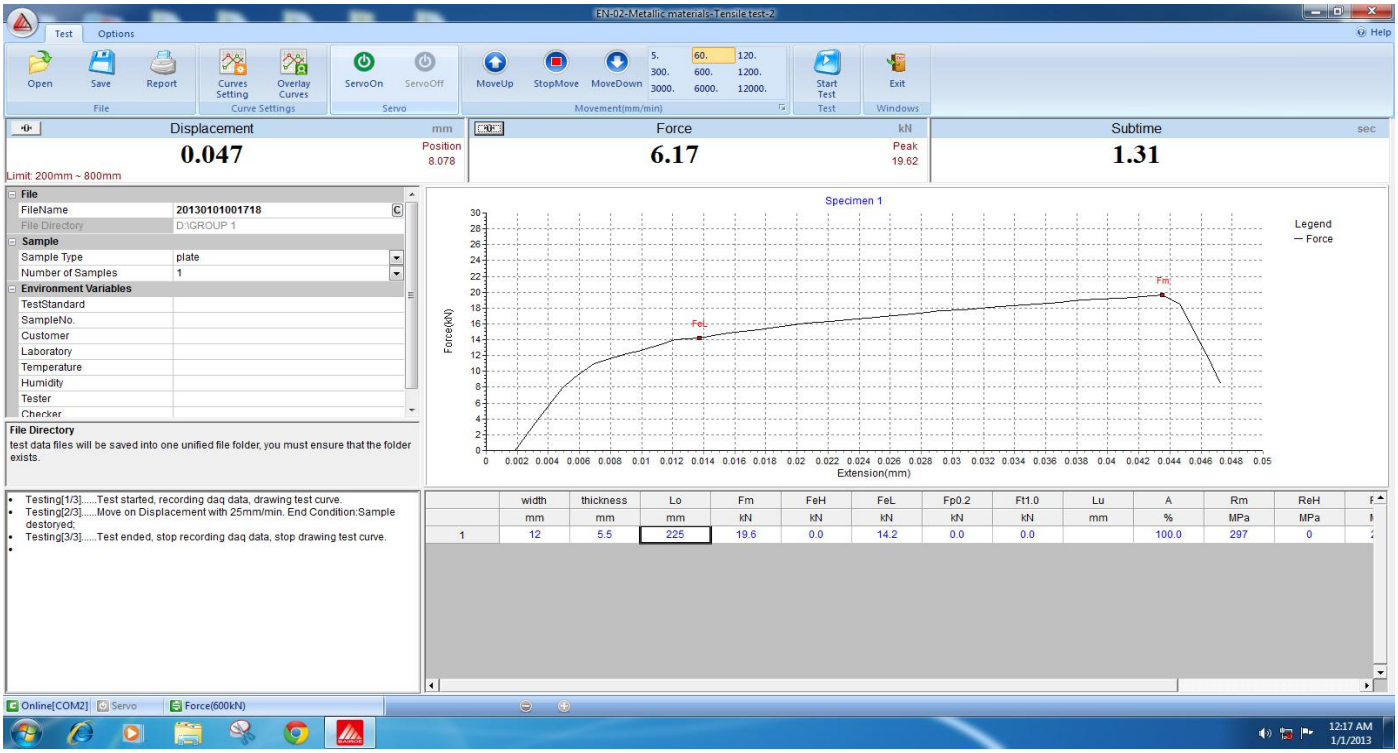

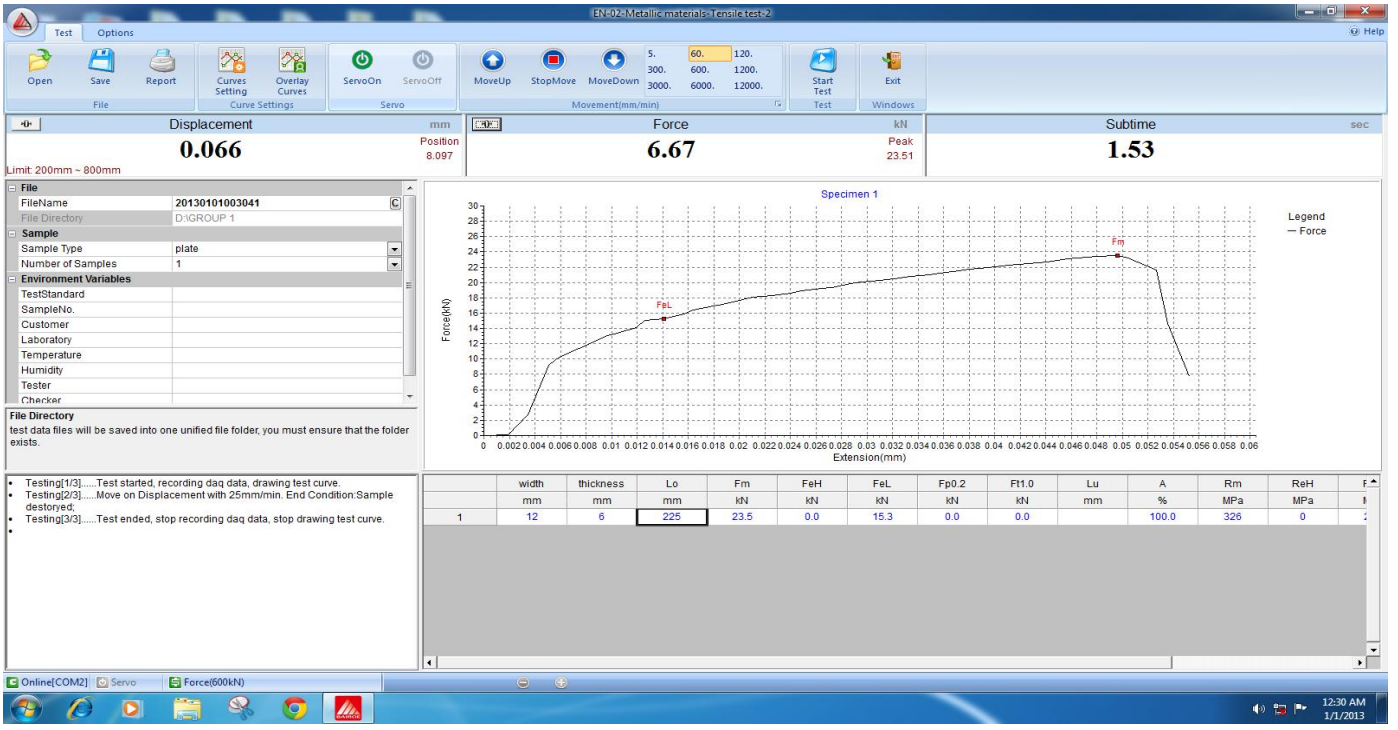

Appendices 6: Test results of Micro-structural

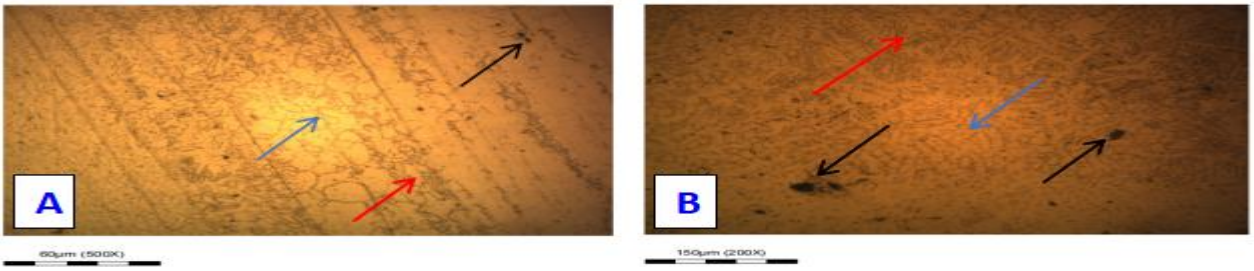

Sample 1 stainless steel Heat affected zone region

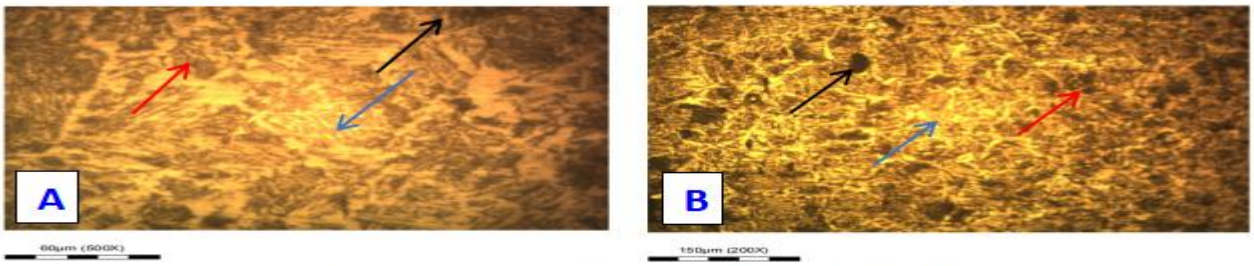

Sample 2 pure copper (CU-2.041) Heat affected zone

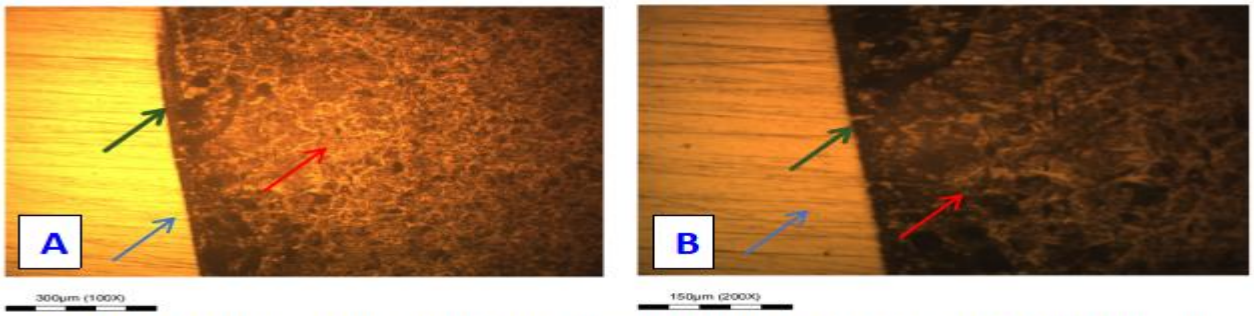

Sample 3 Stainless steel AND pure copper (SS-304L VS CU-2.041) Welding zone

SS-304L HAZ CU-2.041 HAZ VOID DEFICT WZ BOUNDARY

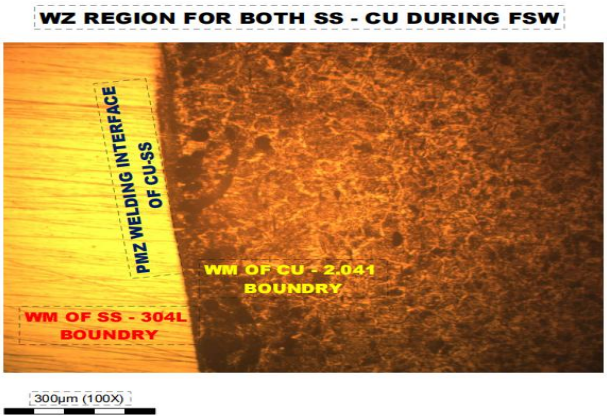

Appendices 7: Test results of Transient thermal simulation Ansys & abacuses software

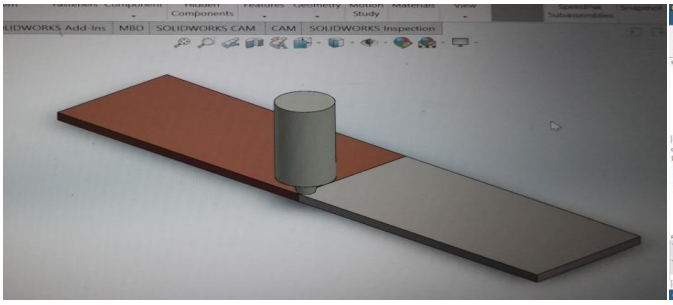

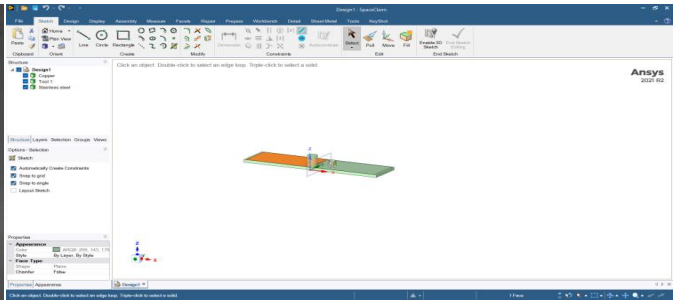

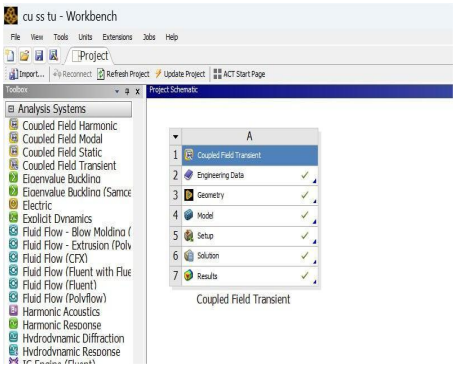

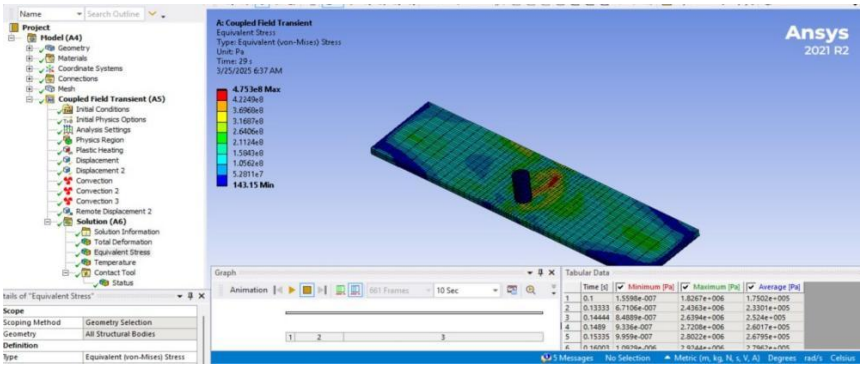

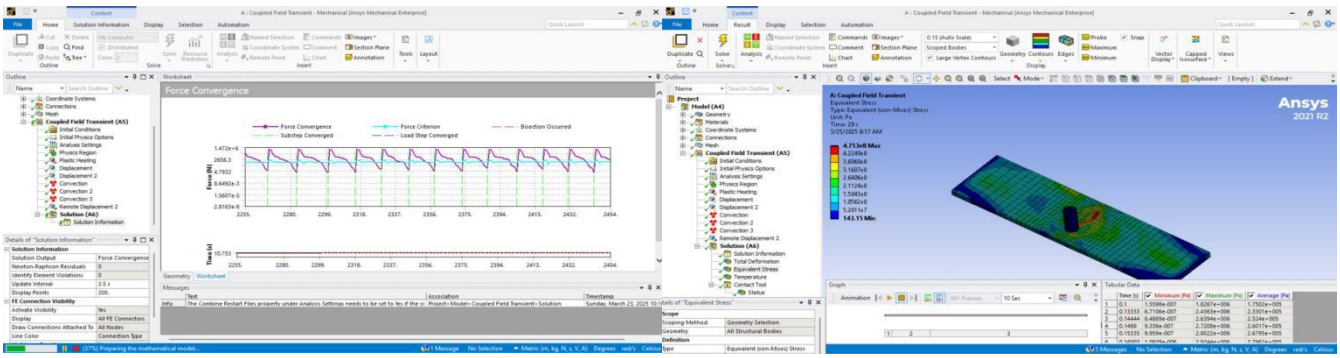

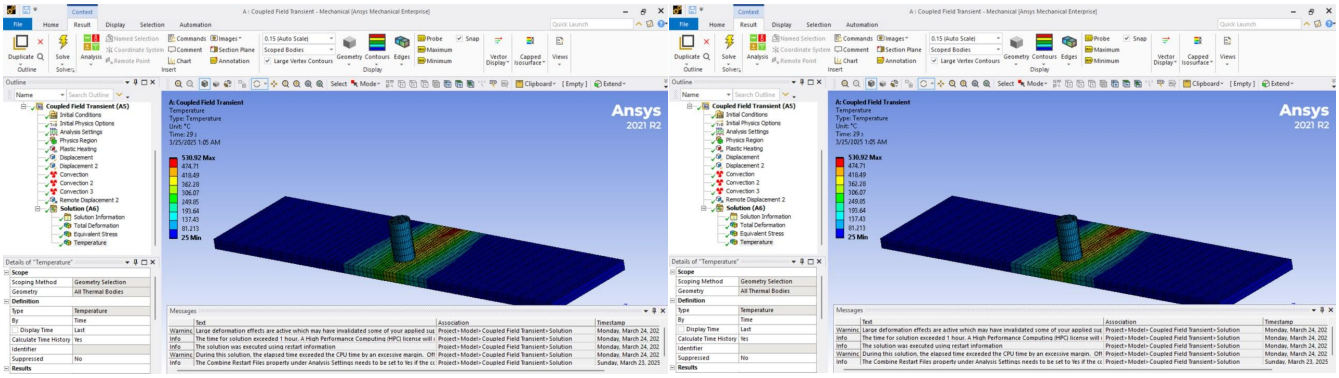

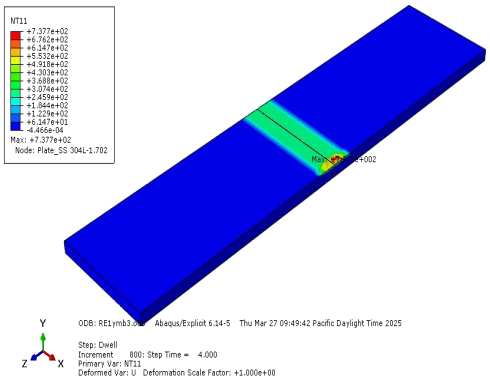
NT11
+7.377e+02
+6.762e+02
+6.147e+02
+5.532e+02
+4.918e+02
+4.303e+02
+3.688e+02
+3.074e+02
+2.459e+02
+1.844e+02
+1.229e+02
+6.147e+01
-4.466e-04
Max: +7.377e+02
Node: Plate_SS 304L-1.702
ODB: RE1ymb3.odb Abaqus/Explicit 6.14-5 Thu Mar 27 09:49:42 Pacific Daylight Time 2025
Step: Dwell
Increment 800: Step Time = 4.000
Primary Var: NT11
Deformed Var: U Deformation Scale Factor: +1.000e+00

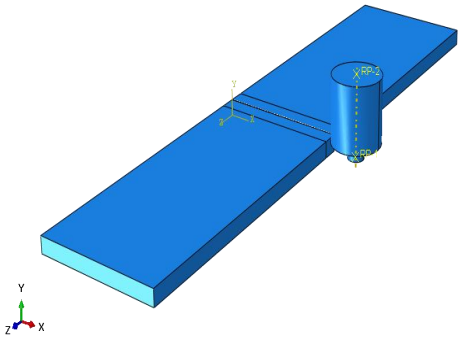
RP-2
RP-1

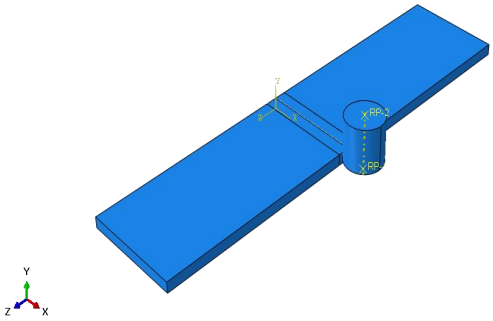
RP-2
RP-1

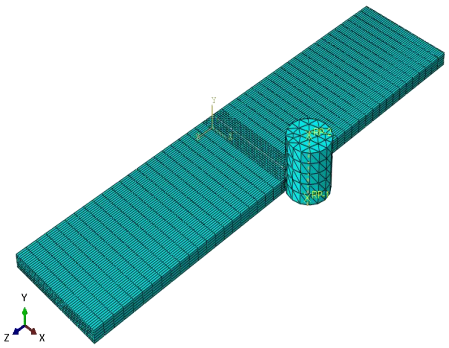
RP-2
RP-1

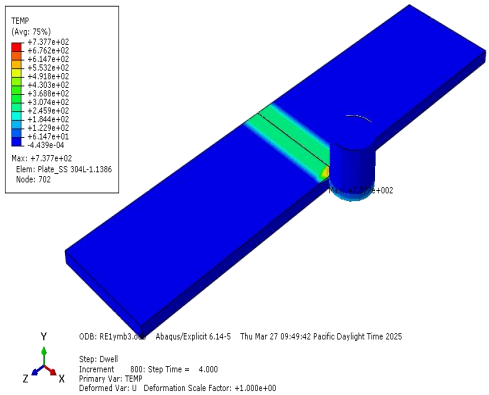
TEMP
(Avg: 75%)
+7.377e+02
+6.762e+02
+6.147e+02
+5.532e+02
+4.918e+02
+4.303e+02
+3.688e+02
+3.074e+02
+2.459e+02
+1.844e+02
+1.229e+02
+6.147e+01
-4.439e-04
Max: +7.377e+02
Elem: Plate_SS 304L-1.1386
Node: 702
ODB: RE1ymb3.odb Abaqus/Explicit 6.14-5 Thu Mar 27 09:49:42 Pacific Daylight Time 2025
Step: Dwell
Increment 800: Step Time = 4.000
Primary Var: TEMP
Deformed Var: U Deformation Scale Factor: +1.000e+00

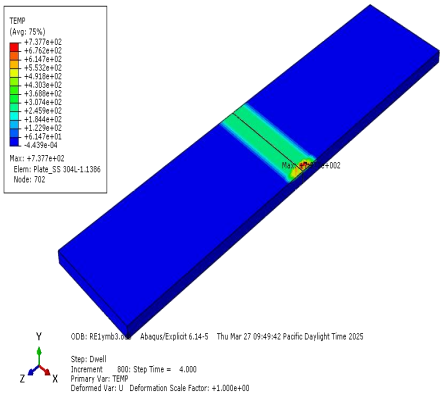
TEMP
(Avg: 75%)
+7.377e+02
+6.762e+02
+6.147e+02
+5.532e+02
+4.918e+02
+4.303e+02
+3.688e+02
+3.074e+02
+2.459e+02
+1.844e+02
+1.229e+02
+6.147e+01
-4.439e-04
Max: +7.377e+02
Elem: Plate_SS 304L-1.1386
Node: 702
ODB: RE1ymb3.odb Abaqus/Explicit 6.14-5 Thu Mar 27 09:49:42 Pacific Daylight Time 2025
Step: Dwell
Increment 800: Step Time = 4.000
Primary Var: TEMP
Deformed Var: U Deformation Scale Factor: +1.000e+00

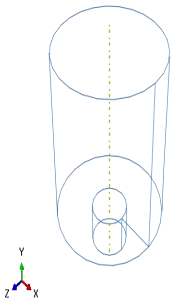

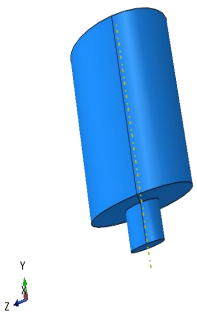

Appendices 8: Budget

The necessary expenditure needed to complete this research is listed in the following table

No	Expenditure Description	Size/thickness	Qty/ size	Unit/ M	Unit price in Birr	Total Price in Birr
	RAW MATERIAL COST					
1	Copper pure base bar	12000 x 1000 x 50 mm	1	M	10,000	10,000
2	Stainless steel pleat	4000 x 4000 x 50 mm	1	M	7,500	7,500
3	Jig and fixture Modefic	known	-	lps	1,500	1,500
	STANDARD FSW TOOL COST BUTT WELDING					
4	Material type company lenght structure Internal diameter	Tungsten Carbide, WO-CO Castle bar 5.91 x 0.79 x 0.79 inches L x W x H Round Rod 20 Millimetres	1	pcs	21,500	21,500
	WELDING OPERATION COST					
5	CNCwelding Operation	203 x 102 x 4.76 mm	9	weld	500	4,500
	INSTRUMENTATION COST					
6	Tensile strength test Measurement	Per welding	27	Per weld	300	8,100
7	Hardness test For FSW welding measurement	Per welding	27	Per weld	100	2,700
8	FSW Microstructural test	Per welding	6	Per weld	500	3,000
9	Others	unkown	lap	-	10,000	10,000
	Total		-	-	-	**68,800**

Appendices 9: Different pictures of experimental process as well as SAMPLES





Bairoe

Bairoe
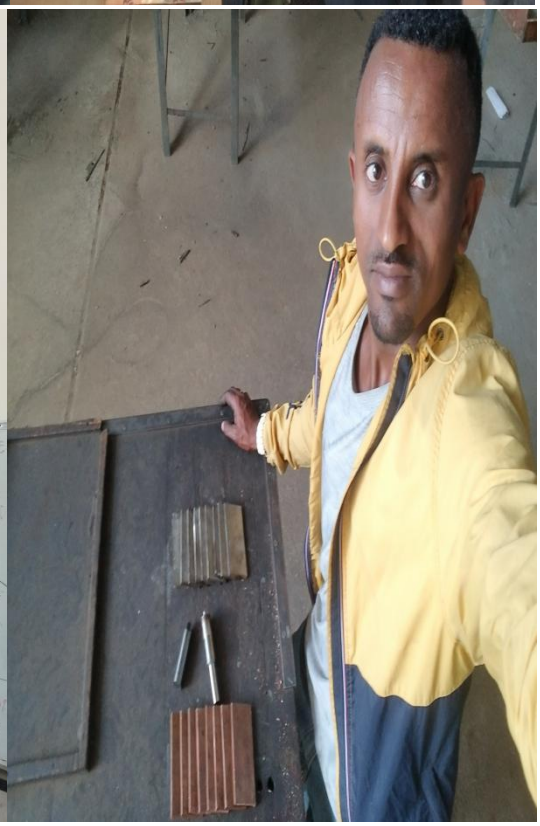

Appendices 10: Minitab result WORKSHEET 1

Taguchi Design

Design Summary

Taguchi Array	L9(3^4)
Factors:	4
Runs:	9

Columns of L9(3^4) array: 1 2 3 4

Taguchi Analysis: HARDNESS versus ROTATINAL SPEED, TRAVERSE SPEED, DWELL TIME, WELDING TOOL PROFILE

Response Table for Signal to Noise Ratios

Larger is better

Level	ROTATINAL SPEED	TRAVERSE SPEED	DWELL TIME	WELDING TOOL PROFILE
1	39.28	39.32	39.07	38.95
2	38.71	39.70	39.41	39.08
3	39.12	38.08	38.62	39.08
Delta	0.56	1.62	0.79	0.13
Rank	3	1	2	4

Response Table for Means

Level	ROTATINAL SPEED	TRAVERSE SPEED	DWELL TIME	WELDING TOOL PROFILE
1	92.60	92.50	90.33	88.70
2	86.47	96.90	93.83	90.60
3	90.57	80.23	85.47	90.33
Delta	6.13	16.67	8.37	1.90
Rank	3	1	2	4


Main Effects Plot for Means
Data Means
ROTATINAL SPEED
TRAVERSE SPEED
DWELL TIME
WELDING TOOL PROFILE
Mean of Means
98
96
94
92
90
88
86
84
82
80
1200
1400
1600
45
55
65
4
8
12
CONICAL
SQUARE
CYLINDRICAL

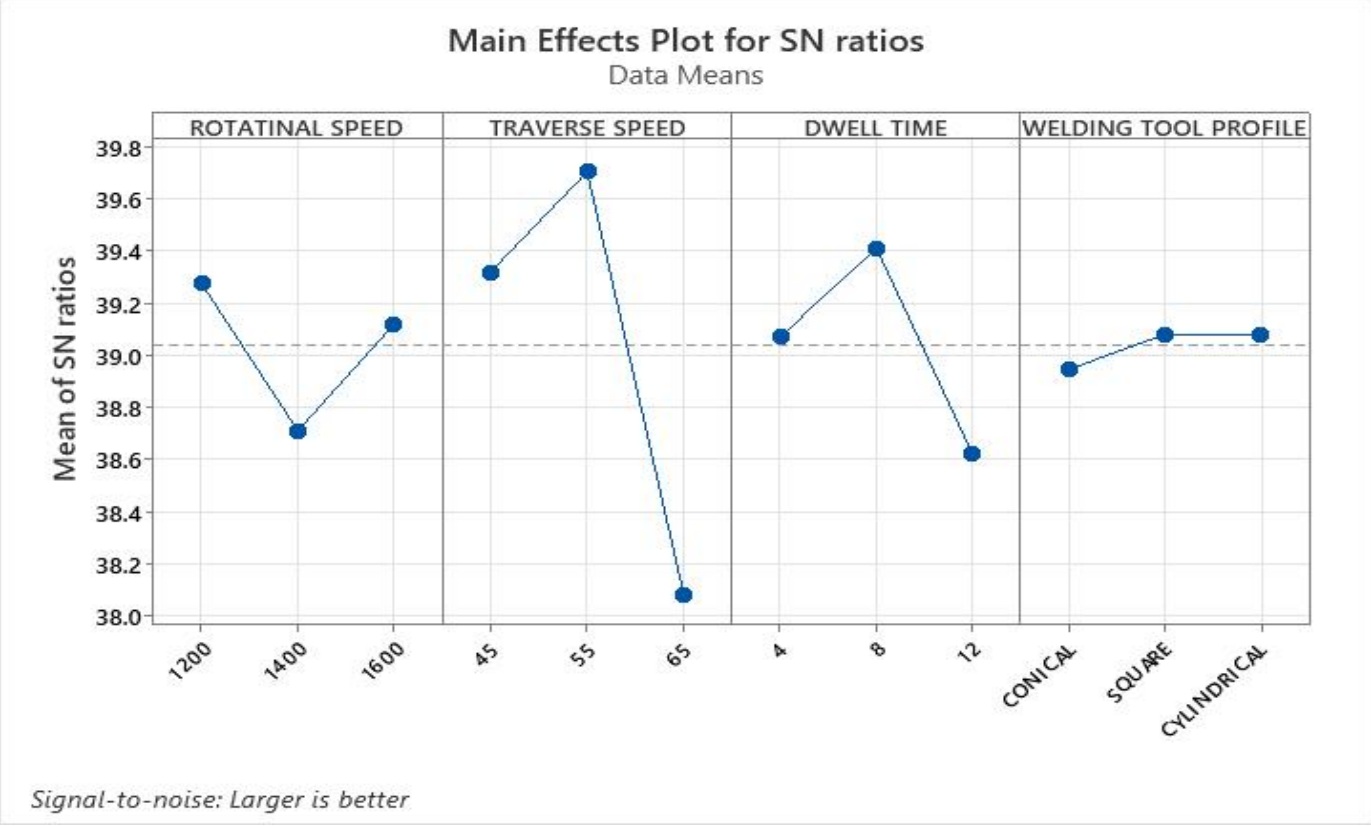
Main Effects Plot for SN ratios
Data Means
ROTATINAL SPEED
TRAVERSE SPEED
DWELL TIME
WELDING TOOL PROFILE
Mean of SN ratios
39.8
39.6
39.4
39.2
39.0
38.8
38.6
38.4
38.2
38.0
1200
1400
1600
45
55
65
4
8
12
CONICAL
SQUARE
CYLINDRICAL
Signal-to-noise: Larger is better

WORKSHEET 2

Taguchi Analysis: TENSILE STRENGTH versus ROTATINAL SPEED, TRAVERSE SPEED, DWELL TIME, WELDING TOOL PROFILE

Response Table for Signal to Noise Ratios

Larger is better

Level	ROTATINAL SPEED	TRAVERSE SPEED	DWELL TIME	WELDING TOOL PROFILE
1	48.01	47.74	47.98	47.75
2	48.38	47.81	47.93	48.14
3	47.52	48.35	48.00	48.02
Delta	0.86	0.61	0.06	0.40
Rank	1	2	4	3

Response Table for Means

Level	ROTATINAL SPEED	TRAVERSE SPEED	DWELL TIME	WELDING TOOL PROFILE
1	251.7	244.0	251.3	244.0
2	262.7	246.0	249.3	256.0
3	237.7	262.0	251.3	252.0
Delta	25.0	18.0	2.0	12.0
Rank	1	2	4	3

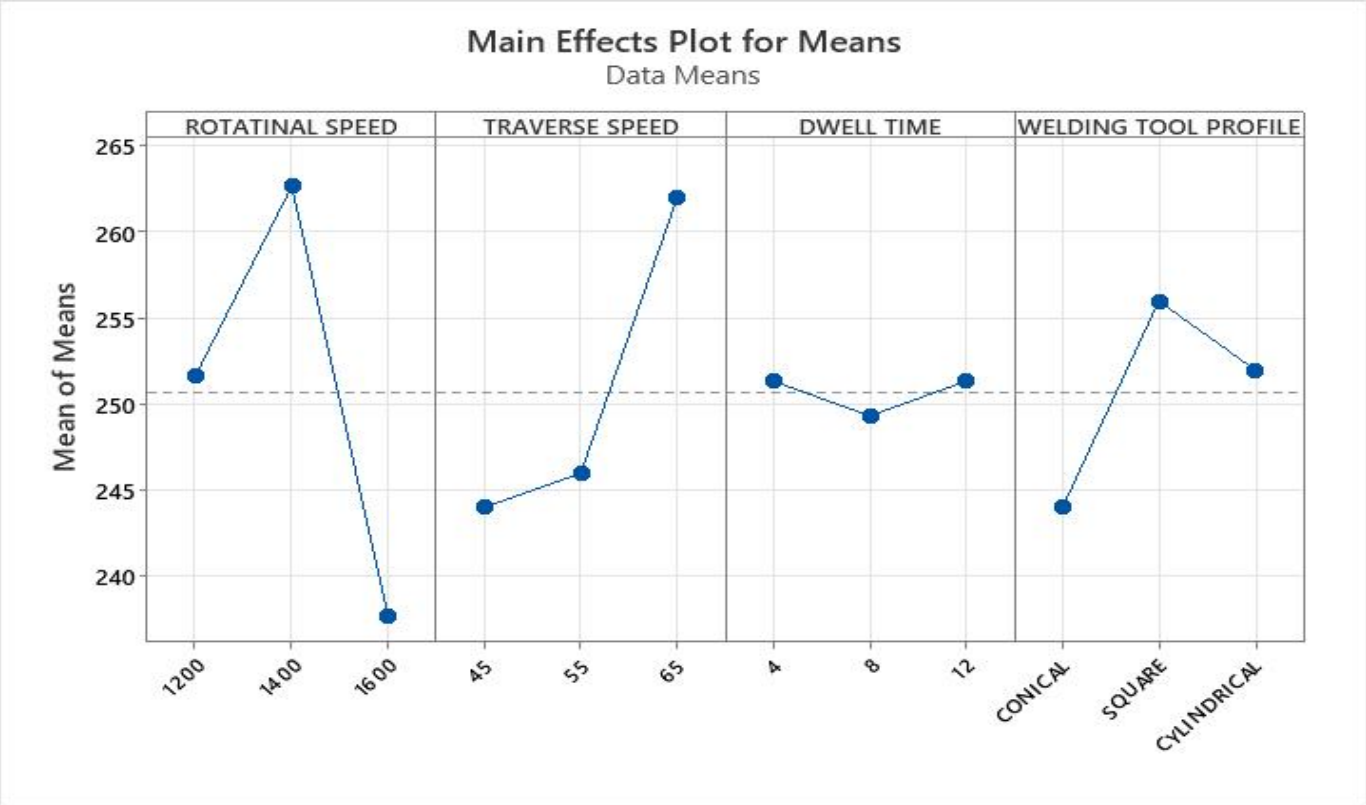
Main Effects Plot for Means
Data Means
ROTATINAL SPEED
TRAVERSE SPEED
DWELL TIME
WELDING TOOL PROFILE
Mean of Means
265
260
255
250
245
240
1200
1400
1600
45
55
65
4
8
12
CONICAL
SQUARE
CYLINDRICAL

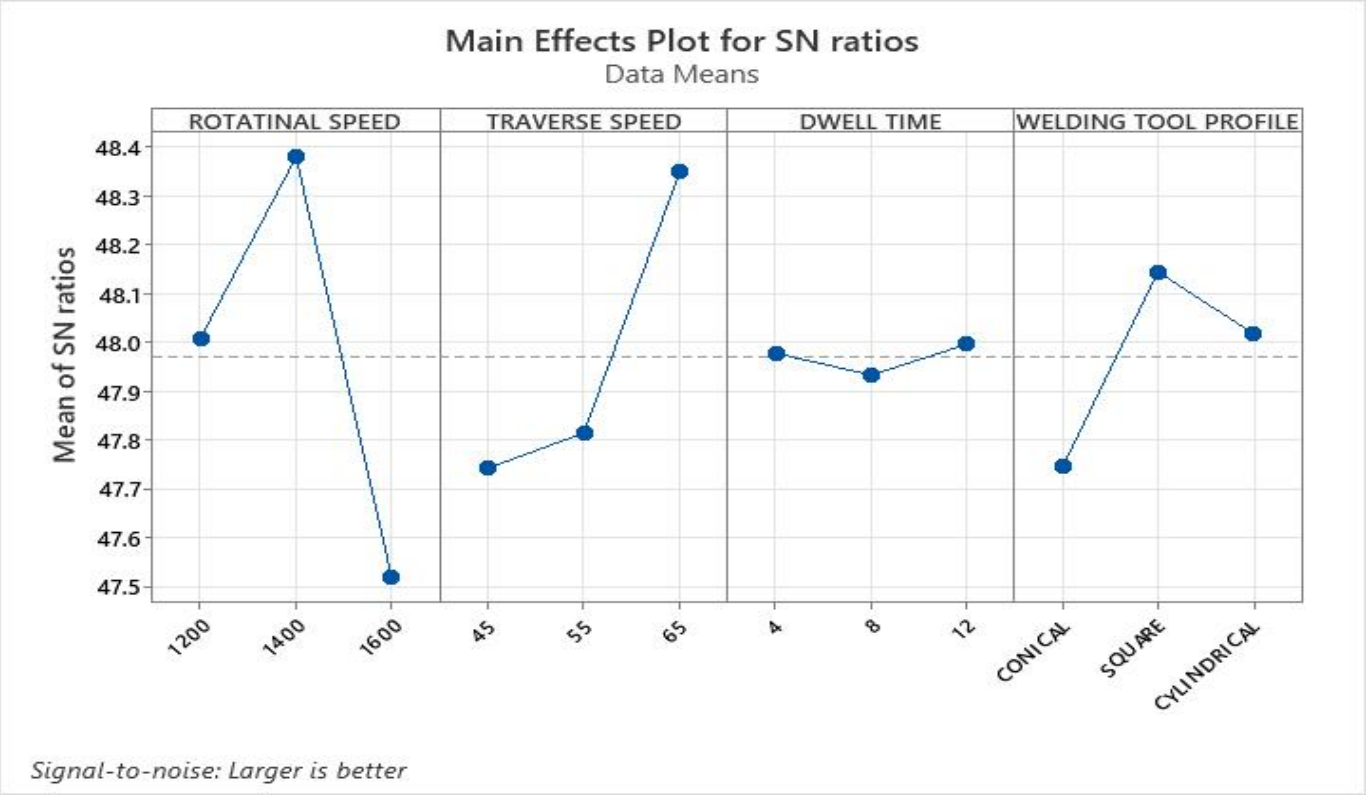
Main Effects Plot for SN ratios
Data Means
ROTATINAL SPEED
TRAVERSE SPEED
DWELL TIME
WELDING TOOL PROFILE
Mean of SN ratios
48.4
48.3
48.2
48.1
48.0
47.9
47.8
47.7
47.6
47.5
1200
1400
1600
45
55
65
4
8
12
CONICAL
SQUARE
CYLINDRICAL
Signal-to-noise: Larger is better

WORKSHEET 3

Probability Plot of TENSILE STRENGTH, HARDNESS

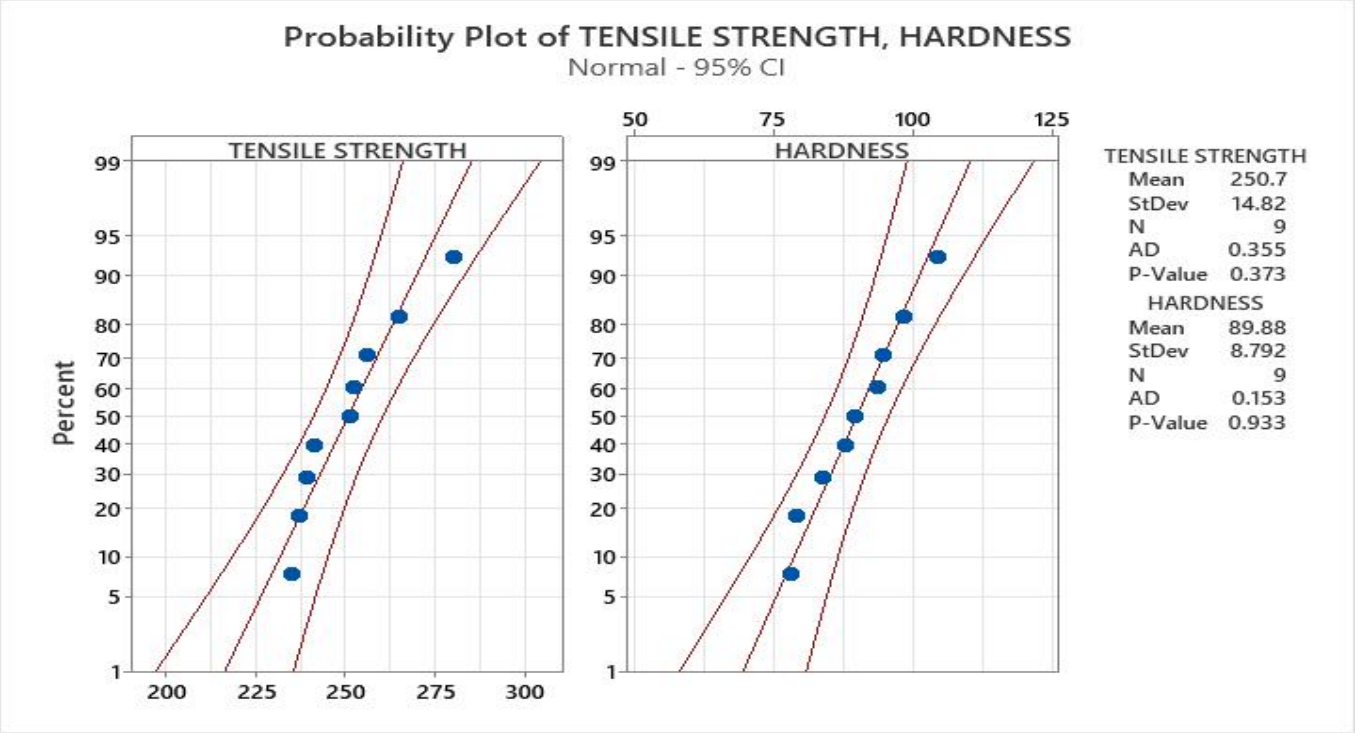

WORKSHEET 1

Principal Component Analysis: ROTATINAL SPEED, TRAVERSE SPEED, DWELL TIME, TENSILE STRENGTH, HARDNESS

Eigen analysis of the Correlation Matrix

Eigenvalue	*1.5821*	*0.4179*
Proportion	*0.791*	*0.209*
Cumulative	*0.791*	*1.000*

Eigenvectors

Variable	PC1	PC2
TENSILE STRENGTH	*-0.707*	*-0.707*
HARDNESS	*0.707*	*-0.707*

Eigen analysis of the Correlation Matrix

Variable	PC1	PC2	PC3	PC4	PC5
ROTATINAL SPEED	-0.151	-0.795	-0.371	-0.197	0.411
TRAVERSE SPEED	0.549	-0.135	-0.289	0.771	0.049
DWELL TIME	0.116	-0.379	0.883	0.169	0.189
TENSILE STRENGTH	0.577	0.319	-0.000	-0.395	0.639
HARDNESS	-0.574	0.324	-0.000	0.426	0.620

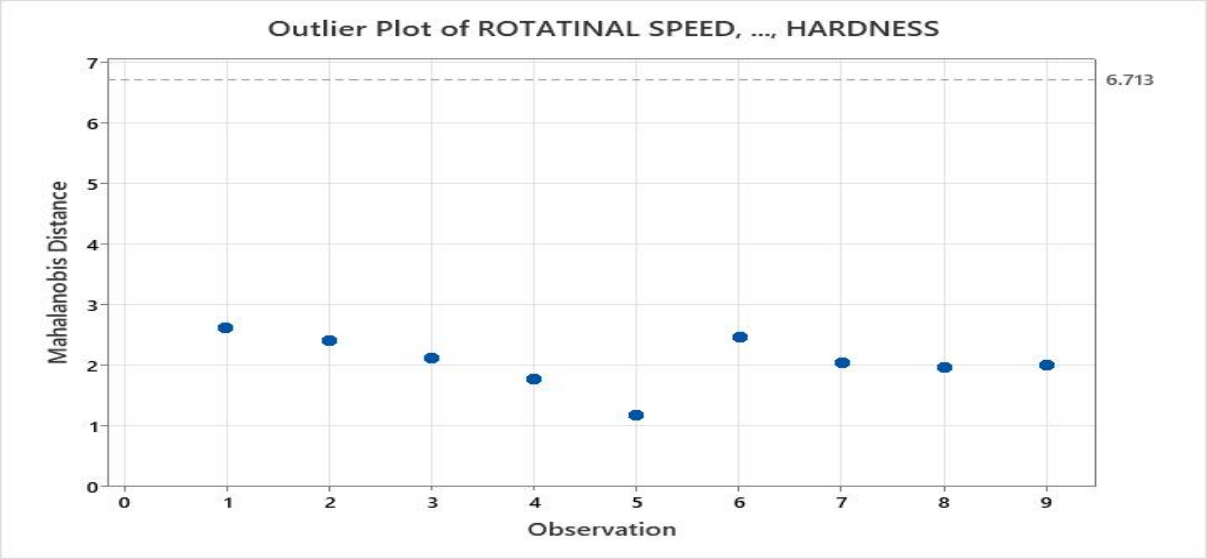

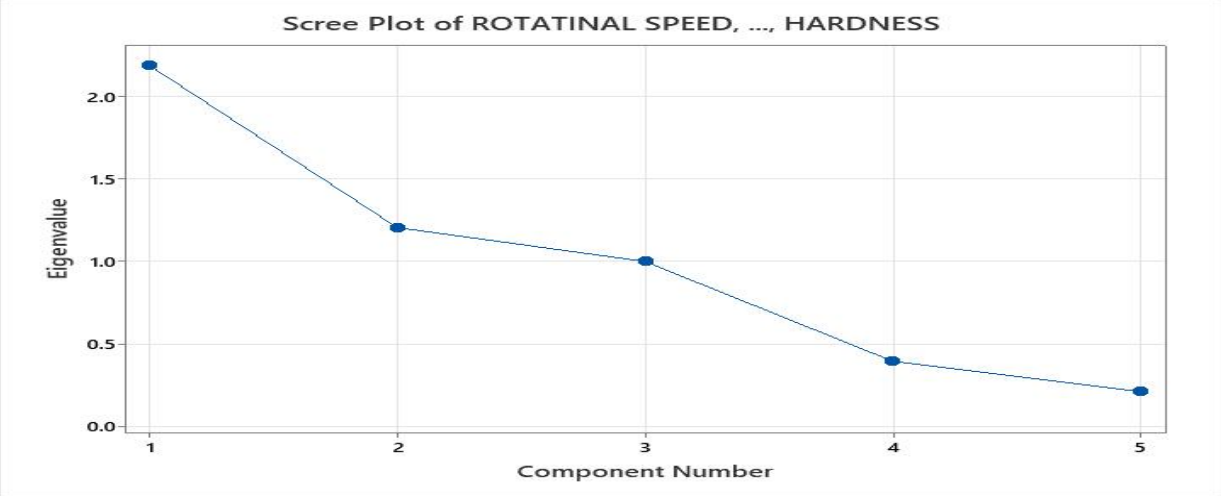

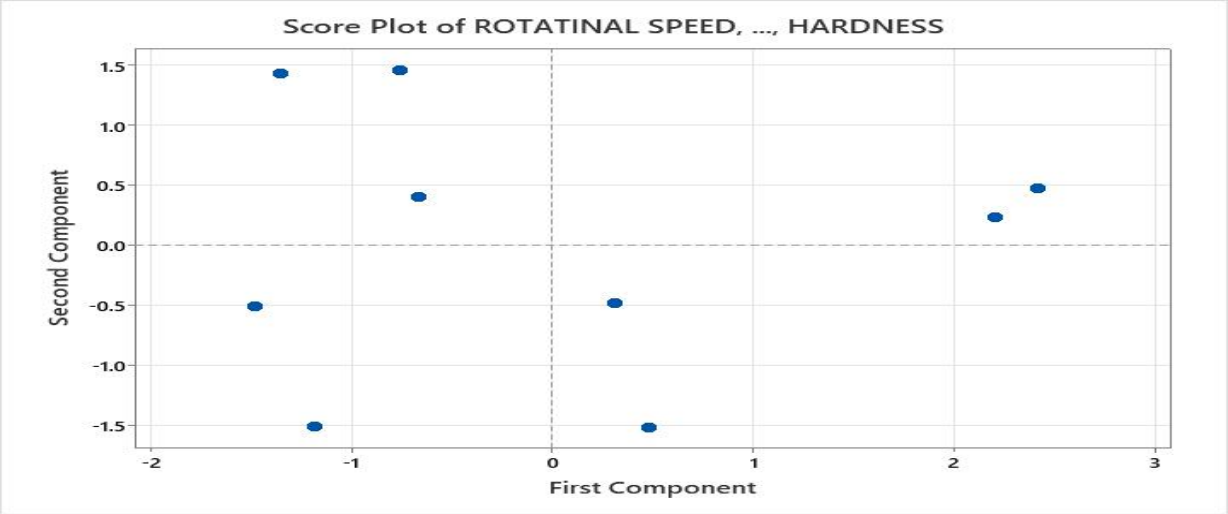

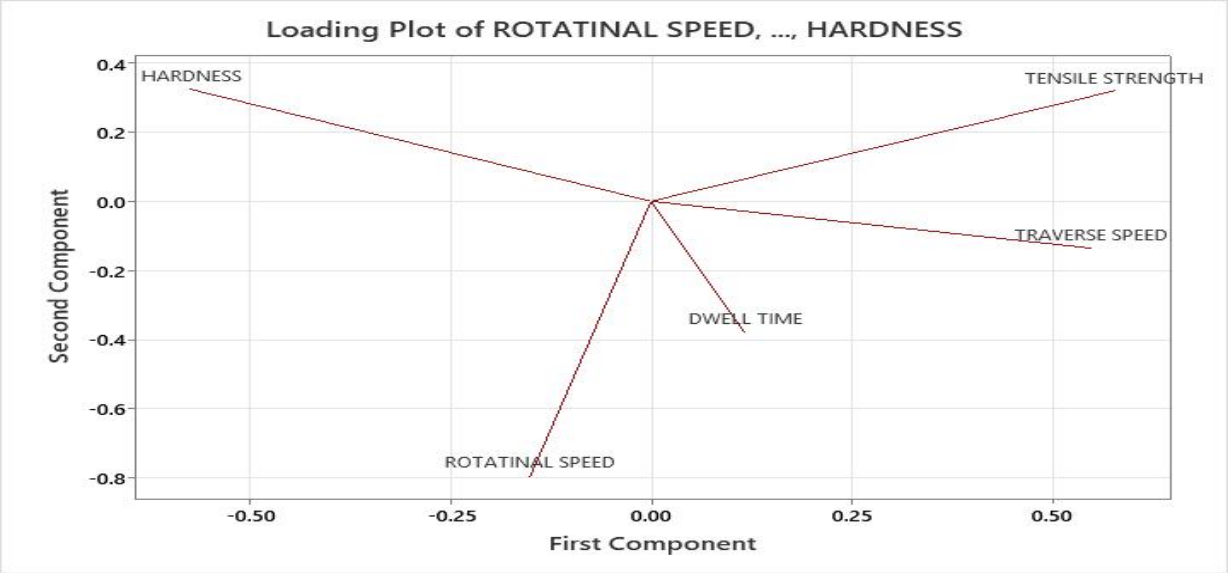

WORKSHEET 1

General Linear Model: GRG versus Rotational speed, Transversal speed, Dwell time, Welding tool profile

Method

Factor coding (-1, 0, +1)

Factor Information

Factor	Type	Levels Values
Rotational speed	Fixed	3 1200, 1400, 1600
Transversal speed	Fixed	3 45, 55, 65
Dwell time	Fixed	3 4, 8, 12
Welding tool profile	Fixed	3 Conical, squier, clyinderical

Analysis of Variance

Source	DF	Adj SS	Adj MS	F-Value	P-Value	PC-% Contribution	Remark
Rotational speed	2	0.12608	0.013038	26.4619	0.098	24.3042	significant
Transversal speed	2	0.07041	0.010206	13.2802	0.002	11.0761	significant
Dwell time	2	0.10338	0.006690	18.1453	0.091	15.5548	significant
Welding tool profile	2	0.28000	0.020001	68.3261	0	47.7176	significant
Error	2	0.00247	0.00201			1.4474	
Total	10	0.58234				100%	

Model Summary

S	R-sq	R-sq(adj)	R-sq(pred)
*	100.00%	*	*

Coefficients

Term	Coef	SE Coef	T-Value	P-Value	VIF
Constant	0.5174	*	*	*	
Rotational speed					
1200	0.04154	*	*	*	1.33
1400	0.03447	*	*	*	1.33
Transversal speed					
45	-0.04276	*	*	*	1.33
55	0.05069	*	*	*	1.33
Dwell time					
4	0.03853	*	*	*	1.33
8	0.02858	*	*	*	1.33
Welding tool profile					
Conical	-0.07889	*	*	*	1.33
squier	0.08415	*	*	*	1.33

Regression Equation

GRG = 0.5174 + 0.04154 Rotational speed_1200 + 0.03447 Rotational speed_1400
- 0.07601 Rotational speed_1600 - 0.04276 Transversal speed_45
+ 0.05069 Transversal speed_55 - 0.007929 Transversal speed_65
+ 0.03853 Dwell time_4
+ 0.02858 Dwell time_8 - 0.06710 Dwell time_12 - 0.07889 Welding tool profile_Conical
+ 0.08415 Welding tool profile_squire - 0.005261 Welding tool profile_cylindrical

Taguchi Analysis: GRG versus Rotational speed, Transversal speed, Dwell time, Welding tool profile

Response Table for Signal to Noise Ratios

Larger is better

Level	Rotational speed	Transversal speed	Dwell time	Welding tool profile
1	-5.225	-6.516	-5.188	-7.197
2	-5.268	-5.075	-5.543	-4.657
3	-7.182	-6.084	-6.944	-5.821
Delta	1.958	1.441	1.756	2.540
Rank	2	4	3	1

Response Table for Means

Level	Rotational speed	Transversal speed	Dwell time	Welding tool profile
1	0.5590*	0.4747	0.5560*	0.4386
2	0.5519	0.5681*	0.5460	0.6016*
3	0.4414	0.5095	0.4503	0.5122
Delta	0.1176	0.0934	0.1056	0.1630
Rank	2	4	3	1

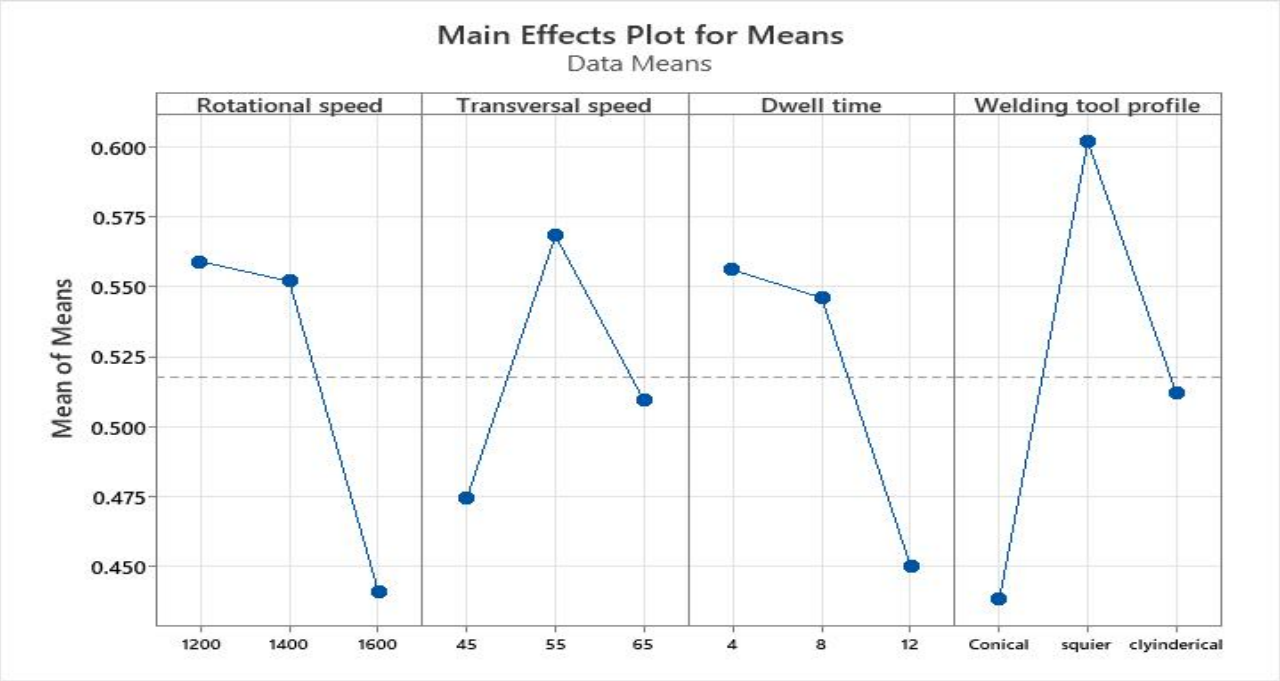
Main Effects Plot for Means
Data Means
Rotational speed
Transversal speed
Dwell time
Welding tool profile
Mean of Means
0.600
0.575
0.550
0.525
0.500
0.475
0.450
1200
1400
1600
45
55
65
4
8
12
Conical
squier
clyinderical

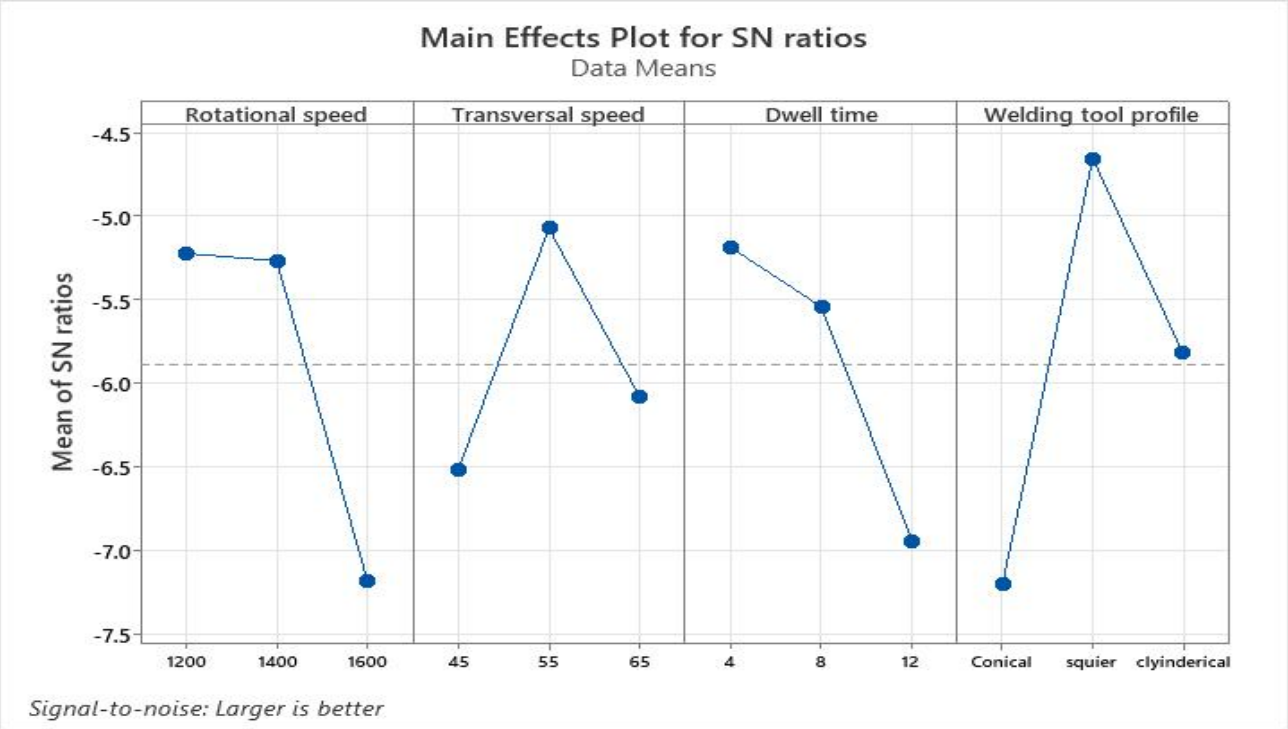
Main Effects Plot for SN ratios
Data Means
Rotational speed
Transversal speed
Dwell time
Welding tool profile
Mean of SN ratios
-4.5
-5.0
-5.5
-6.0
-6.5
-7.0
-7.5
1200
1400
1600
45
55
65
4
8
12
Conical
squier
clyinderical
Signal-to-noise: Larger is better

Appendices 11: Degree of freedom

TABLE E

F critical values

Degrees of freedom in the denominator		Degrees of freedom in the numerator								
	p	1	2	3	4	5	6	7	8	9
1	.100	39.86	49.50	53.59	55.83	57.24	58.20	58.91	59.44	59.86
	.050	161.45	199.50	215.71	224.58	230.16	233.99	236.77	238.88	240.54
	.025	647.79	799.50	864.16	899.58	921.85	937.11	948.22	956.66	963.28
	.010	4052.2	4999.5	5403.4	5624.6	5763.6	5859.0	5928.4	5981.1	6022.5
	.001	405284	500000	540379	562500	576405	585937	592873	598144	602284
2	.100	8.53	9.00	9.16	9.24	9.29	9.33	9.35	9.37	9.38
	.050	18.51	19.00	19.16	19.25	19.30	19.33	19.35	19.37	19.38
	.025	38.51	39.00	39.17	39.25	39.30	39.33	39.36	39.37	39.39
	.010	98.50	99.00	99.17	99.25	99.30	99.33	99.36	99.37	99.39
	.001	998.50	999.00	999.17	999.25	999.30	999.33	999.36	999.37	999.39
3	.100	5.54	5.46	5.39	5.34	5.31	5.28	5.27	5.25	5.24
	.050	10.13	9.55	9.28	9.12	9.01	8.94	8.89	8.85	8.81
	.025	17.44	16.04	15.44	15.10	14.88	14.73	14.62	14.54	14.47
	.010	34.12	30.82	29.46	28.71	28.24	27.91	27.67	27.49	27.35
	.001	167.03	148.50	141.11	137.10	134.58	132.85	131.58	130.62	129.86
4	.100	4.54	4.32	4.19	4.11	4.05	4.01	3.98	3.95	3.94
	.050	7.71	6.94	6.59	6.39	6.26	6.16	6.09	6.04	6.00
	.025	12.22	10.65	9.98	9.60	9.36	9.20	9.07	8.98	8.90
	.010	21.20	18.00	16.69	15.98	15.52	15.21	14.98	14.80	14.66
	.001	74.14	61.25	56.18	53.44	51.71	50.53	49.66	49.00	48.47
5	.100	4.06	3.78	3.62	3.52	3.45	3.40	3.37	3.34	3.32
	.050	6.61	5.79	5.41	5.19	5.05	4.95	4.88	4.82	4.77
	.025	10.01	8.43	7.76	7.39	7.15	6.98	6.85	6.76	6.68
	.010	16.26	13.27	12.06	11.39	10.97	10.67	10.46	10.29	10.16
	.001	47.18	37.12	33.20	31.09	29.75	28.83	28.16	27.65	27.24
6	.100	3.78	3.46	3.29	3.18	3.11	3.05	3.01	2.98	2.96
	.050	5.99	5.14	4.76	4.53	4.39	4.28	4.21	4.15	4.10
	.025	8.81	7.26	6.60	6.23	5.99	5.82	5.70	5.60	5.52
	.010	13.75	10.92	9.78	9.15	8.75	8.47	8.26	8.10	7.98
	.001	35.51	27.00	23.70	21.92	20.80	20.03	19.46	19.03	18.69
7	.100	3.59	3.26	3.07	2.96	2.88	2.83	2.78	2.75	2.72
	.050	5.59	4.74	4.35	4.12	3.97	3.87	3.79	3.73	3.68
	.025	8.07	6.54	5.89	5.52	5.29	5.12	4.99	4.90	4.82
	.010	12.25	9.55	8.45	7.85	7.46	7.19	6.99	6.84	6.72
	.001	29.25	21.69	18.77	17.20	16.21	15.52	15.02	14.63	14.33

TABLE E

F critical values (continued)

Degrees of freedom in the denominator		Degrees of freedom in the numerator								
	p	1	2	3	4	5	6	7	8	9
8	.100	3.46	3.11	2.92	2.81	2.73	2.67	2.62	2.59	2.56
	.050	5.32	4.46	4.07	3.84	3.69	3.58	3.50	3.44	3.39
	.025	7.57	6.06	5.42	5.05	4.82	4.65	4.53	4.43	4.36
	.010	11.26	8.65	7.59	7.01	6.63	6.37	6.18	6.03	5.91
	.001	25.41	18.49	15.83	14.39	13.48	12.86	12.40	12.05	11.77
9	.100	3.36	3.01	2.81	2.69	2.61	2.55	2.51	2.47	2.44
	.050	5.12	4.26	3.86	3.63	3.48	3.37	3.29	3.23	3.18
	.025	7.21	5.71	5.08	4.72	4.48	4.32	4.20	4.10	4.03
	.010	10.56	8.02	6.99	6.42	6.06	5.80	5.61	5.47	5.35
	.001	22.86	16.39	13.90	12.56	11.71	11.13	10.70	10.37	10.11
10	.100	3.29	2.92	2.73	2.61	2.52	2.46	2.41	2.38	2.35
	.050	4.96	4.10	3.71	3.48	3.33	3.22	3.14	3.07	3.02
	.025	6.94	5.46	4.83	4.47	4.24	4.07	3.95	3.85	3.78
	.010	10.04	7.56	6.55	5.99	5.64	5.39	5.20	5.06	4.94
	.001	21.04	14.91	12.55	11.28	10.48	9.93	9.52	9.20	8.96
11	.100	3.23	2.86	2.66	2.54	2.45	2.39	2.34	2.30	2.27
	.050	4.84	3.98	3.59	3.36	3.20	3.09	3.01	2.95	2.90
	.025	6.72	5.26	4.63	4.28	4.04	3.88	3.76	3.66	3.59
	.010	9.65	7.21	6.22	5.67	5.32	5.07	4.89	4.74	4.63
	.001	19.69	13.81	11.56	10.35	9.58	9.05	8.66	8.35	8.12
12	.100	3.18	2.81	2.61	2.48	2.39	2.33	2.28	2.24	2.21
	.050	4.75	3.89	3.49	3.26	3.11	3.00	2.91	2.85	2.80
	.025	6.55	5.10	4.47	4.12	3.89	3.73	3.61	3.51	3.44
	.010	9.33	6.93	5.95	5.41	5.06	4.82	4.64	4.50	4.39
	.001	18.64	12.97	10.80	9.63	8.89	8.38	8.00	7.71	7.48
13	.100	3.14	2.76	2.56	2.43	2.35	2.28	2.23	2.20	2.16
	.050	4.67	3.81	3.41	3.18	3.03	2.92	2.83	2.77	2.71
	.025	6.41	4.97	4.35	4.00	3.77	3.60	3.48	3.39	3.31
	.010	9.07	6.70	5.74	5.21	4.86	4.62	4.44	4.30	4.19
	.001	17.82	12.31	10.21	9.07	8.35	7.86	7.49	7.21	6.98
14	.100	3.10	2.73	2.52	2.39	2.31	2.24	2.19	2.15	2.12
	.050	4.60	3.74	3.34	3.11	2.96	2.85	2.76	2.70	2.65
	.025	6.30	4.86	4.24	3.89	3.66	3.50	3.38	3.29	3.21
	.010	8.86	6.51	5.56	5.04	4.69	4.46	4.28	4.14	4.03
	.001	17.14	11.78	9.73	8.62	7.92	7.44	7.08	6.80	6.58
15	.100	3.07	2.70	2.49	2.36	2.27	2.21	2.16	2.12	2.09
	.050	4.54	3.68	3.29	3.06	2.90	2.79	2.71	2.64	2.59
	.025	6.20	4.77	4.15	3.80	3.58	3.41	3.29	3.20	3.12
	.010	8.68	6.36	5.42	4.89	4.56	4.32	4.14	4.00	3.89
	.001	16.59	11.34	9.34	8.25	7.57	7.09	6.74	6.47	6.26
16	.100	3.05	2.67	2.46	2.33	2.24	2.18	2.13	2.09	2.06
	.050	4.49	3.63	3.24	3.01	2.85	2.74	2.66	2.59	2.54
	.025	6.12	4.69	4.08	3.73	3.50	3.34	3.22	3.12	3.05
	.010	8.53	6.23	5.29	4.77	4.44	4.20	4.03	3.89	3.78
	.001	16.12	10.97	9.01	7.94	7.27	6.80	6.46	6.19	5.98
17	.100	3.03	2.64	2.44	2.31	2.22	2.15	2.10	2.06	2.03
	.050	4.45	3.59	3.20	2.96	2.81	2.70	2.61	2.55	2.49
	.025	6.04	4.62	4.01	3.66	3.44	3.28	3.16	3.06	2.98
	.010	8.40	6.11	5.19	4.67	4.34	4.10	3.93	3.79	3.68
	.001	15.72	10.66	8.73	7.68	7.02	6.56	6.22	5.96	5.75